

Field Investigation of a Hanging Dam
in the St. Lawrence River,
Winter of 1981-82

Hung Tao Shen, William A. VanDeValk, Gordon B. Batson
and Iury L. Maytin

Department of Civil and Environmental Engineering
Clarkson College of Technology
Potsdam, N.Y. 13676



CIRCULATING COPY
Sea Grant Depository

August, 1982

Final Report

Prepared for

U.S. Department of Transportation
St. Lawrence Seaway Development Corporation
Office of Plans and Policy Development
Washington, D.C. 20591

NATIONAL SEA GRANT DEPOSITORY
PELL LIBRARY BUILDING
URI, NARRAGANSETT BAY CAMPUS
NARRAGANSETT, RI 02882

Field Investigation of a Hanging Dam
in the St. Lawrence River,
Winter of 1981-82

Hung Tao Shen, William A. VanDeValk, Gordon B. Batson
and Iury L. Maytin

Department of Civil and Environmental Engineering
Clarkson College of Technology
Potsdam, N.Y. 13676



August, 1982

Final Report

Prepared for

U.S. Department of Transportation
St. Lawrence Seaway Development Corporation
Office of Plans and Policy Development
Washington, D.C. 20591

1. Report No. DTSL55-82-C-C0198A		2. Government Accession No.		3. Recipient's Catalog No.	
4. Title and Subtitle Field Investigation of a Hanging Dam in the St. Lawrence River, Winter of 1981-82				5. Report Date	
				6. Performing Organization Code	
				8. Performing Organization Report No.	
7. Author(s) H.T. Shen, W.A. VanDeValk, G.B. Batson, I.L. Martin				10. Work Unit No. (TRAIS)	
9. Performing Organization Name and Address Department of Civil and Environmental Engrg. Clarkson College of Technology Potsdam, NY 13676				11. Contract or Grant No. DTSL55-82-C-C0198	
				13. Type of Report and Period Covered Final Report Feb.-Aug., 1982	
12. Sponsoring Agency Name and Address U.S. Department of Transportation St. Lawrence Seaway Development Corporation Washington, D.C. 20591				14. Sponsoring Agency Code	
				15. Supplementary Notes	
16. Abstract <p>In this study, field surveys were carried out for a large hanging ice dam in the St. Lawrence River near Sparrowhawk Point, during the winter of 1981-82. Cross section profiles of the dam and the channel, the headloss characteristics, and velocity profiles underneath the dam were monitored during the season. Based on the field data, hydraulic resistance characteristics of the dam are analyzed. The effect of channel geometry and flow pattern on the formation and shape of the ice dam are discussed.</p>					
17. Key Words Flow Resistance, Frazil Ice, Hanging Dam, Ice Cover, River			18. Distribution Statement		
19. Security Classif. (of this report)		20. Security Classif. (of this page)		21. No. of Pages	22. Price

NOTICE

This document is disseminated under the sponsorship of the Department of Transportation in the interest of information exchange. The United States Government assumes no liability for the contents or use thereof.

NOTICE

The United States Government does not endorse products or manufacturers. Trade or manufacturer's names appear herein solely because they are considered essential to the object of this report.

METRIC CONVERSION FACTORS

To convert	To	Multiply by
inches (in)	millimeters (mm)	25.40
inches (in)	centimeters (cm)	2.540
inches (in)	meters (m)	0.0254
feet (ft)	meters (m)	0.305
miles (miles)	kilometers (km)	1.61
square inches (sq in)	square centimeters (cm ²)	6.45
square feet (sq ft)	square meters (m ²)	0.093
cubic feet (cu ft)	cubic meters (m ³)	0.028
Fahrenheit temperature (°F)	Celsius temperature (°C)	5/9 after subtracting 32
Btu	Calories	252
Btu/hr. ft. °F	Watts/cm °C	0.0173

ACKNOWLEDGEMENTS

This study is supported by the Office of Plans and Policy Development, St. Lawrence Seaway Development Corporation, Washington, D.C. Particular thanks are extended to Mr. Stephen C. Hung for his cooperation and assistance in expediting the project throughout the study period.

Mr. P.N.D.D. Yapa and Mr. G.C. Pasquarell, research assistants, Clarkson College of Technology, assisted in some computations and analyses. The field work was carried out with the assistance of the Atlantic Testing Laboratory.

The cooperation and assistance of the following individuals and organizations are gratefully acknowledged: J.B. Adams, St. Lawrence Seaway Development Corporation; J.L. Bartholomew, Power Authority of the State of New York; G. Graham, St. Lawrence Seaway Authority; T.E. Wigle and J.A. Keon, Ontario Hydro; and D.F. Witherspoon, Environment Canada.

Partial support provided by the New York Sea Grant Institute through Grant No. 344-5129G is also acknowledged.

The contents of this report are not to be used for advertising or promotional purposes. Citation of brand names does not constitute an official endorsement or approval of the use of such commercial products.

TABLE OF CONTENTS

	Page
I. INTRODUCTION	1
Formation of Hanging Dams	1
The St. Lawrence River Ice Cover	2
II. FIELD MEASUREMENTS	6
Hanging Dam Profiles and the Channel Geometry	10
Water Levels	11
Velocity Profiles	17
Other Flow and Ice Condition Data	26
III. ANALYSIS AND DISCUSSIONS	27
Formation and Geometry of the Hanging Dam	27
Hydraulic Resistance of the Hanging Dam	33
IV. SUMMARY AND CONCLUSIONS	40
REFERENCES	41
APPENDIX A FLOW DISTRIBUTIONS AND HANGING DAM PROFILES	44
APPENDIX B WATER LEVELS AND DISCHARGE	68
APPENDIX C ICE COVER THICKNESS AT SELECTED CROSS SECTIONS	74
APPENDIX D ICE COVER CONDITION MAPS	79

LIST OF FIGURES

Figure		Page
1	Location of the Hanging Dam Near Sparrowhawk Point, 1981-82	7
2	Location of Control Lines at the Hanging Dam Site	8
3	Coordinates of Grid Points on the Control Lines	9
4	Hanging Dam Profiles Along Longitudinal Line L-L	12
5	Hanging Dam Profile Along Transverse Line 1-1	13
6	Hanging Dam Profiles Along Transverse Line 6-6	14
7	Hanging Dam Profile Along Transverse Line 12-12	15
8	The Assembly for Velocity Meters	18
9	Velocity Measurement in the Field	19
10	Velocity Profile at Station L-1; Feb. 24, 1982	20
11	Velocity Profile at Station L-3; Feb. 24, 1982	21
12	Velocity Profile at Station L-5; Feb. 25, 1982	22
13	Velocity Profile at Station L-7; Feb. 25, 1982	23
14	Velocity Profile at Station L-9; Feb. 18, 1982	24
15	Velocity Profile at Station L-12; Feb. 18, 1982	25
16	Flow Pattern and Hanging Dam Cross Sections Near Sparrowhawk Point	30
17	Channel Bottom Topography	31
18	Manning's Coefficients, Air Temperature (FDD) at Massena, Discharge (Q) at the Power Dam Site, Winter of 1981-82	39

LIST OF TABLES

Table		Page
1	Water Surface Slopes Along the Hanging Dam	16
2	Depth-Averaged Velocity Underneath the Maximum Ice Thickness	34
3	Local Roughness Coefficients Calculated from Measured Velocity Profiles	35
4	Cross-Sectional Geometry at the Reference Water Level (19)	38

Chapter I

INTRODUCTION

The existence of hanging dams in rivers with an ice cover has been known to hydraulic engineers for many years. The presence of hanging dams in a river constricts the flow cross section and, in many cases, could cause large head losses in addition to the loss caused by a normal sheet ice cover. A number of field studies have been reported in the literature (5,6,8,9,13,26) on the formation and characteristics of hanging dams. In this report, a field study on the hydraulic characteristics of a hanging dam located in the St. Lawrence River near Sparrowhawk Point during the winter of 1981-82 is presented.

Formation of Hanging Dams

Although all hanging dams are massive accumulations of ice particles on the underside of an ice cover, the formation processes of these hanging dams may be significantly different. According to their formation processes, hanging dams may be classified into two categories. The first type of hanging dams, which will be referred to as fragment ice hanging dams, are accumulations of large ice plates or frazil ice pans. These dams are formed near the leading edge of an ice cover during its upstream progression. This process can occur either at the beginning of the winter during the formation of the new ice cover or during the spring break-up period when ice floes, which are released from an upstream reach of a river, reaches a stationary downstream obstacle or ice cover. Fragment ice dams are formed either by the submergence, transport, and arrest of ice floes

underneath an ice cover or through the internal collapse and subsequent thickening of floating ensembles of large ice particles caused by the action of external forces. The second type of hanging dams, which will be referred to as frazil ice hanging dams, are formed by the deposition of suspended frazil ice particles which are produced in open water areas upstream of a stable ice cover during periods of supercooling of the river surface. The deposition of frazil suspensions could occur when suspended ice particles reach the undersurface of the ice cover. Near the leading edge of the ice cover, when frazil ice particles are active, particles that reach the ice-water interface are deposited. Further downstream, when ice particles become inactive they will deposit only in low flow velocity regions. For a fragment ice dam, which is located near the leading edge of an ice cover, and is formed at the beginning of the ice covered season, a relatively soft outer layer of frazil slush could form on the surface of the fragment ice dam due to the accumulation of active frazil ice particles produced in the open water area during the winter. In the St. Lawrence River both the fragment ice hanging dams and the frazil ice hanging dams, and the combination of both could form.

The St. Lawrence River Ice Cover

The Upper St. Lawrence River is being utilized for hydro-power production and serves as the only navigation passage for shipping between the Atlantic Ocean and the Great Lakes. The existence of hanging ice dams in the river has been an important consideration in the planning and management of the river flow

during the winter. The flow of the river is regulated by the Moses-Saunders Power Dam located near Massena. This dam is part of the St. Lawrence Project, which was completed in 1959 as a joint venture of the United States and Canada. The planning for the flow regulation is closely related to the ice conditions in the river which affect the length of the navigation season and the amount of power that can be generated.

With the present regulation plan, ice covers are initiated at artificial obstacles such as dams and booms at the beginning of each winter (18). Stable ice covers are formed between Lake Ontario and Cardinal with the installation of Ogdensburg-Prescott ice booms in the Galop Island area. Ice cover conditions in the International Rapids Section (see Appendix C) between Cardinal and Massena, however, are more complicated. Early in the winter, when the water temperature is supercooled, frazil ice forms in the river. This frazil ice develops into large ice floes and fragmented ice sheets which flow into Lake St. Lawrence. Beginning initially at the face of the Power Dam, these ice floes pack against each other to form a solid cover. The ice front formed by the edge of the ice floes then progresses upstream as more ice floes arrive. Due to the low flow velocity, the progression of the ice cover from the Power Dam to Morrisburg can be completed with no flow regulation. When the leading edge of the ice cover reaches Morrisburg, the progression of the ice cover still further upstream is accomplished by a short period of flow reduction which is created when favorable cold weather develops. With the flow reduction, the ice cover will progress

upstream towards the region of high velocity flow near Pinetree Point. At this stage the incoming ice floes which pass through Iroquois Dam will become entrained by the flow and are transported under the ice cover. When these floes come to rest under the ice cover they form a hanging dam. The size of this hanging dam will increase either due to the arrest of additional ice floes underneath the hanging dam or due to the thickening caused by the collapse of the accumulated floating ice mass. The collapse of the ice mass occurs when the hydrodynamic drag and streamwise gravity force acting on the ice mass surpasses the strength of the fragmented ice cover. The lowering of the gates at the Iroquois Control Dam can control the size of the hanging dam at Pinetree Point by preventing the inflow of additional ice floes. The lowering of these gates also initiates the progression of an ice sheet upstream from Iroquois Dam towards Sparrowhawk Point and Cardinal. The ice cover upstream of Iroquois Dam can only progress to the vicinity of Sparrowhawk Point because of high flow velocities in the Galop Island Region. Another hanging dam will then form near Sparrowhawk Point.

Due to the high flow velocity, open water reaches always remain downstream of the Galop Booms and Iroquois Dam, throughout the winter. These open water areas can produce large amounts of frazil ice. Because of the relatively short reaches in these open water areas, the frazil ice generated in these areas is entrained in the flow in the form of buoyant suspensions. The suspended frazil ice particles will gradually accumulate under the ice cover and lead to the growth of existing hanging dams

and form additional hanging dams further downstream (3,4,21).

Field measurements in the St. Lawrence River indicated that major fragment ice hanging dams are formed each winter in the vicinity of Sparrowhawk Point and Pinetree Point. Frazil ice hanging dams have also been observed in the Ogden Island region (3,4). During the winter of 1981-82 a major hanging dam located near the Sparrowhawk Point was monitored and studied for its hydraulic characteristics. The result of this field study will be presented in the following chapters.

Chapter II

FIELD MEASUREMENTS

During the winter of 1981-82, ice covers in the International Rapids Section of the St. Lawrence River were formed during the period between Jan. 11 and Jan. 18, 1982 (18). Preliminary surveys made by Ontario Hydro in late January showed that a large hanging dam existed near Sparrowhawk Point and a smaller one existed near Pinetree Point. Considering the time and resources available, the larger hanging dam near Sparrowhawk Point was selected for detailed study. A reconnaissance survey was then made on Jan. 28, 1982 to determine the exact location of the dam. This survey indicated that the hanging dam had a length of about 2,000 ft with a maximum thickness of more than 20 ft. Since a full three-dimensional mapping of the hanging dam is not feasible, a grid system, which includes a longitudinal control line and three transverse control lines, at the site of the dam was established with grid points marked on the ice surface to serve as a reference for locating measuring stations later. The location of the hanging dam and control lines for the grid system are presented in Figs. 1 and 2. Coordinates of grid points along control lines are summarized in Fig. 3. Based on the grid system defined, the hanging dam was monitored on a weekly basis during the whole period. The data measured include i) longitudinal and transverse profiles of the dam, the corresponding channel bottom profiles, ii) drop in the water surface level along the hanging dam, and iii) velocity distribution underneath the hanging dam. These measurements are discussed in detail in the following

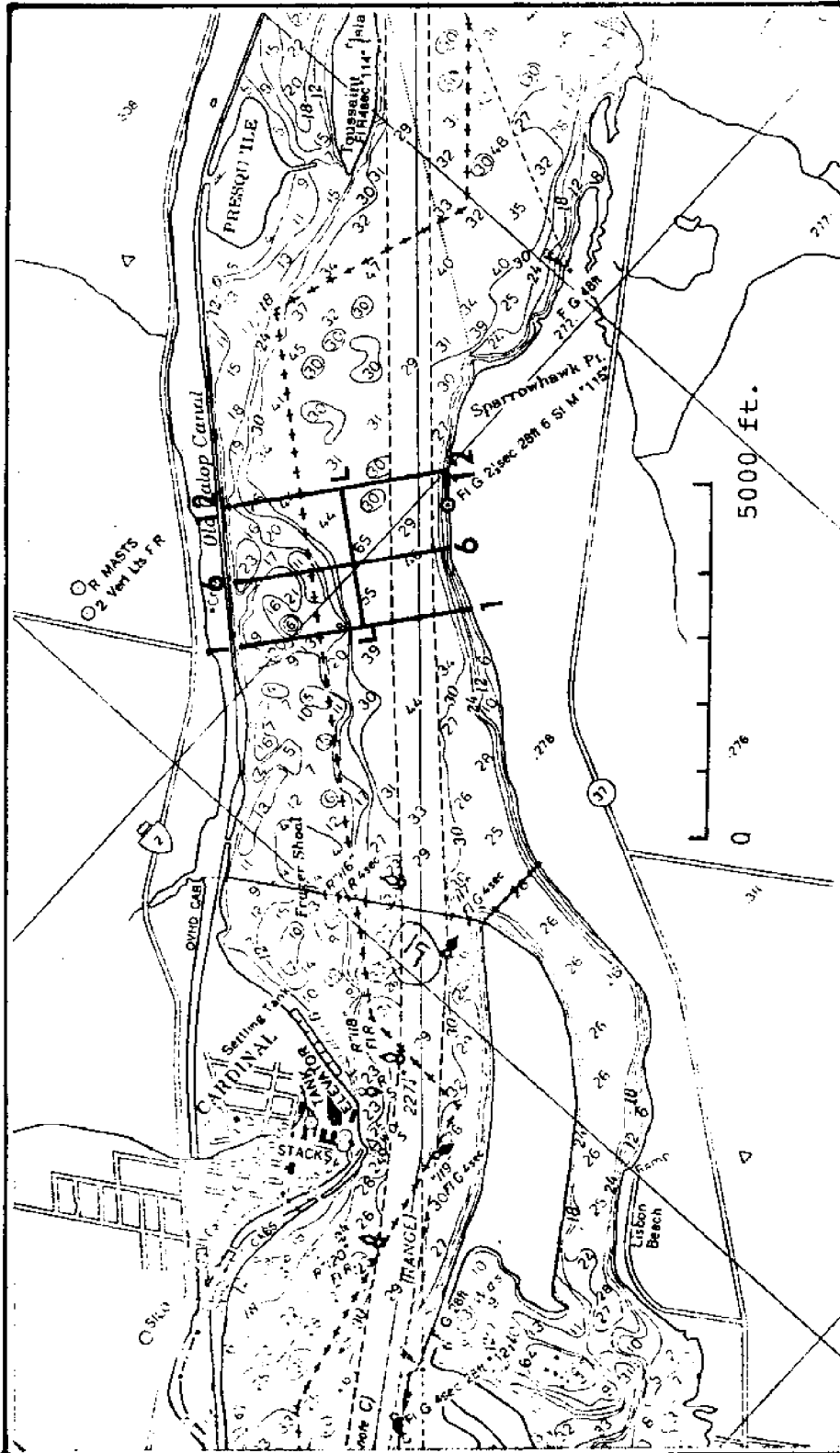


Figure 1. Location of the Hanging Dam Near Sparrowhawk Point, 1981-82

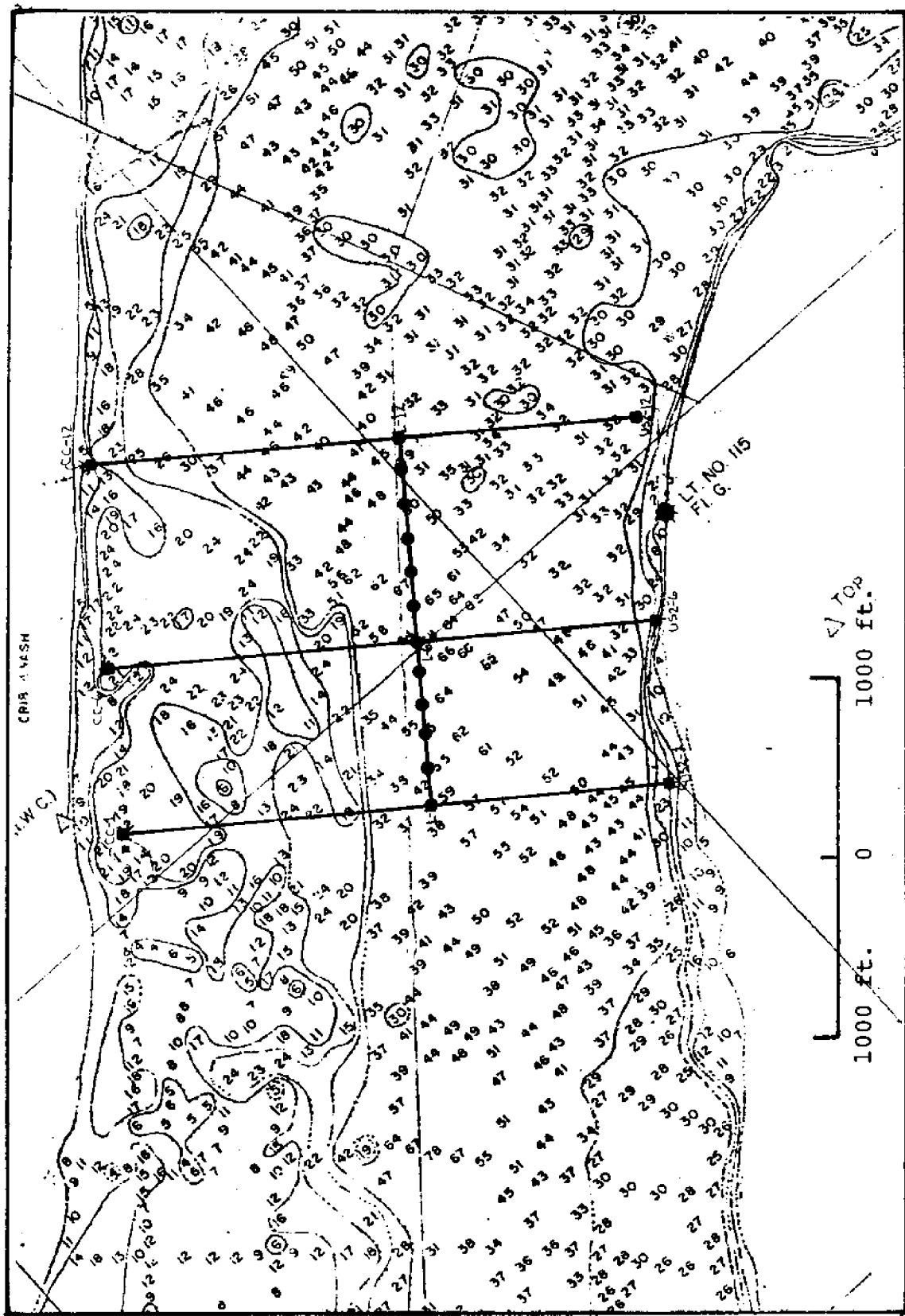


Figure 2. Location of Control Lines at the Hanging Dam Site.

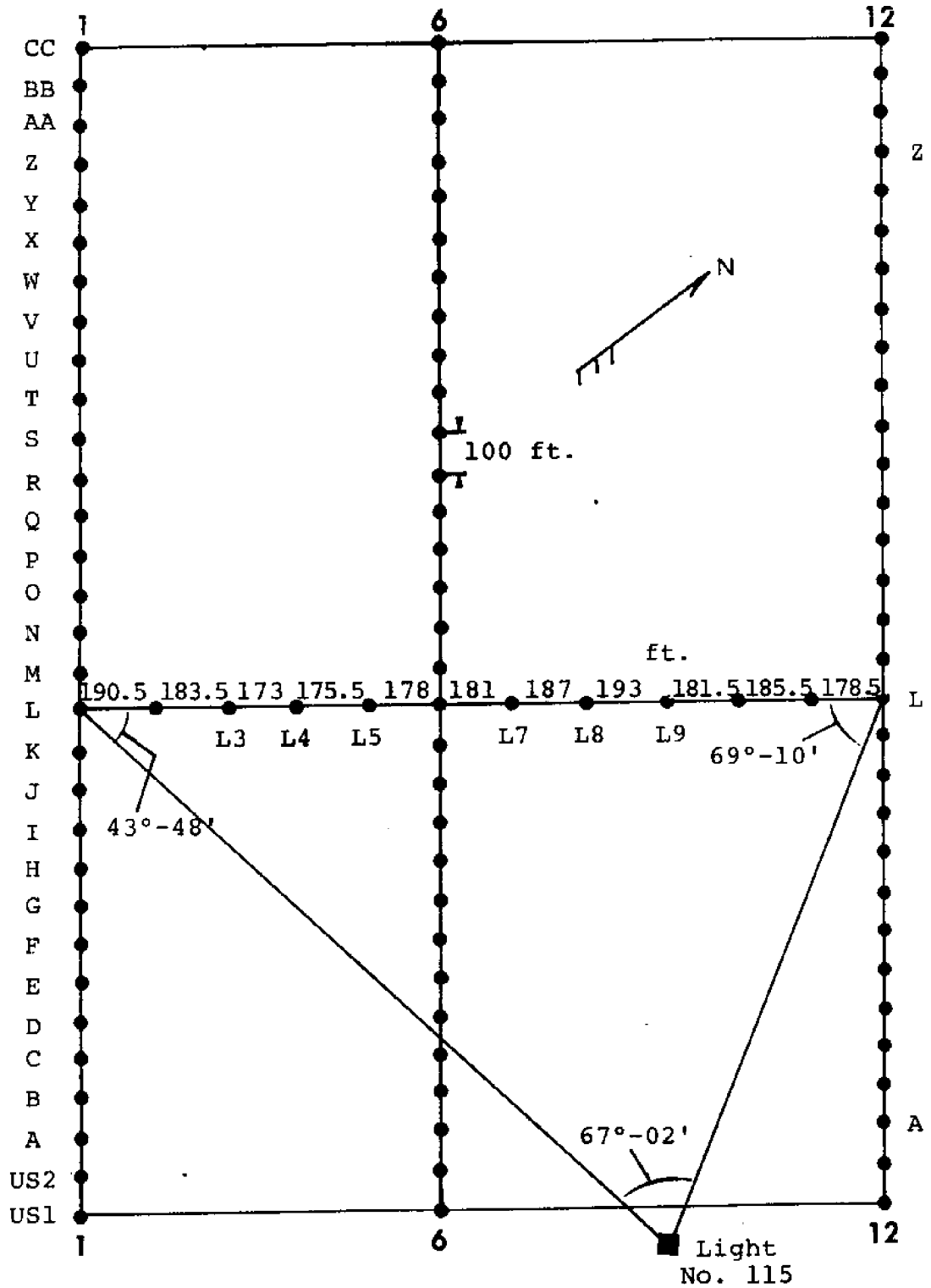


Figure 3. Coordinates of Grid Points on the Control Lines

sections.

Hanging Dam Profiles and the Channel Geometry

The field measurement procedures adopted in this study to obtain ice thickness and channel cross sectional geometries were the same as those reported in previous surveys conducted during the winters of 1977-78 and 1978-79 on flow and ice conditions in the Upper St. Lawrence River (3,4). When measurements were to be made, holes were first drilled through the ice sheet at a selected grid point. The thickness of the ice sheet was then measured with an L-shaped metal rod which was hooked onto the underside of the ice sheet. The location of the undersurface of the hanging dam and the depth to the channel bottom were measured using a Lowrance Fish Lo-K-Tor Sonic Meter. The measurement procedure consisted of first lowering the depth sensing portion of the meter through the ice mass with a scaled metal pipe. When the sensor was no longer inside the hanging dam, the meter would indicate the depth from the sensor to the river bottom. The thickness of the hanging dam and the flow depth could then be determined.

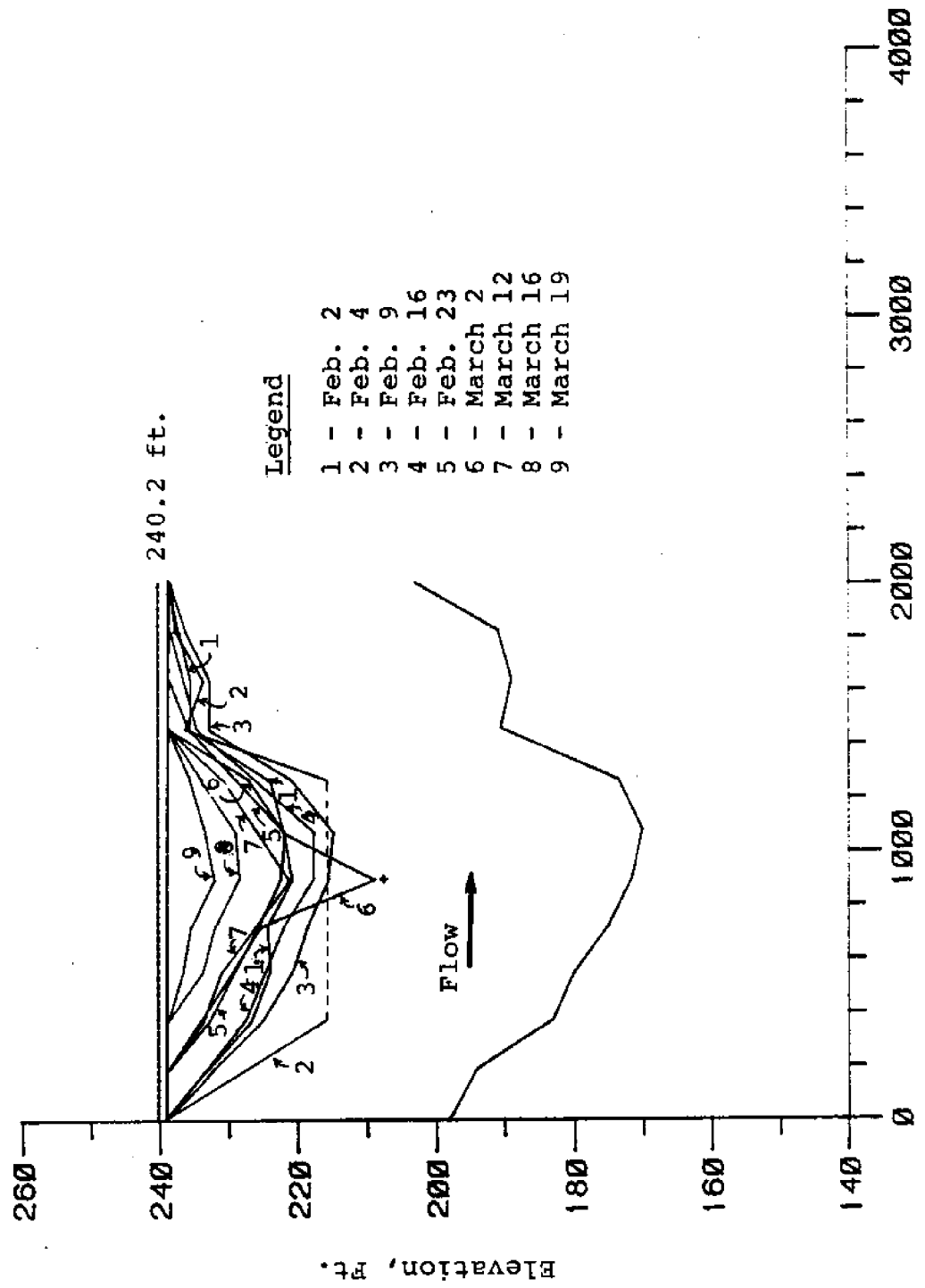
Geometry of channel cross sections - The elevation of the channel bottom along all four control lines was determined based on the average of flow depth readings obtained by the sonic meter during ice thickness measurements. Additional information obtained from the detailed hydrographic charts prepared by the U.S. Army Corps of Engineers in 1960 are also used. The channel bottom profiles given by the hydrographic charts compared very well with the sonic meter data. This shows that relatively little change in channel bottom profiles has occurred since 1960. All channel

bottom elevation data were adjusted to measure from the 1955 IGLD.

Hanging dam profiles - Hanging dam thickness profiles along control lines were measured. Since the thickness of the hanging dam along both transverse lines 1-1 and 12-12 at the upstream and the downstream ends were small, only the longitudinal profile and the transverse profile along line 6-6 were monitored periodically. All measured profiles are presented in Appendix A. A summary of these results are presented in Figs. 4, 5, 6, and 7. These figures show that the hanging dam has a three-dimensional form. The shape of the dam is affected by the channel geometry, the amount of ice supply from the upstream, and the flow pattern in the vicinity and upstream of the site of the hanging dam. Both the length along the longitudinal control line and the width along the transverse control line 6-6 of the hanging dam decreased as winter progressed. The thickness of the dam along these two control lines, however, both increased and decreased during this period. The variation of thickness during the winter was closely related to the variation of the air temperature.

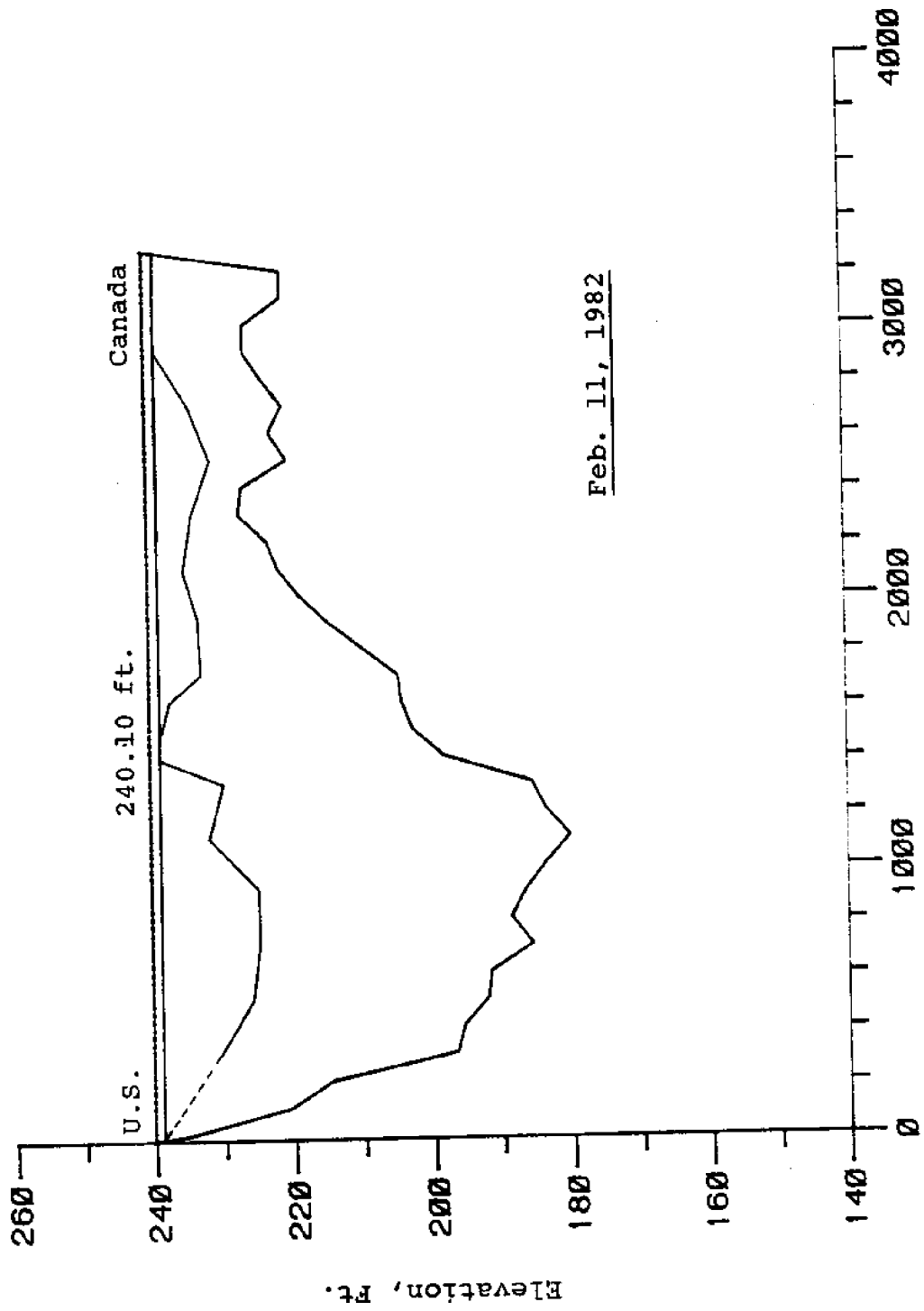
Water Levels

The resistance characteristics of a hanging dam is an important parameter in ice hydraulics. For this purpose, water levels at both the upstream and downstream ends of the hanging dam; i.e., at stations L-1 and L-12; were measured using a surveyor's level. The water surface slope along the hanging dam could then be determined. Table 1 summarizes measured water surface slopes.



Distance from Point L-1 (Ft.)

Figure 4. Hanging Dam Profiles Along Longitudinal Line L-L



Distance from U.S. Shore (Ft.)

Figure 5. Hanging Dam Profile Along Transverse Line 1-1-1

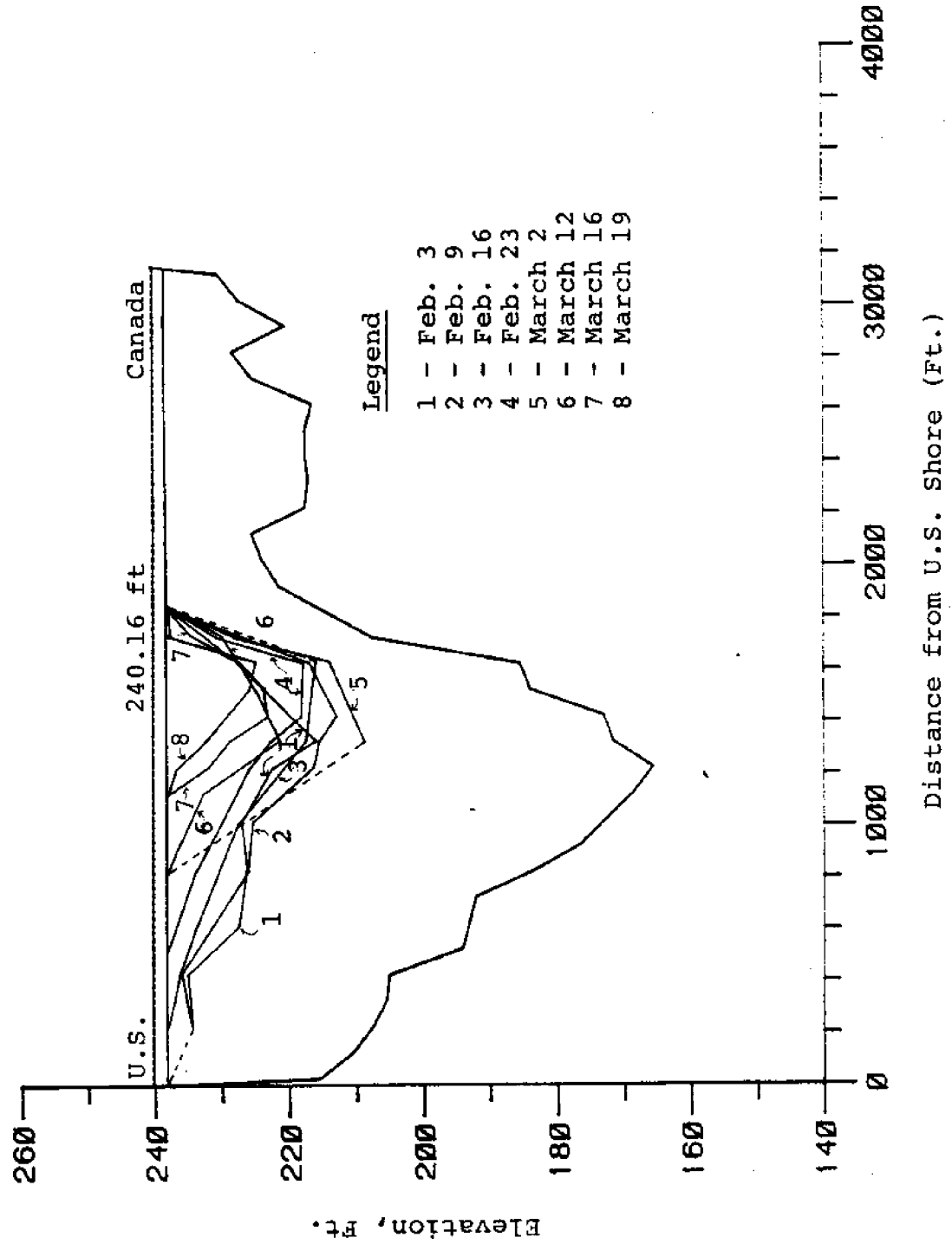
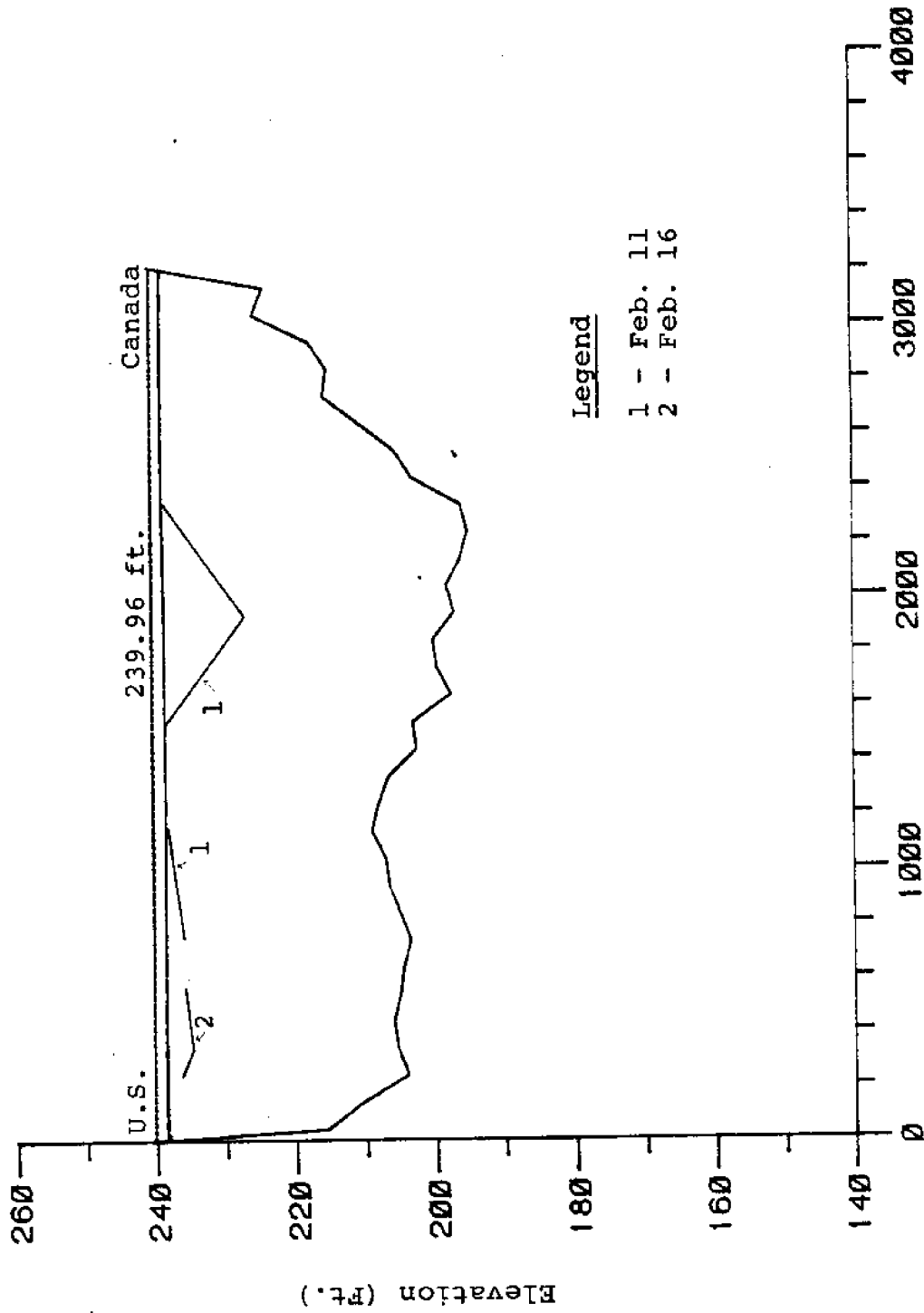


Figure 6. Hanging Dam Profiles Along Transverse Line 6-6



Legend

- 1 - Feb. 11
- 2 - Feb. 16

Distance from U.S. Shore (Ft.)

Figure 7. Hanging Dam Profile Along Transverse Line 12-12

Table 1. Water Surface Slopes Along the Hanging Dam

Date	Slope, s_f
Feb. 2, 1982	5.98×10^{-5}
Feb. 4, 1982	4.98×10^{-5}
Feb. 9, 1982	5.48×10^{-5}
Feb. 16, 1982	6.48×10^{-5}
Feb. 18, 1982	6.98×10^{-5}
Feb. 23, 1982	8.72×10^{-5}
Feb. 25, 1982	4.48×10^{-5}
Mar. 2, 1982	8.47×10^{-5}
Mar. 12, 1982	3.49×10^{-5}

Velocity Profiles

Velocity profiles underneath the hanging dam were measured using a Marsh-McBirney electromagnetic current meter (3,4) and a gimbal-mounted, vane-type photoelectric current meter (12). Both meters were attached to a winch-cable assembly with a standard 75-lb USGS lead weight attached at the lower end of the cable to maintain the vertical position of the meters (Figs. 8 and 9). Even with the successive pounding of the 75-lb lead weight, it was often difficult to send the meter assembly through the inner portion of the hanging dam which consisted of hardened fragment ice pieces. Only a few measured velocity profiles were obtained along the longitudinal control line. These profiles are presented in Figs. 10-15. Most of these profiles have the shape of composite logarithmic profiles commonly observed in rivers with sheet ice cover (11). Velocity profiles at stations L3 and L5, however, are rather irregular. A velocity defect at the upper portion of the velocity profile at station L3 can be observed. This velocity defect is similar to that commonly observed in convergent pipe flows when the adverse pressure gradient exists (30). In the present case, although the flow area remains fairly uniform in the vicinity of station L3, an adverse pressure gradient may exist due to the change in pressure at the ice-water interface caused by the streamwise variation of ice thickness. At station L5, large fluctuations in velocity readings were experienced during the measurement. The mean velocity profile is extremely irregular. This is believed to be caused by the cross currents and large eddies which existed in this region where

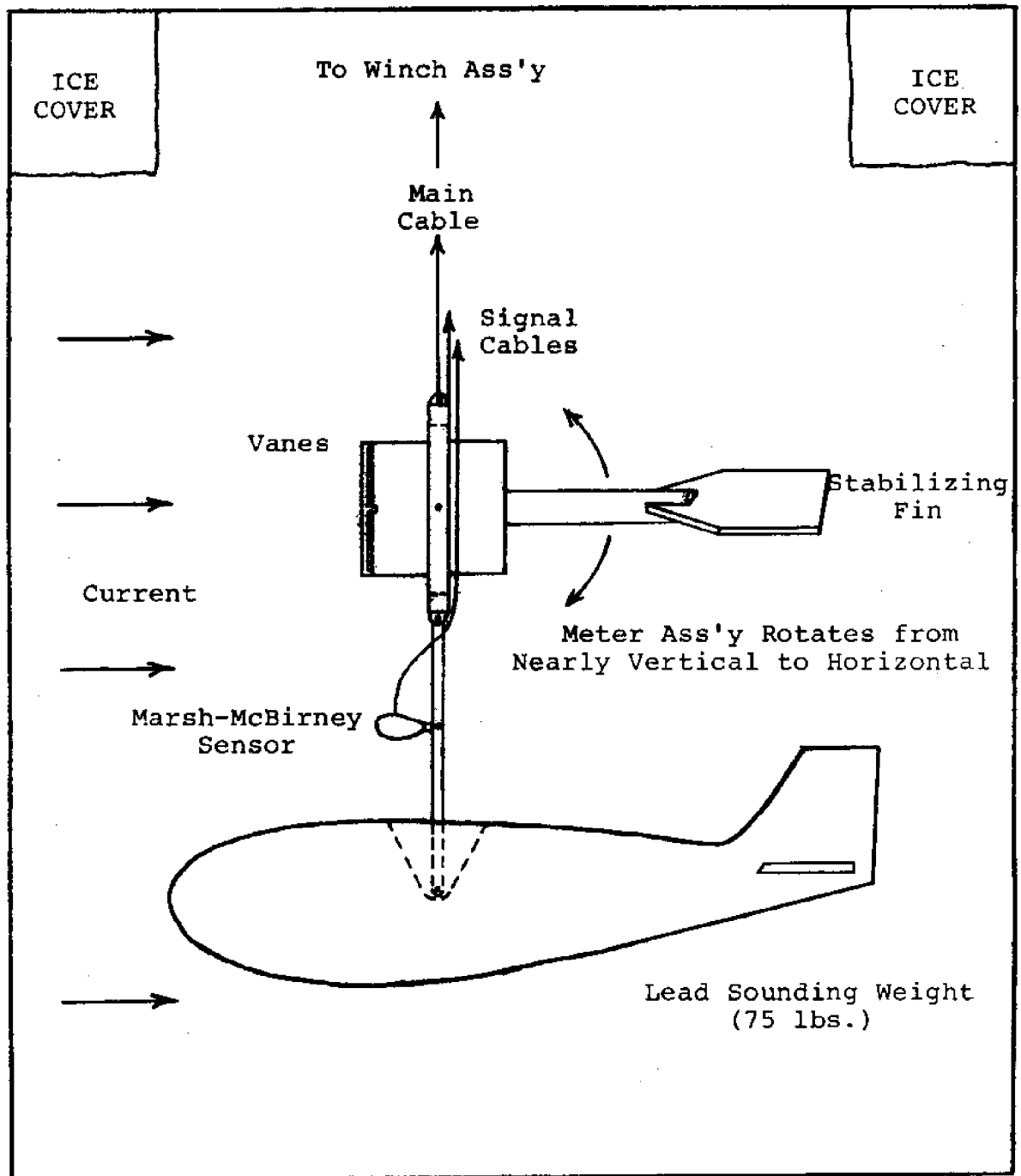
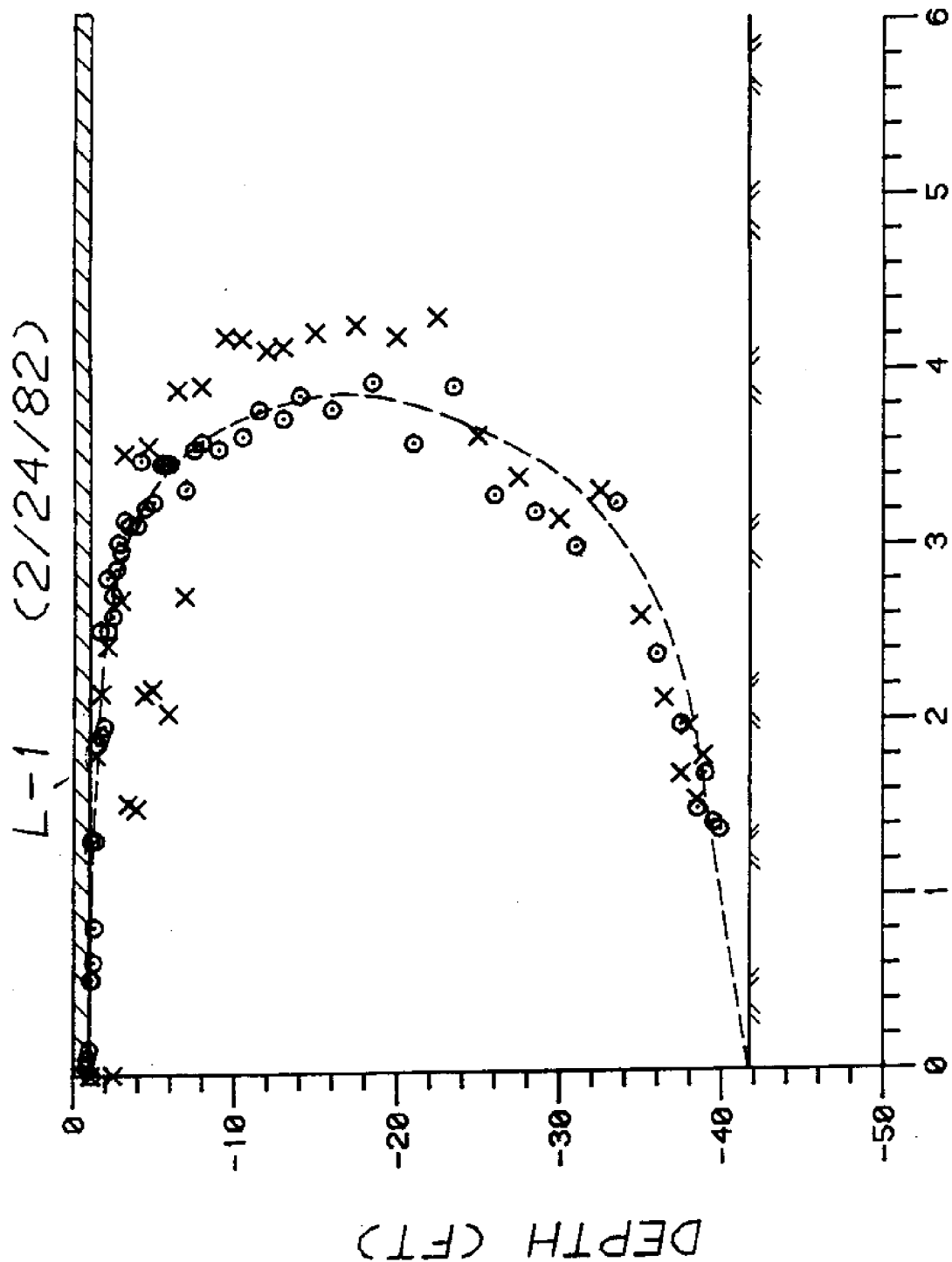


Figure 8. The Assembly for Velocity Meters



Figure 9. Velocity Measurement in the Field



VELOCITY (FT/SEC)

Figure 10. Velocity Profile at Station L-1; Feb. 24, 1982

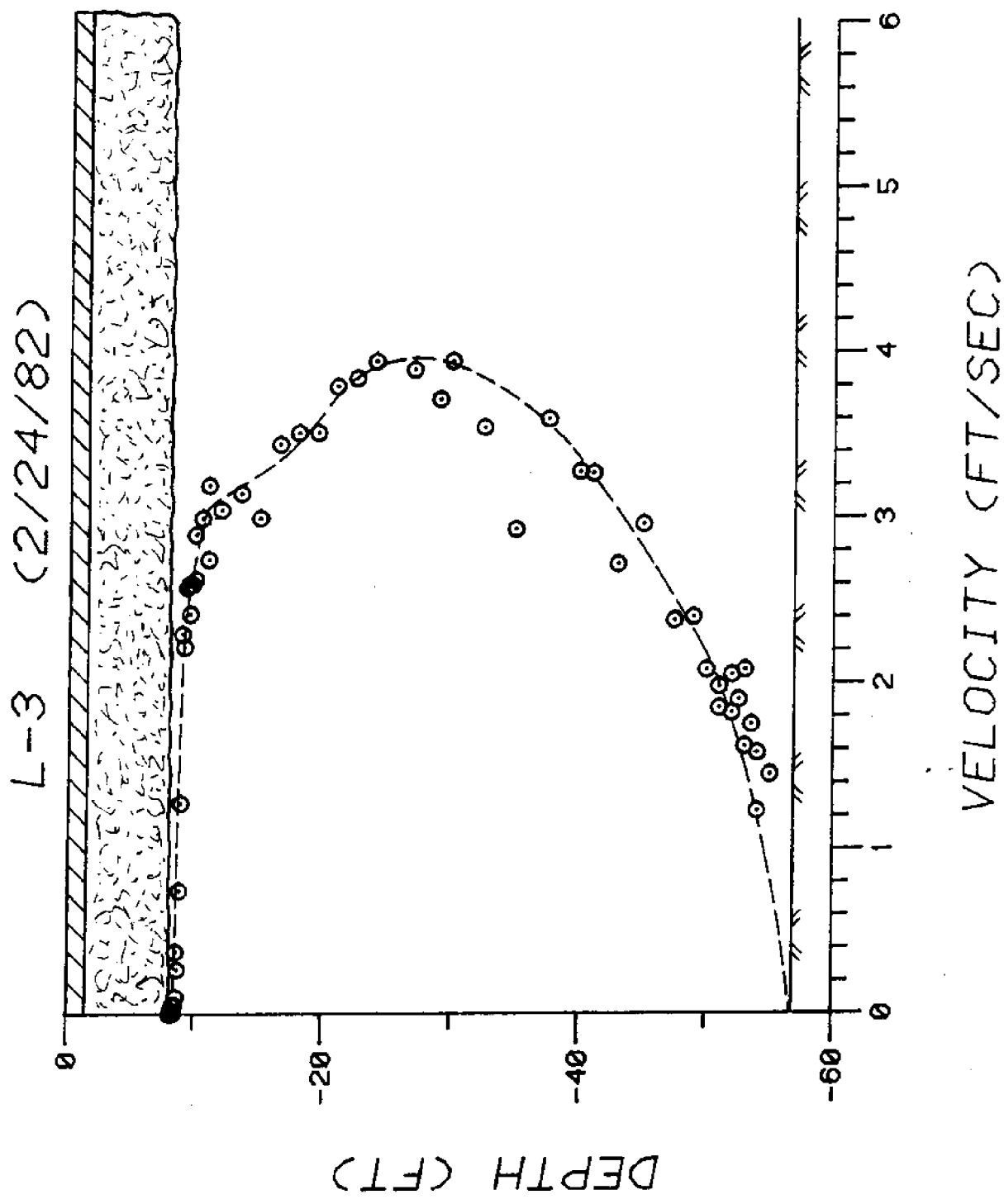


Figure 11. Velocity Profile at Station L-3; Feb. 24, 1982

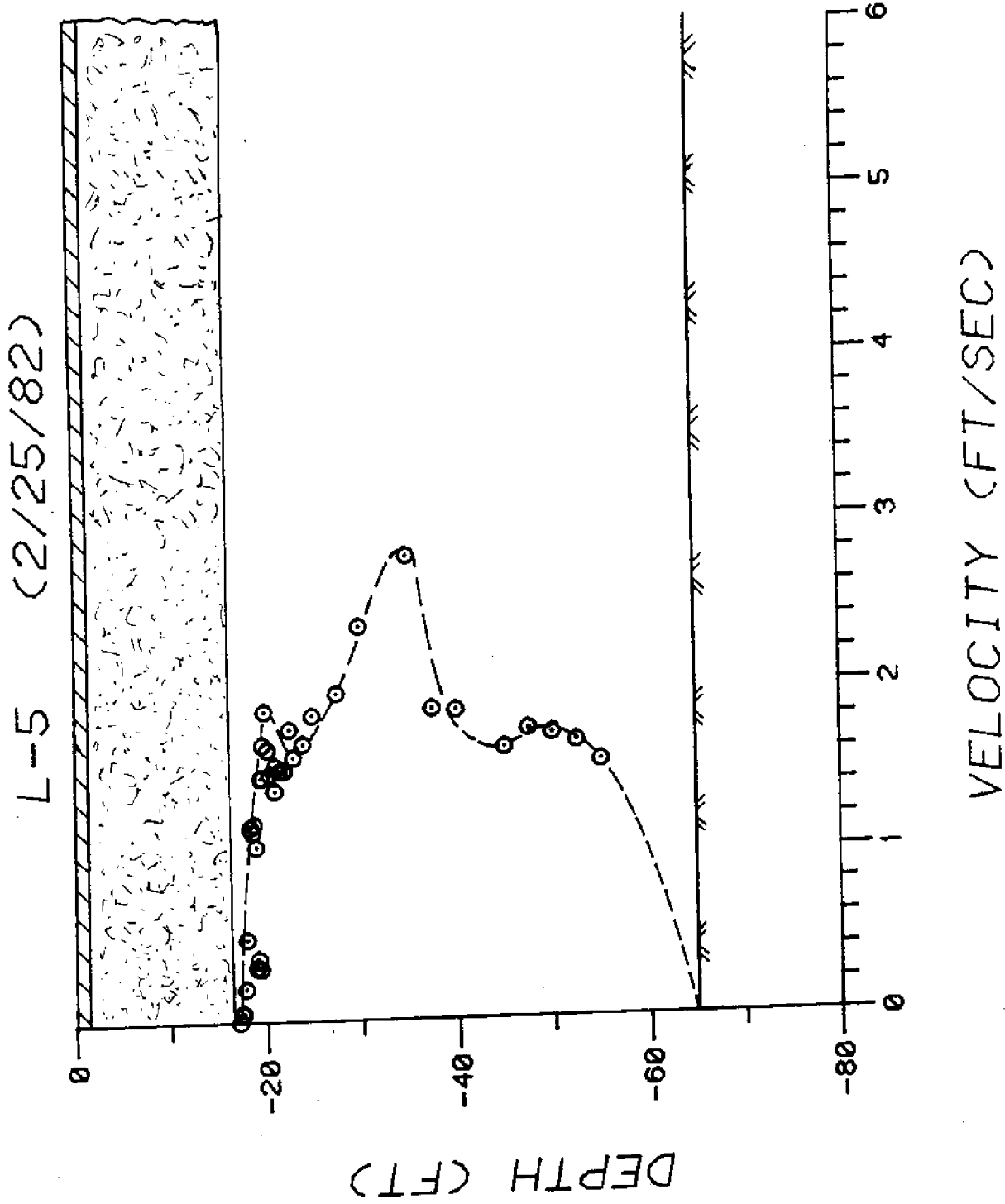
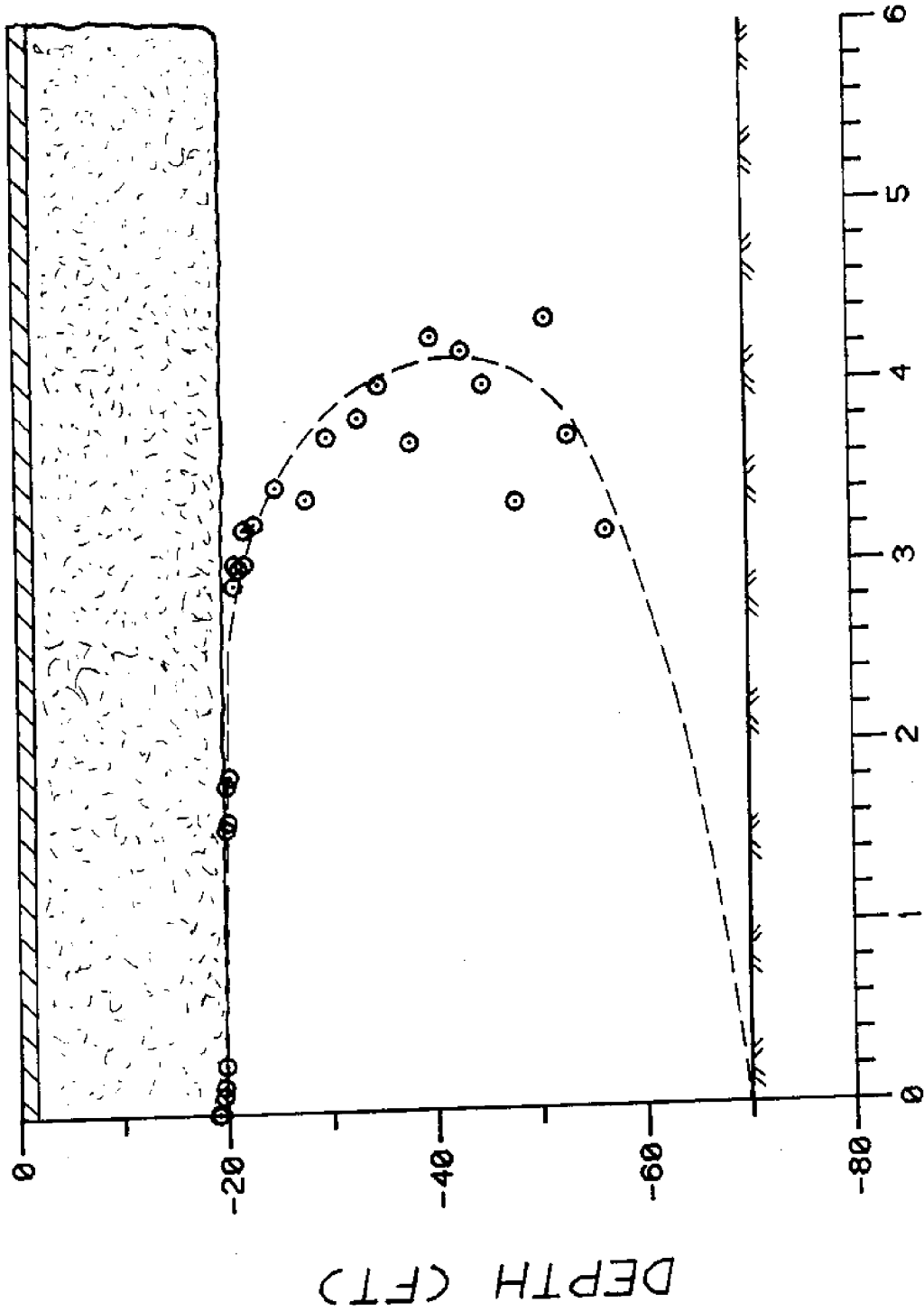


Figure 12. Velocity Profile at Station L-5; Feb. 25, 1982

L-7 (2/25/82)



VELOCITY (FT/SEC)

Figure 13. Velocity Profile at Station L-7; Feb. 25, 1982

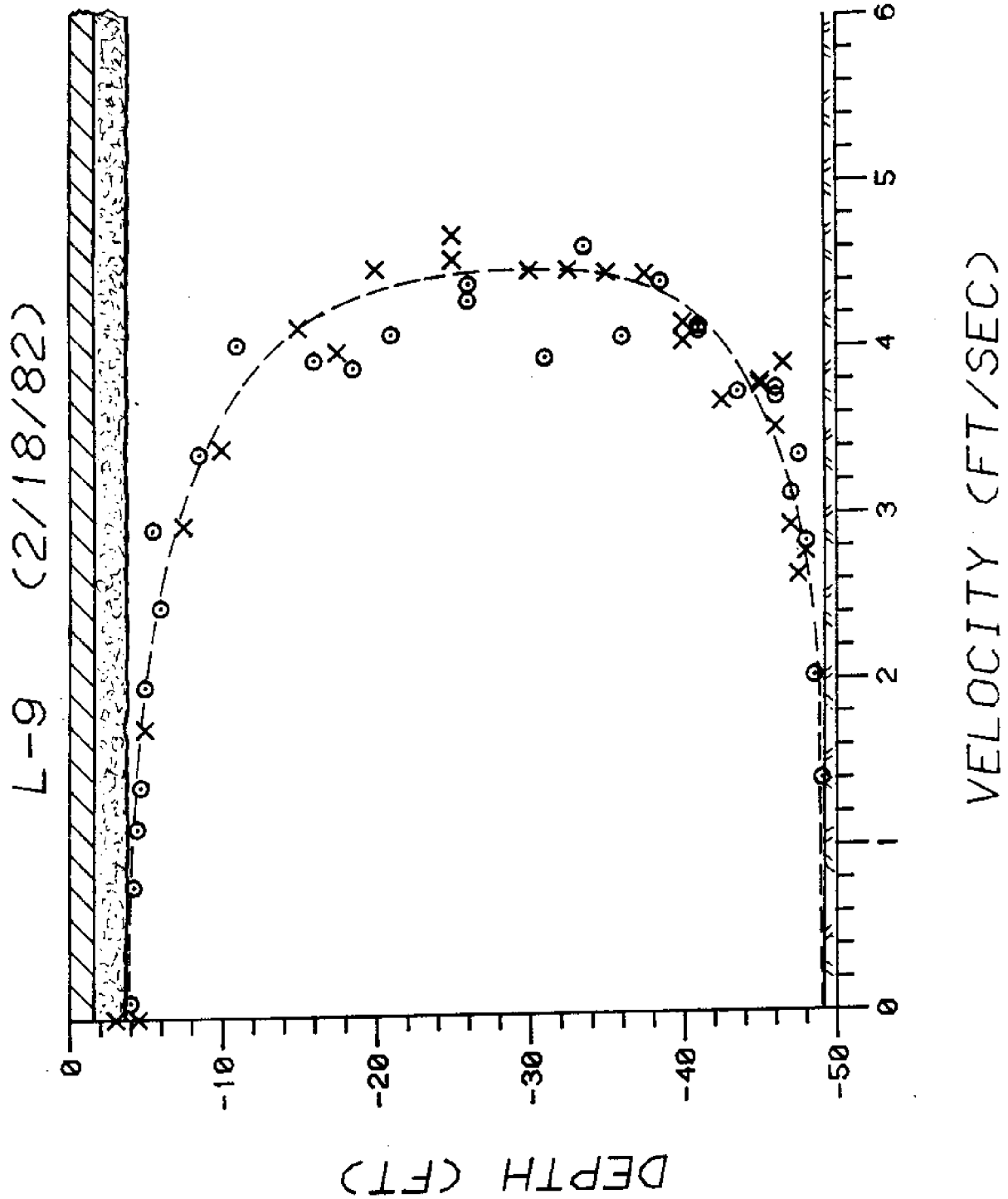


Figure 14. Velocity Profile at Station L-9; Feb. 18, 1982

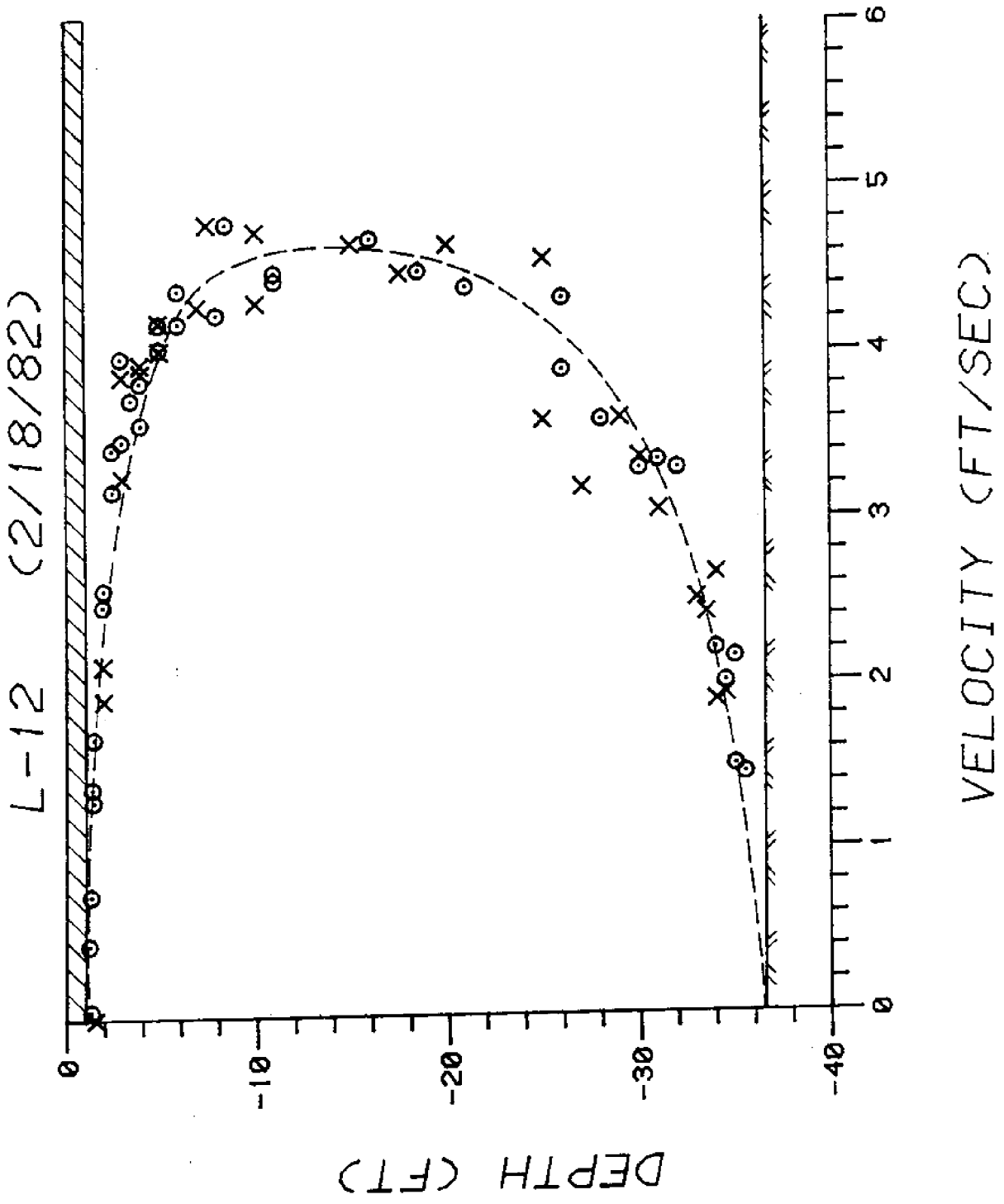


Figure 15. Velocity Profile at Station L-12; Feb. 18, 1982

the flow is distinctly three-dimensional.

Other Flow and Ice Condition Data

Since flow and ice cover conditions can provide useful information for interpreting the field survey results related to the hanging ice dam, additional data obtained by various agencies are presented in the Appendices. These data include: 1) water levels along the river and discharge at the Power Dam; 2) ice cover thickness measured near the Power Dam, Waddington, Pinetree Point, and Cardinal; and 3) ice cover condition maps.

Chapter III

ANALYSIS AND DISCUSSIONS

The importance of effects of hanging ice dams on winter flow conditions of a river have often been discussed in the literature on ice hydraulics. The present understanding on the formation process and hydraulic effect of hanging dams is, however, still rather qualitative. This is due partly to the complex nature of the evolution process, and partly to the difficulty involved in carrying out comprehensive field studies. In this chapter, the field data presented in Chapter II will be analyzed and interpreted.

Formation and Geometry of the Hanging Dam

In order to better interpret the field data, a brief description of the formation process of a typical fragment hanging ice dam will be given. This description is based on the understanding accumulated from previously reported analytical, laboratory, and field studies. Most of these studies are limited to idealized uniform rectangular channels. As winter begins, large quantities of ice floes will form in the river. These floes are carried downstream until they reach an artificial obstacle or form an ice bridge. With any additional supply of ice floes from upstream, the front of the ice cover will progress upstream against the river flow. In river reaches with low velocity, a relatively thin initial ice sheet can be formed and progress smoothly in the upstream direction. This upstream progression will be impeded when the leading edge of the cover enters a fast flowing reach where the Froude number exceeds a critical value (1,9,10,16,17, 27,29). At this time additional incoming ice floes will be

carried under the ice cover to form a hanging dam. The local thickening of an ice cover can also be induced by internal collapse of the ice cover when the total force acting on the cover exceeds its strength (16,17,28). During the build up of the hanging dam the surface slope of the river will change. This change will alter the Froude number upstream of the leading edge, the strength of the cover, and magnitude of forces acting on the cover. All of these changes could again allow the cover to progress in the upstream direction. The thickness of the hanging dam is limited by the available supply of ice floes, and the stability of the ice floes within the accumulation. This stability criteria may be expressed in terms of a critical Froude number, a critical velocity, or a critical shear stress (2,7,9, 10,14,25,29).

In the reach of the St. Lawrence River between Cardinal and Iroquois Dam, a hanging ice dam usually forms in the vicinity of Sparrowhawk Point. No effort has been made in the past to determine the location of the hanging dam. The only hanging dam location surveyed other than that reported in Chapter II is the hanging dam of the winter of 1978-79 (3). The location and typical cross sectional geometry of both the 1978-79 hanging dam and the 1981-82 hanging dam are presented in Fig. 16 along with major currents estimated from stream-tube analysis (22). The dam of 1978-79 was formed between Jan. 16, 1979 and Jan. 18, 1979 when the discharge was 219,000 cfs. The dam of 1981-82 was formed between Jan. 15, 1982 and Jan. 18, 1982 when the discharge was 210,000 cfs (18). The larger discharge in 1979 is believed to

have caused the hanging dam of that season to form approximately 3,000 ft downstream from the 1981-82 hanging dam. The leading edge of the ice covers of both winters are located approximately two thousand feet upstream from the mid-section of the hanging dams. The cross sectional profiles of the hanging dam also indicate that these hanging dams have irregular three-dimensional shapes. The shapes of these hanging dams are governed by the flow pattern upstream as well as in the region where the hanging dams are formed. A comparison of Fig. 16 with the channel bottom topography, shown in Fig. 17, indicates further that when a hanging dam is formed in a river reach which has nearly constant width and total river channel cross sectional area, the dam tends to form at a cross section where there exists a large variation in depth across the river's width. This phenomena can be explained by noticing that the transverse distribution of the depth-averaged velocity at a given cross section can be approximately described by Eq. 1.

$$\frac{V(z)}{U} = \left[\frac{d(z)}{D} \right]^{2/3} \quad (1)$$

in which, z = transverse distance from a bank; $V(z)$ = depth-averaged flow velocity at z ; $d(z)$ = depth of flow at z ; U = cross sectional average velocity, Q/A ; and D = average flow depth of the flow cross section. Eq. 1, which can be obtained from the Manning Equation by neglecting interfacial shear stresses (22), indicates that the local depth-averaged flow velocity increases with the local flow depth. Thus, at a cross section where a

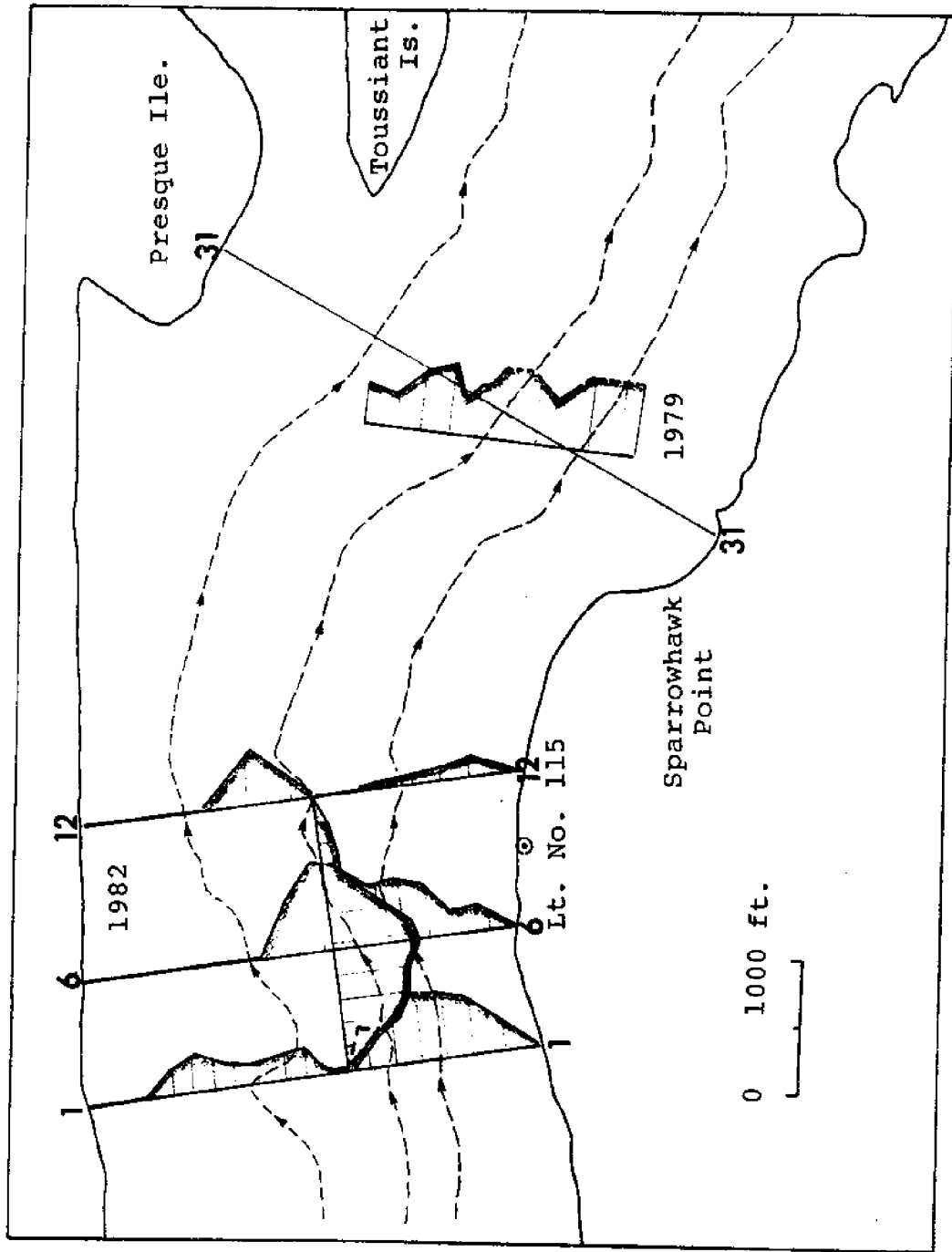


Figure 16. Flow Pattern and Hanging Dam Cross Sections Near Sparrowhawk Point

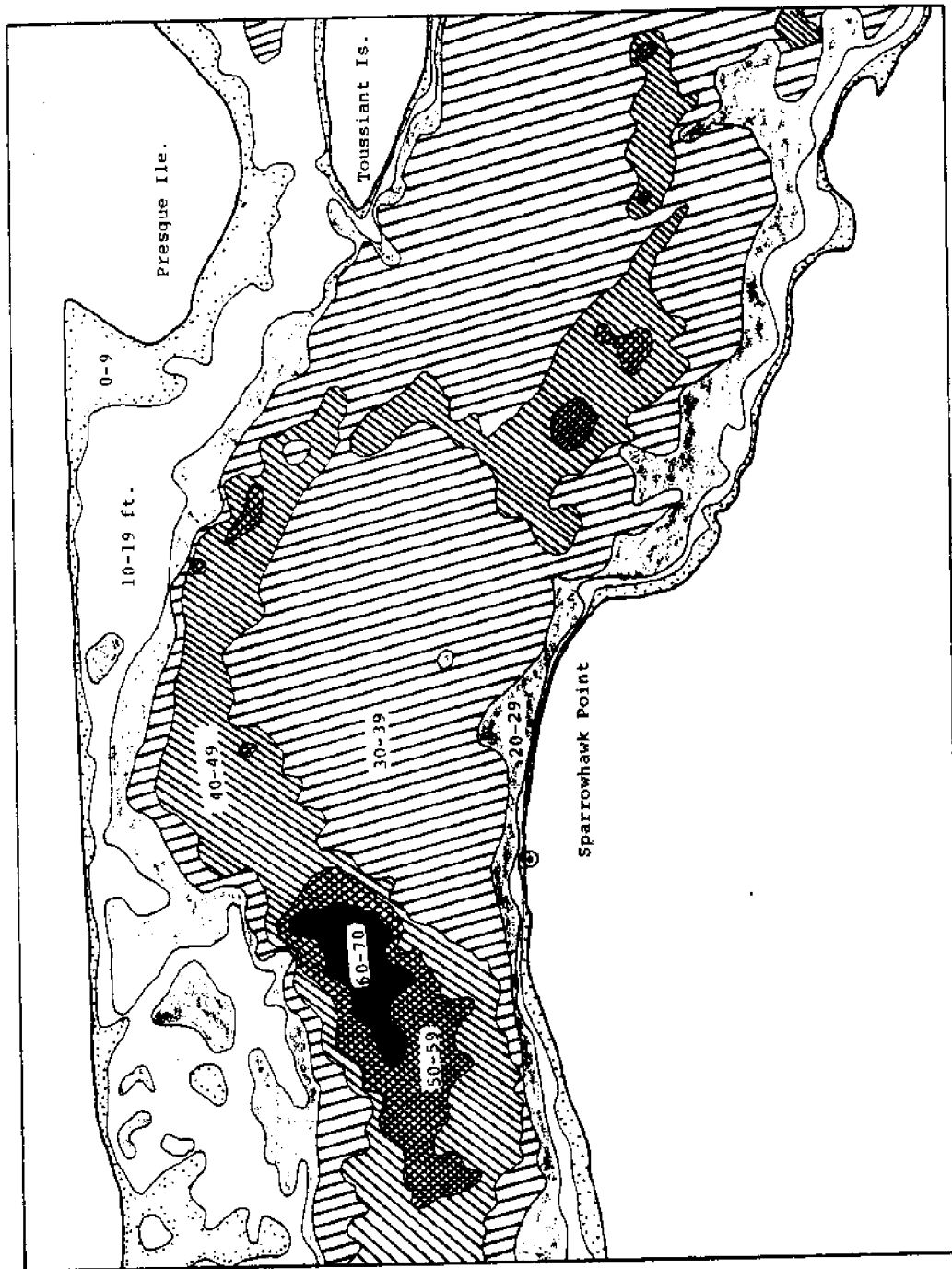


Figure 17. Channel Bottom Topography

large transverse variation in depth exists, there will usually be areas of high velocity which may cause the overturning of ice floes. The overturning of ice floes will prevent further progression of the ice cover until the formation of a hanging dam changes the flow condition.

In order to obtain quantitative estimates of the critical Froude number for leading edge progression and the critical velocity of ice deposition, depth-averaged velocity distributions at all four cross sections shown in Fig. 16 are determined for both the free surface condition and the condition with hanging dams. Flow distributions for free surface conditions at times of ice cover initiation are presented in Appendix A. These figures indicate that the critical Froude number for the progression of the leading edge of the ice cover is approximately equal to 0.06 for the 1978-79 ice cover and is 0.052 for the 1981-82 ice cover. Flow distributions at channel cross sections underneath the hanging dam are presented in Appendix A. To determine the critical velocity of deposition from these figures the criteria used are: a) at each cross section, only the velocity at the location where the ice thickness is a maximum will be considered; b) when the hanging dam was decaying, the velocity distribution was not used to determine critical velocities; c) during cold periods, active frazil ice produced in the upstream open water area may remain active when the ice particles reach the upstream end of the hanging dam. The attachment of active frazil ice particles to the existing hanging dam is not then limited by the critical velocity of deposition. Based on these considerations, velocity

distributions presented in Appendix A are examined along with the air temperature data given in Fig. 18. The depth-averaged velocity distributions underneath the maximum thickness of the ice cover at each cross section are summarized in Table 2. Based on this information it is estimated that the critical velocity of deposition for inactive frazil ice particles is approximately equal to 3 fps, which is in agreement with the observation of Michel and Drouin (13) in the La Grande River.

Hydraulic Resistance of the Hanging Dam

The hydraulic resistance of a hanging ice dam can have an important effect on the flow conditions in an ice covered river. Data presented in Chapter II will be used to obtain some quantitative information on the hydraulic resistance of the hanging dam.

Local roughness coefficients - The local roughness of the undersurface of the ice cover and the channel bottom are calculated from information obtained from the measured velocity profiles. These roughnesses, expressed in terms of Manning's coefficient, are determined using the information developed by Larsen (11). As summarized in Table 3, ice surface roughness coefficients at the upstream side of the dam are lower than those at the downstream side. The average ice cover roughness coefficient is 0.03, which is slightly lower than the value reported by Beltaos and Dean (5) for a Smoky River hanging dam. The average value of bed roughness coefficients at the hanging dam site is 0.047, which is much higher than the gross bed roughness coefficient value of 0.026 for the reach between

Table 2. Depth-Averaged Velocity Underneath
the Maximum Ice Thickness

Cross Section	Date	Velocity	Remarks
Line 1	Feb. 11, 1982	3.7 fps	Accumulation of active frazil
Line 6	Feb. 3, 1982	3.1 fps*	Cold weather.
	Feb. 9, 1982	2.9 fps*	Hanging dam size increased from Feb. 3, 1982.
	Feb. 16, 1982	2.3 fps	Hanging dam size decreased slightly from Feb. 9, 1982.
	Feb. 23, 1982	2.3 fps	Hanging dam size decreased from Feb. 16, 1982.
	Mar. 2, 1982	~3.0 fps*	Very cold weather. Dam size increased. Measured dam cross section was not complete.
	Mar. 12-19, 1982		Dam size decreased continuously.
Line 2	Feb. 11, 1982	3.0 fps*	Very cold weather.

*Estimated critical velocity for the deposition of inactive frazil ice particles.

Table 3. Local Roughness Coefficients Calculated from Measured Velocity Profiles

Station No.	Date	n_i	n_b
L1	Feb. 24, 82	0.028	0.048
L3	Feb. 24, 82	0.026	0.055
L7	Feb. 25, 82	0.022	0.057
L9	Feb. 18, 82	0.037	0.029
L12	Feb. 18, 82	0.036	0.047

Cardinal and the Iroquois Dam reported by Potok (19).

Roughness coefficient of the ice cover - The gross Manning roughness coefficients of the ice cover in the reach between Cardinal and Iroquois Dam, n_i^{CI} , are calculated for the entire winter using the scheme developed by Shen and Ruggles (24). Water levels at Cardinal and Iroquois headwater, and the discharge at the Iroquois Dam are used in the calculation. Gross Manning's coefficients of the ice cover between upstream and downstream ends of the hanging dam, n_i^D , are also determined from the measured water surface slopes given in Table 1. The Manning Equation and Belokon-Sabaneev (15) formula are used in the calculation.

$$Q = \frac{1.49}{n} A R^{2/3} s_f^{1/2} \quad (2)$$

$$n_i^D = n_b \left[2 \left(\frac{n}{n_b} \right)^{3/2} - 1 \right]^{2/3} \quad (3)$$

Both n_i^{CI} and n_i^D are computed using $n_b = 0.026$ and the channel geometries given by Potok (19), as shown in Table 4. The calculated gross roughness coefficients of the ice cover are presented in Fig. 18 along with the discharge at the Iroquois Dam and the air temperature at Massena.

As shown in Figs. 4 and 6 the size of the hanging dam varies with time even though the general shape of the hanging dam changes very little before the break up period. It is, therefore, reasonable to assume that the form loss of the hanging dam remains nearly constant. The variation in the gross hydraulic

resistance of the hanging dam will be mainly due to the variation in surface roughness of the dam. Fig. 18 shows that the resistance coefficient of the ice cover at the hanging dam section, n_i^D , remains relatively constant during a major portion of the winter. The range of the variation of the magnitude of n_i^D is about the same as that of n_i^{CI} . A comparison between n_i^D and the air temperature also indicates that the variation in n_i^D is affected by the air temperature. This appears to be reasonable since the air temperature governs the production of frazil in the open water area upstream and hence influence the surface roughness of the ice cover.

Table 4. Cross-Sectional Geometry at the Reference Water Level (19)

Parameter	Cardinal	Iroquois H.W.
Reference Water Level	240.80 ft.	239.90 ft.
Width	2620 ft.	2620 ft.
Wetted Perimeter	2690.916 ft.	2683.1298 ft.
Cross Sectional Area	92900 sq. ft.	82700 sq. ft.

*Water surface levels are measured from the International Great Lakes Datum (1955).

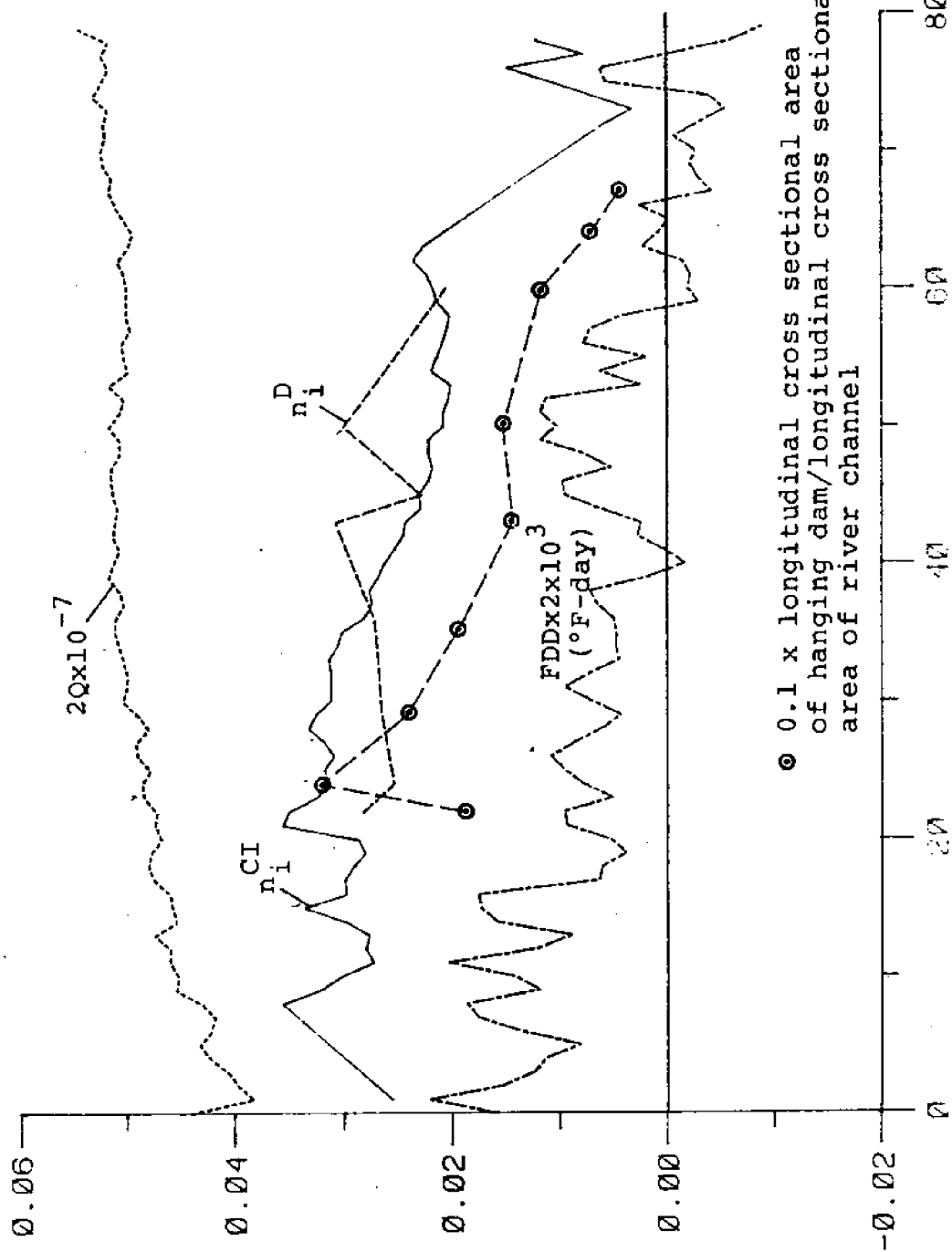


Figure 18. Manning's Coefficients. Air Temperature (FDD) at Massena, Discharge (Q) at the Power Dam Site, Winter of 1981-82

Chapter IV

SUMMARY AND CONCLUSIONS

In this report, results are presented and analyzed of a field survey on a large hanging ice dam in the St. Lawrence River near Sparrowhawk Point during the winter of 1981-82. The major conclusions obtained are: a) the channel bottom topography may be used to provide a convenient guide for determining the location where a hanging dam will form beneath the ice cover in the study reach; b) the shape of a hanging dam is affected by the pattern of currents immediately upstream; c) the critical Froude number for the progression of the ice cover and the critical velocity of deposit of ice particles underneath the dam in the reach between Cardinal and Iroquois Dam are approximately 0.06 and 3 fps, respectively; d) the ice surface roughness at the upstream side of the hanging dam is smaller than that of the downstream side; e) the gross roughness coefficient of the hanging dam remains relatively constant during the winter even though it is slightly affected by the air temperature. These conclusions provide useful insights to the formation process and resistance characteristics of hanging dams in the Upper St. Lawrence River. The information obtained will lead to the further development of simulation models for the dynamics of ice cover formation and its hydraulic effects in the Upper St. Lawrence River. It would be desirable to conduct additional field surveys of hanging ice dams in subsequent winters in order to substantiate and extend these conclusions.

REFERENCES

1. Ashton, G.D., "Froude Criterion for Ice-Block Stability," Journal of Glaciology, Vol. 13, No. 68, 1974, pp. 307-313.
2. Ashton, G.D., "Stability of Ice Blocks Beneath a Cover," Technical Note, U.S. Army Cold Regions Research and Engineering Laboratory, Hanover, N.H., June 1974, 21 pp.
3. Batson, G.B., Shen, H.T., Ackermann, N.L., Candee, K.I., and Landry, S.J., "Investigation of Flow and Ice Conditions, Sparrowhawk Point to Murphy Island, St. Lawrence River, Winter 1978-79," Report No. DOT-SL-79-552, U.S. Department of Transportation, Washington, D.C., July 1979.
4. Batson, G.B., Ackermann, N.L., Shen, H.T., Candee, K.I., "Survey of Flow and Ice Conditions in the Ogden Island Reach, St. Lawrence River, Winter of 1977-78," Report No. DOT-SL-78-519, U.S. Department of Transportation, Washington, D.C., June 1978.
5. Beltaos, S., and Dean, A.M., Jr., "Field Investigation of a Hanging Dam," Proceedings, IAHR International Symposium on Ice, Vol. II, Quebec City, Canada, July 1981, pp. 475-488.
6. Gold, L.W., and William, G.P., "An Unusual Ice Formation on the Ottawa River," Journal of Glaciology, Vol. 4, pp. 569-573.
7. Hausser, R., and Galina, G., "Transportation and Deposit of Frazil Ice," Proceedings, 8th Congress of the International Assoc. of Hydraulic Research, Montreal, Canada, Aug. 1959, pp. 6-SI-1 ~ 6-SI-6.
8. Hopper, H.R., and Raban, R.R., "Hanging Dams in the Manitoba Hydro System," Proceedings of Workshop on Hydraulic Resistance of River Ice, National Water Research Institute, CCIW, Burlington, Canada, Sept. 1980, pp. 195-208.
9. Kivisild, H.R., "Hanging Ice Dams," Proceedings, 8th Congress of the International Assoc. of Hydraulic Research, Montreal, Canada, Aug. 1959, pp. 1-SI-1 ~ 1-SI-3.
10. Kivisild, H.R., "Hydrodynamical Analysis of Ice Floods," Proceedings, 8th Congress of the International Assoc. of Hydraulic Research, Montreal, Canada, Aug. 1959, pp. 23-F-1 ~ 23-F-30.
11. Larsen, P.A., "Head Losses Caused by an Ice Cover on Open Channels," Journal of the Boston Society of Civil Engineers, Vol. 56, No. 1, Jan. 1969, pp. 45-67.

12. Maytin, I.L, and Henderson, P.B., "Hydrological Data Acquisition and the Instrumentation Gap," Journal of the American Water Resources Assoc., Vol. 6, No. 2, Apr. 1970.
13. Michel, B., and Drouin, M., "Equilibrium of an Underhanging Dam at the LaGrande River," Report GCS-75-03-01, Department of Civil Engineering, Université Laval, Quebec City, Canada, 1975.
14. Michel, B., "Ice Accumulations at Freeze-Up or Break-Up," Proceedings, 4th International Symposium on Ice Problems, Lulea, Sweden, 1978, pp. 301-317.
15. Nezhikhovskiy, R.A., "Coefficients of Roughness of Bottom Surface of Slush Ice Cover," Soviet Hydrology: Selected Papers, No. 2, 1964, pp. 127-126.
16. Pariset, E., and Hausser, R., "Formation and Evolution of Ice Covers in Rivers," Transactions of the Engineering Institute of Canada, Vol. 5, No. 1, 1961, pp. 41-49.
17. Pariset, E., Hausser, R., and Gagnon, A., "Formation of Ice Covers and Ice Dams in Rivers," Journal of the Hydraulics Division, ASCE, Vol. 92, No. HY6, Nov. 1966, pp. 1-24.
18. PASNY/Ontario Hydro, "St. Lawrence Power Project Report on Winter Operation, 1981 to 1982," June 1982, 12 pp.
19. Potok, A.J., "Upper St. Lawrence River Hydraulic Transient Model," NOAA Tech. Memorandum ERL GLERL-25, Ann Arbor, Michigan, Oct. 1978, 96 pp.
20. Shen, H.T., and Ackermann, N.L., "Wintertime Flow Distribution in River Channels," Journal of the Hydraulics Division, ASCE, Vol. 106, No. HY5, May 1980.
21. Shen, H.T., Ackermann, N.L., Landry, S.J., "Formation of Hanging Ice Dam," Proceedings, Symposium on Surface-Water Impoundments, ASCE/AGU/AWRA, Minneapolis, Sept. 1980.
22. Shen, H.T., and Ackermann, N.L., "Wintertime Flow and Ice Conditions in the Upper St. Lawrence River," Proceedings, IAHR International Symposium on Ice, Quebec City, Canada, July 1981.
23. Shen, H.T., and Yapa, P.N.D.D., "Winter Flow, Ice, and Weather Conditions of the Upper St. Lawrence River, 1971-81, Vol. II," Technical Report 82-3, Department of Civil and Environmental Engineering, Clarkson College of Technology, July 1982.

24. Shen, H.T., and Ruggles, R.W., "Analysis of River Ice Cover Roughness," Proceedings, 1982 ASCE Hydraulics Division Specialty Conference, Jackson, Mississippi, Aug. 1982.
25. Tatinclaux, J.C., and Gogus, M., "Stability of Floes Below a Floating Cover," Proceedings, IAHR International Symposium on Ice, Vol. I, July 1981, pp. 298-308.
26. Tesaker, E., "Accumulation of Frazil Ice in an Intake Reservoir," Proceeding, Third International Symposium on Ice Problems, Hanover, N.H., 1975, pp. 25-35.
27. Uzuner, M.S., and Kennedy, J.F., "Stability of Floating Ice Blocks," Journal of the Hydraulics Division, ASCE, Vol. 98, No. HY12, Dec. 1972, pp. 2117-2133.
28. Uzuner, M.S., and Kennedy, J.F., "A Theoretical Model of River Ice Jams," Journal of the Hydraulics Division, ASCE, Vol. 102, No. HY9, Sept. 1976, pp. 1365-1383.
29. Uzuner, M.S., "Stability Analysis of Floating and Submerged Ice Floes," Journal of the Hydraulics Division, ASCE, Vol. 103, No. HY7, July 1977, pp. 713-722.
30. White, F.M., Viscous Fluid Flow, McGraw-Hill, Inc., N.Y., 1974, 725 pp.
31. Wigle, T.E., Bartholomew, J.L., and Lawrie, C.J.R., "Winter Operations International Rapids Section of the St. Lawrence River," Proceedings, IAHR International Symposium on Ice, Vol. I, Quebec City, July 1981, pp. 193-210.

APPENDIX A
Flow Distributions and Hanging Dam Profiles

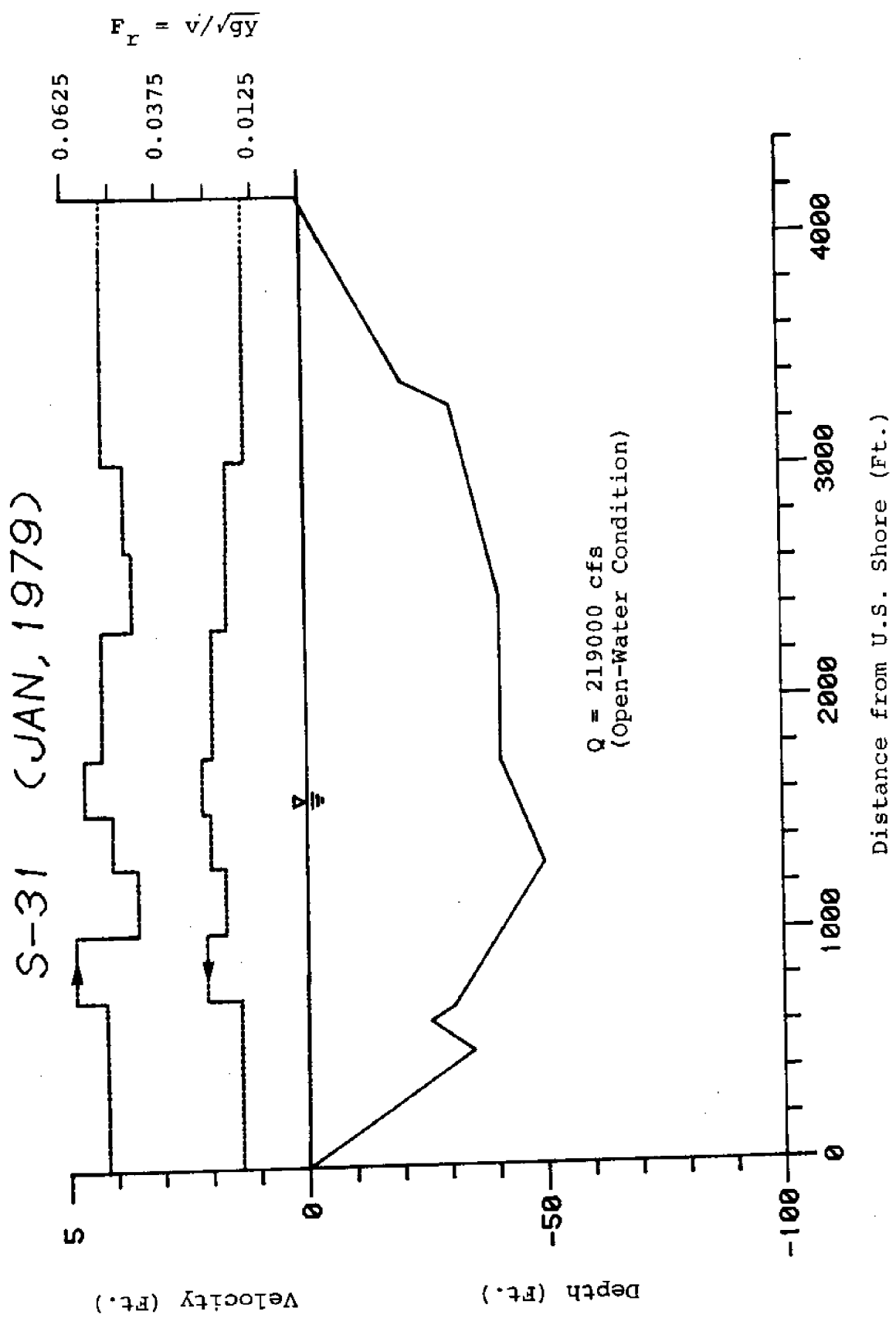


Figure A1. Velocity and Froude Number Distributions at Cross Section 31-31, Jan. 1979

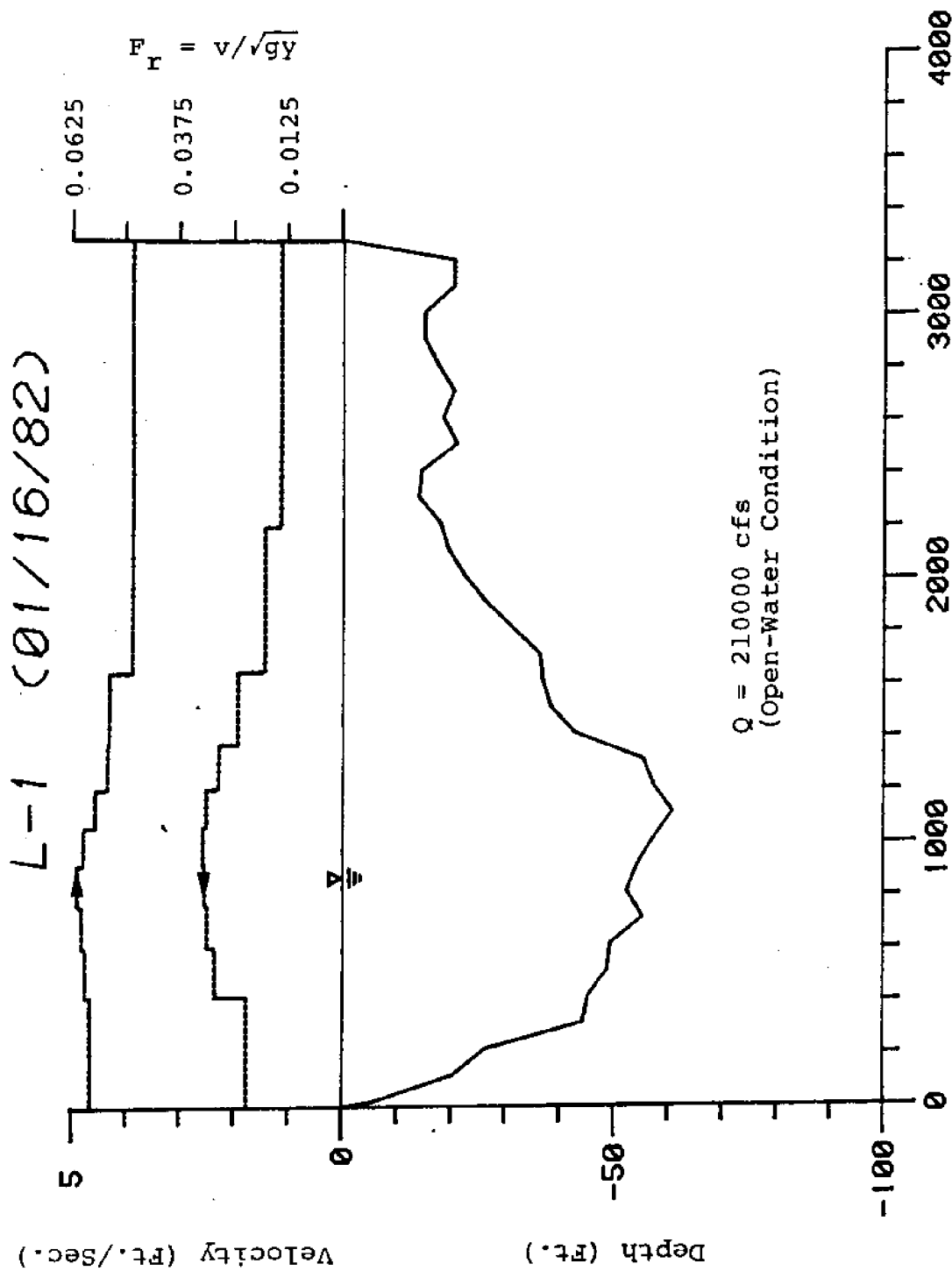


Figure A2. Velocity and Froude Number Distribution at Cross Section 1-1; Jan. 16, 1982

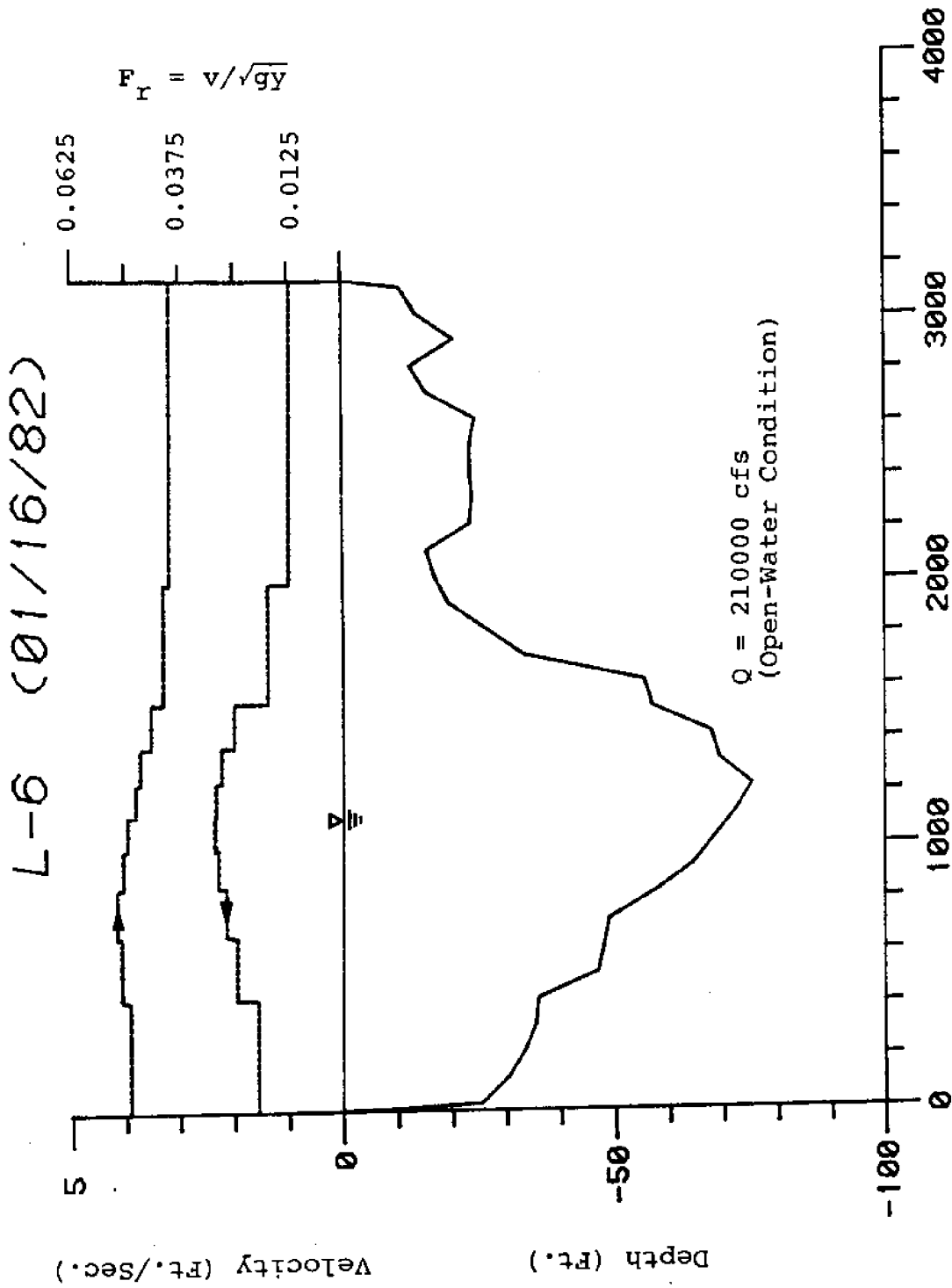


Figure A3. Velocity and Froude Number Distribution at Cross Section 6-6; Jan. 16, 1982

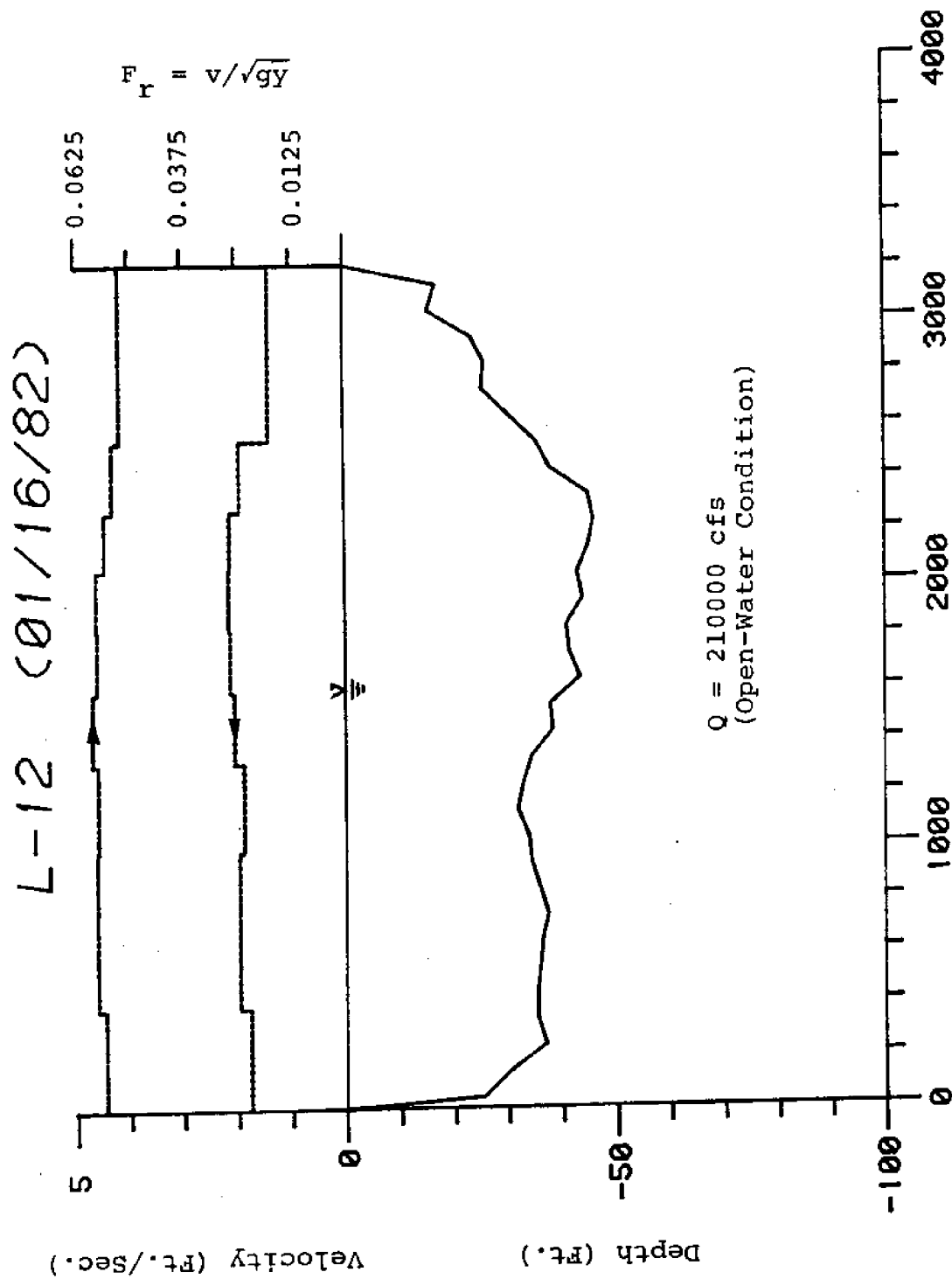


Figure A4. Velocity and Froude Number Distribution at Cross Section 12-12; Jan. 16, 1982

L-1 (FEB 11, 1982)

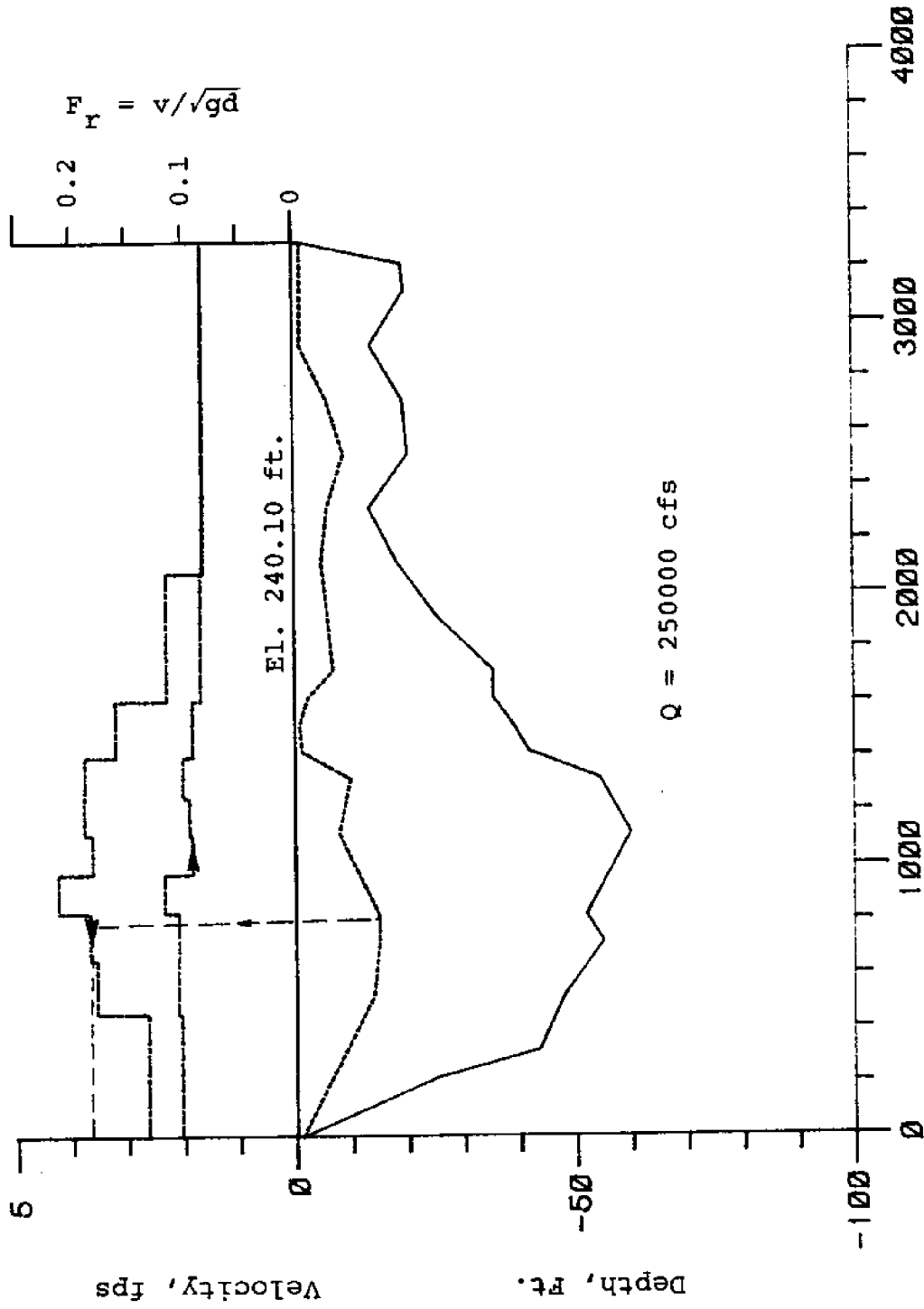


Figure A5. Velocity and Froude Number Distributions at Cross Section L-1; Feb. 11, 1982

L-6 (FEB 3, 1982)

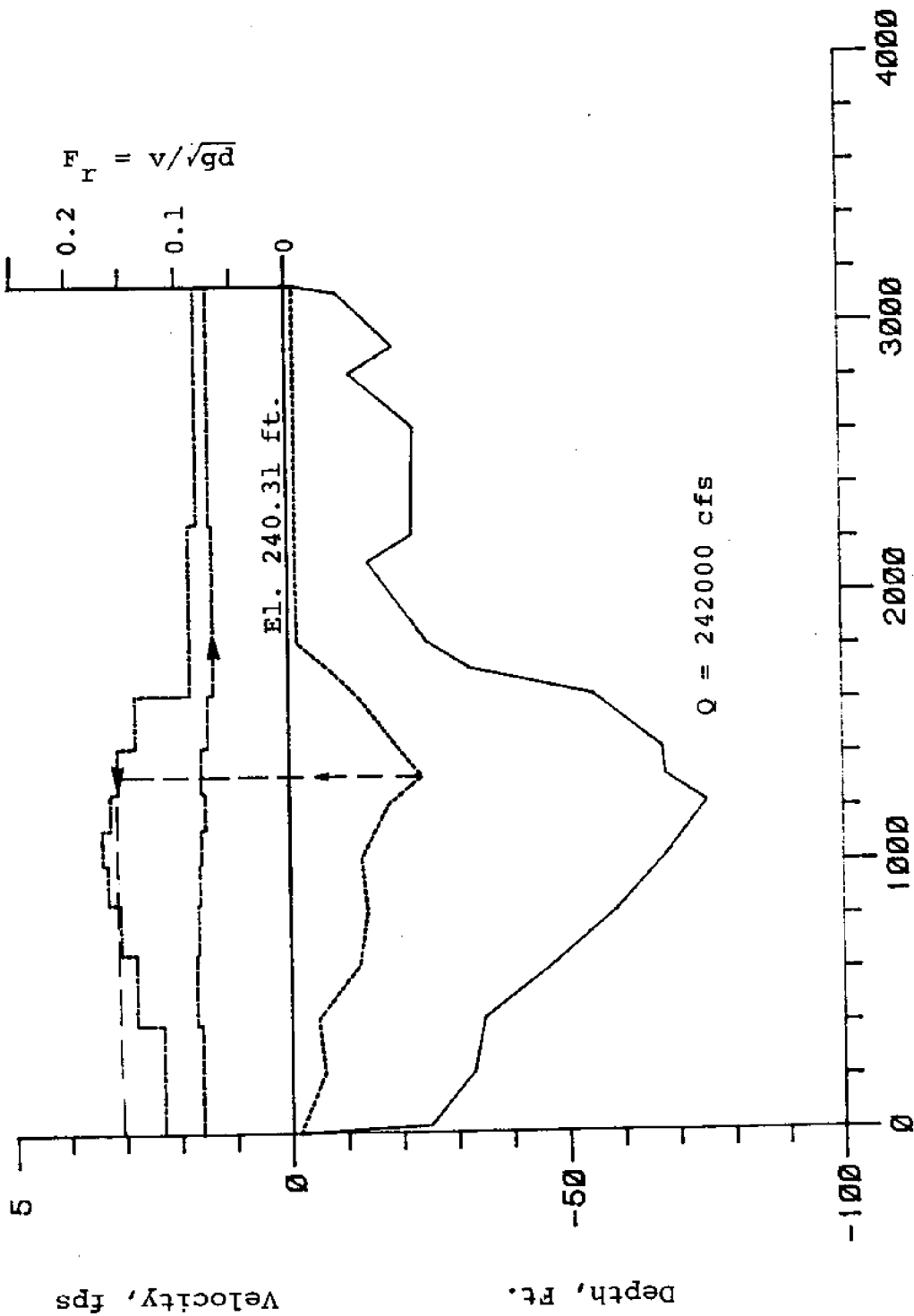


Figure A6. Velocity and Froude Number Distribution at Cross Section 6-6; Feb. 3, 1982

L-6 (FEB 9, 1982)

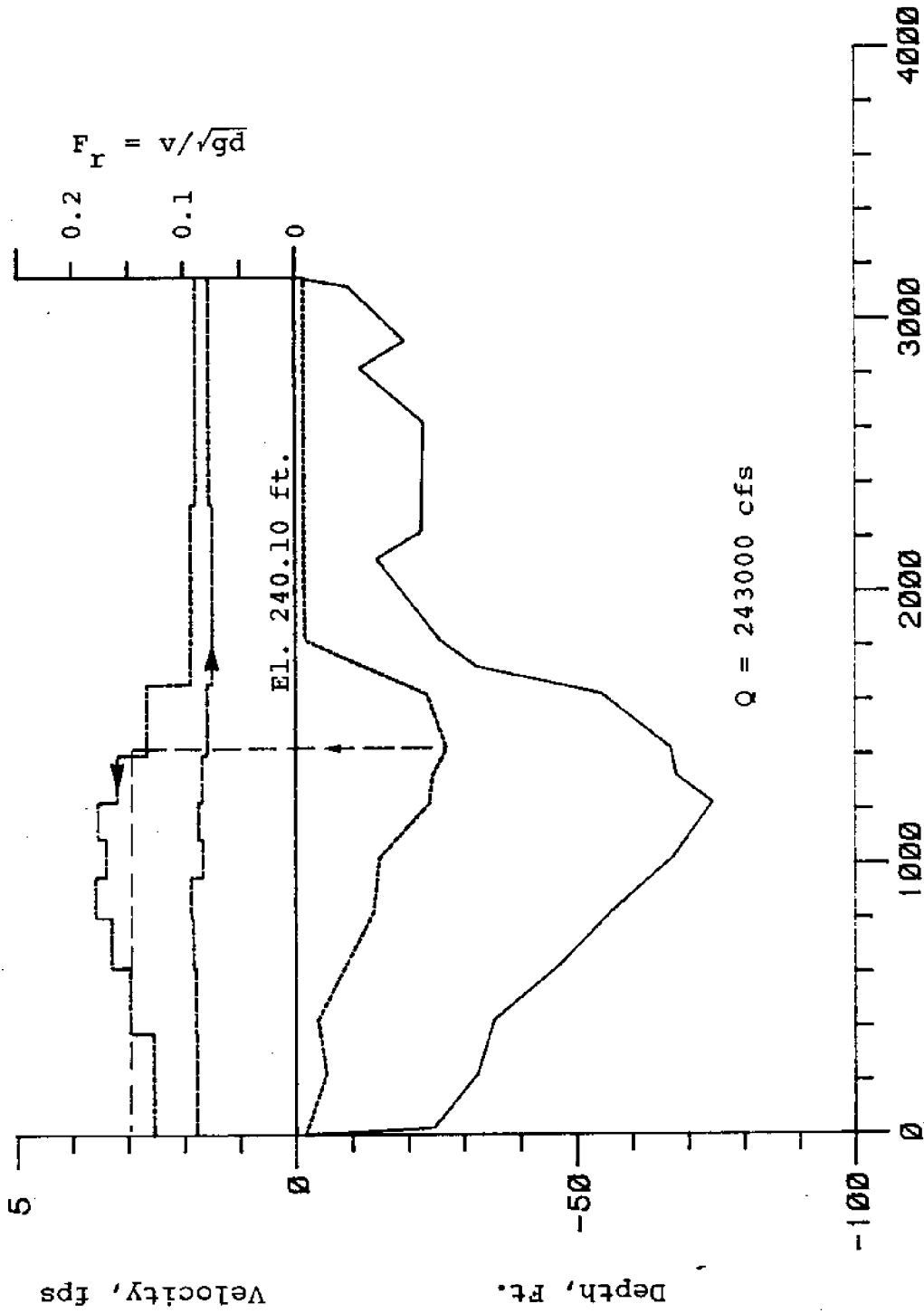
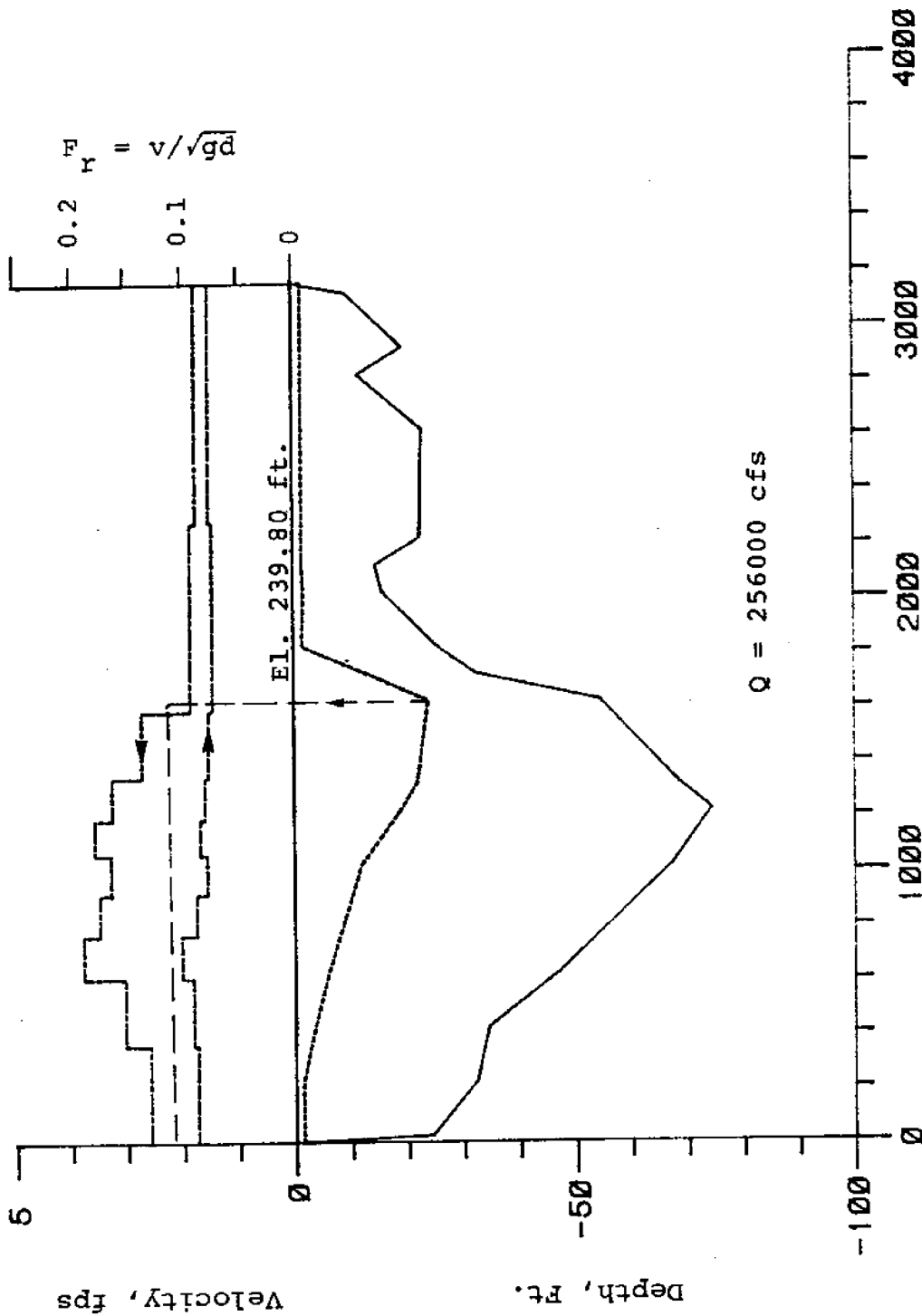


Figure A7. Velocity and Froude Number Distributions at Cross Section 6-6; Feb. 9, 1982

L-6 (FEB 16, 1982)



Distance from U.S. Shore (Ft.)

Figure A8. Velocity and Froude Number Distributions at Cross Section 6-6; Feb. 16, 1982

L-6 (FEB 23, 1982)

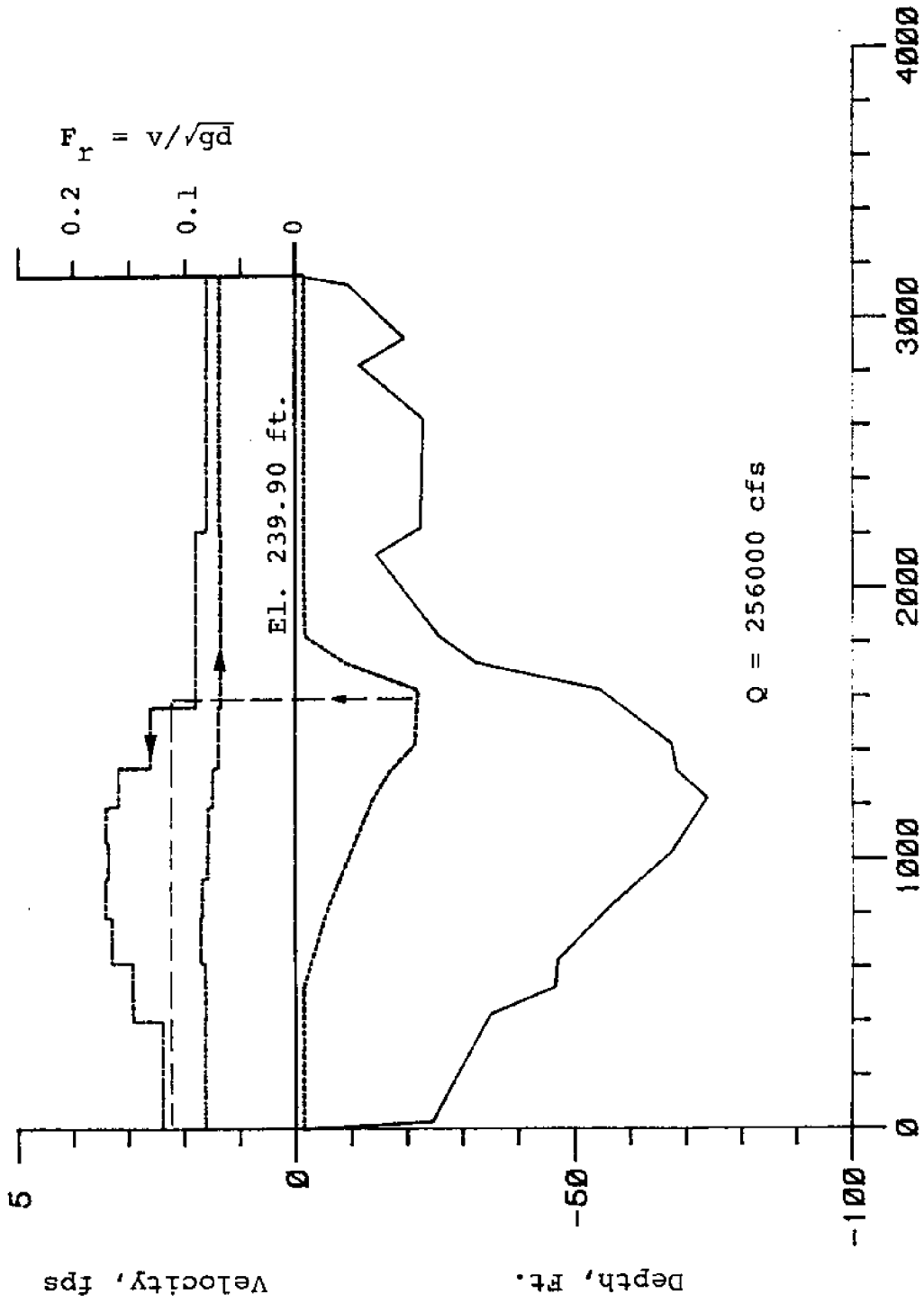


Figure A9. Velocity and Froude Number Distributions at Cross Section 6-6; Feb. 23, 1982

L-6 (MARCH 2, 1982)

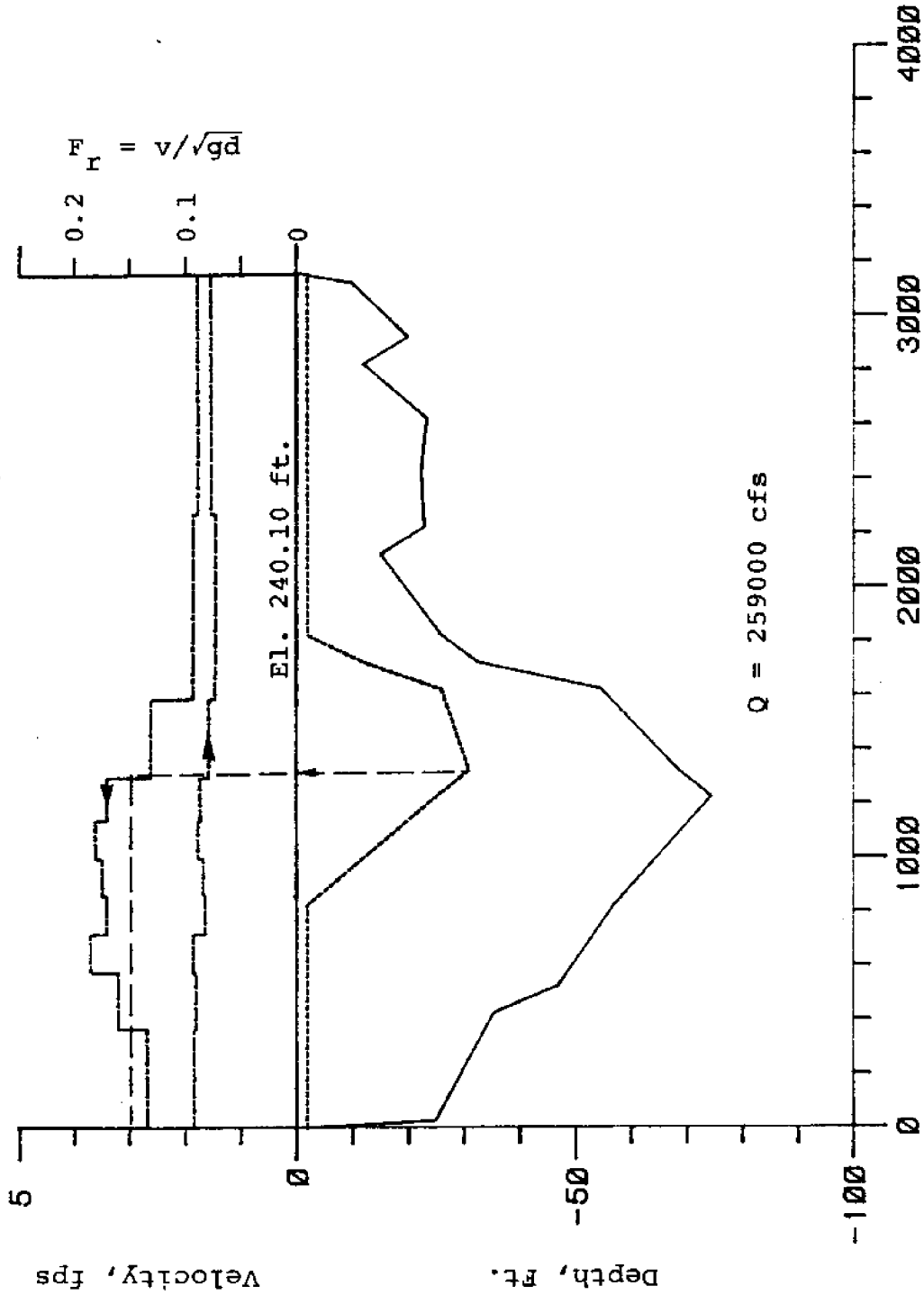


Figure A10. Velocity and Froude Number Distributions at Cross Section 6-6; Mar. 2, 1982

L-6 (MARCH 12, 1982)

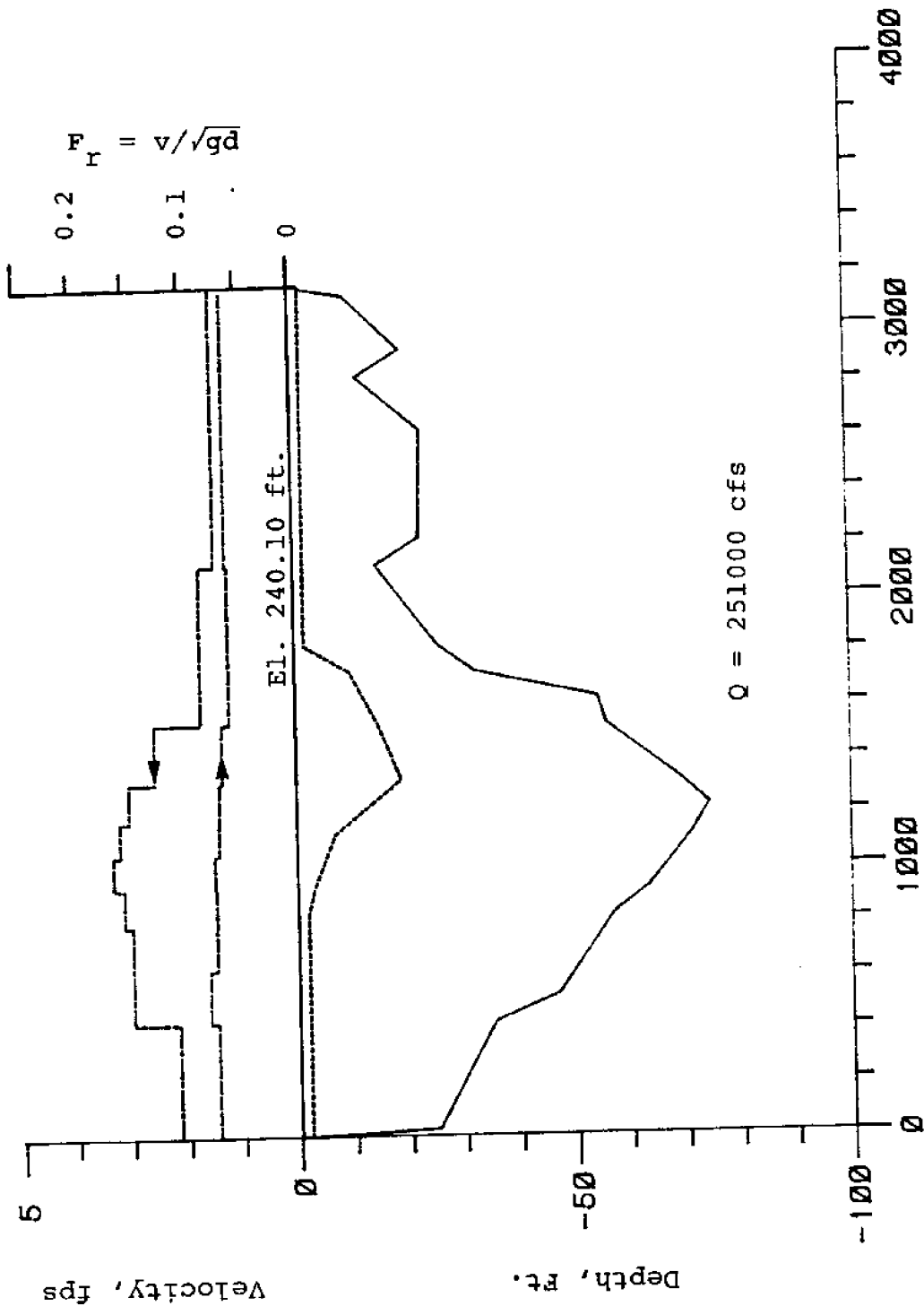


Figure All. Velocity and Froude Number Distributions at Cross Section 6-6; Mar. 12, 1982

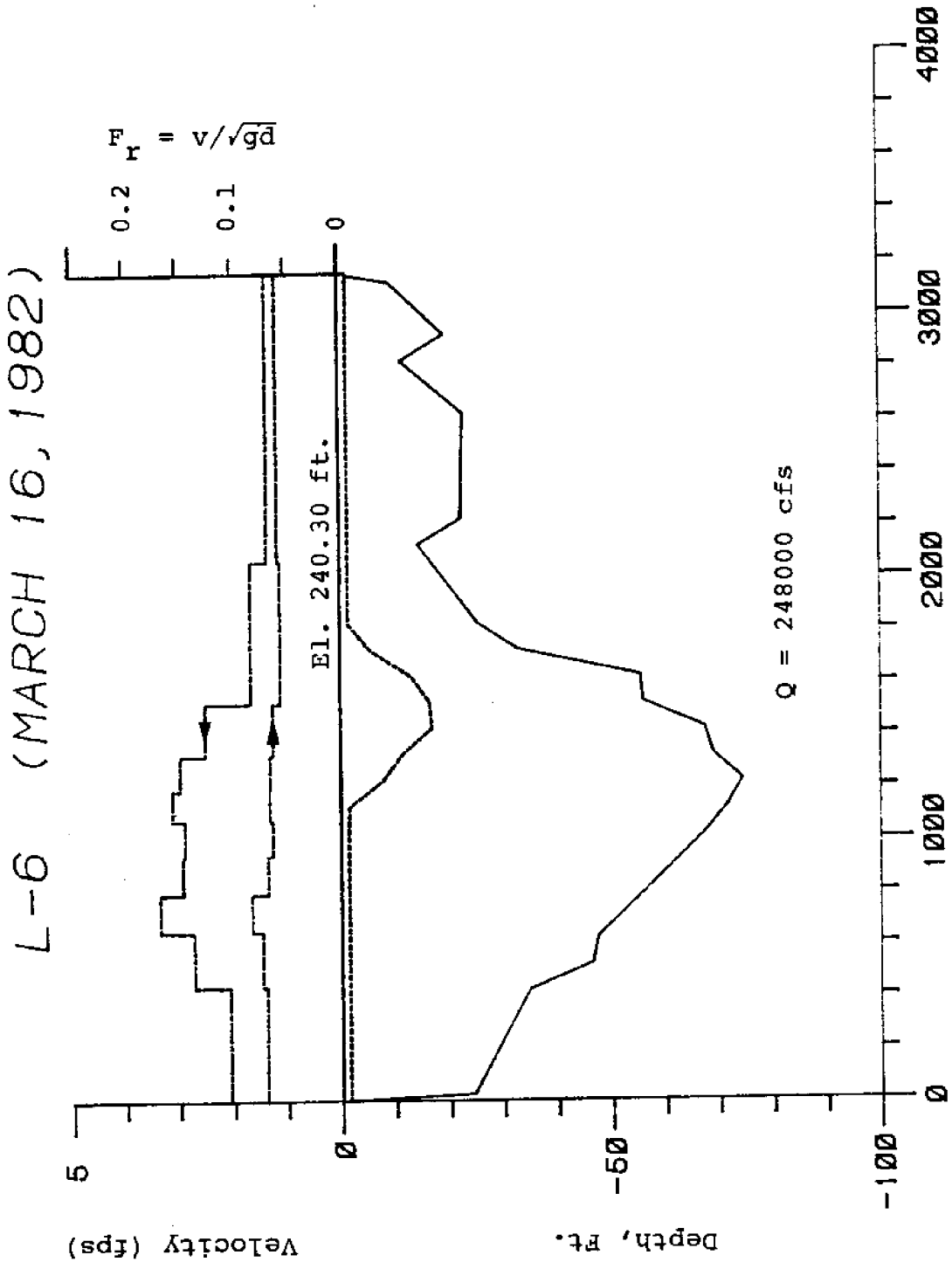


Figure A12. Velocity and Froude Number Distributions at Cross Section 6-6; Mar. 16, 1982

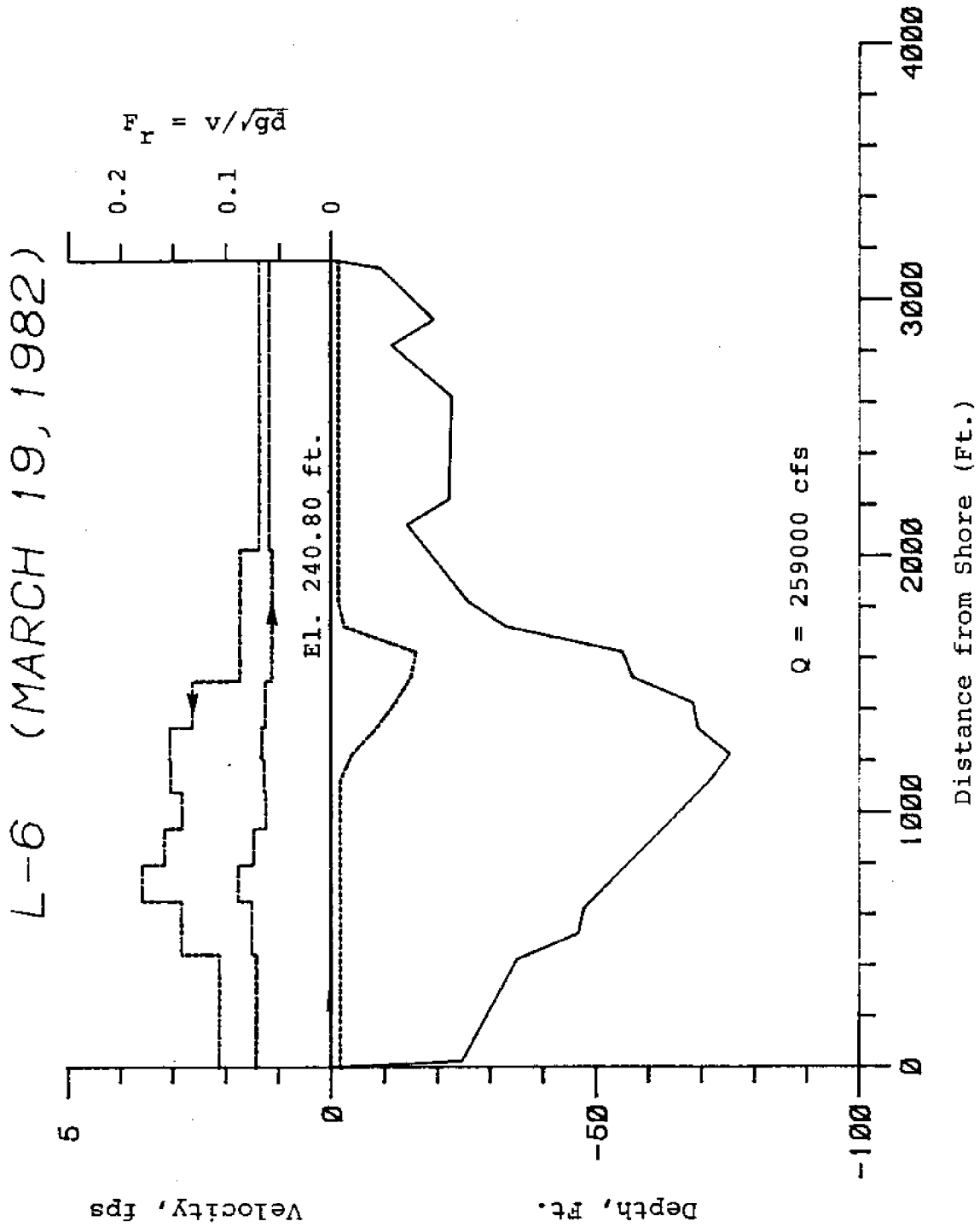


Figure A13. Velocity and Froude Number Distributions at Cross Section 6-6; Mar. 19, 1982

L-12 (FEB 11 & 16, 1982)

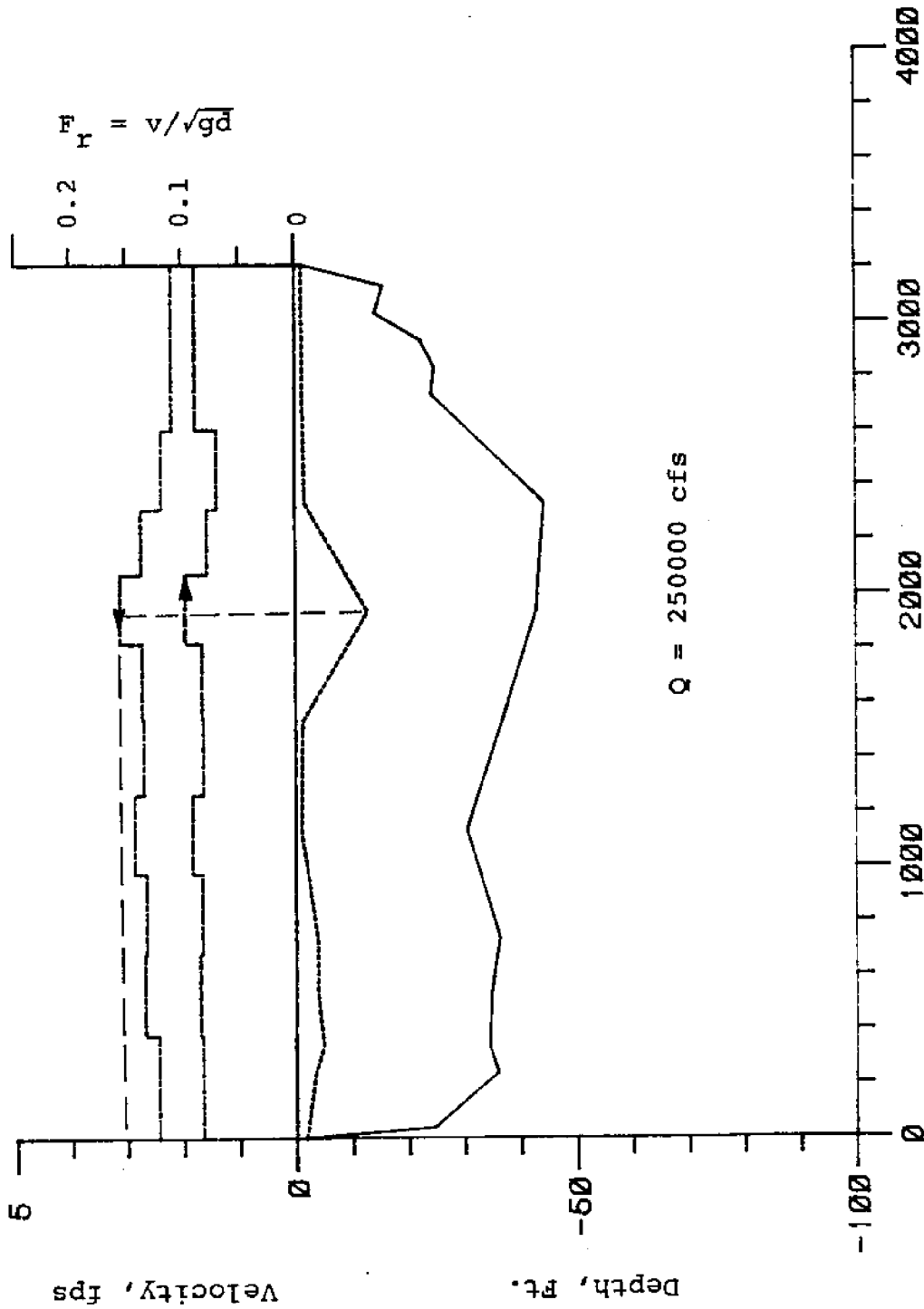
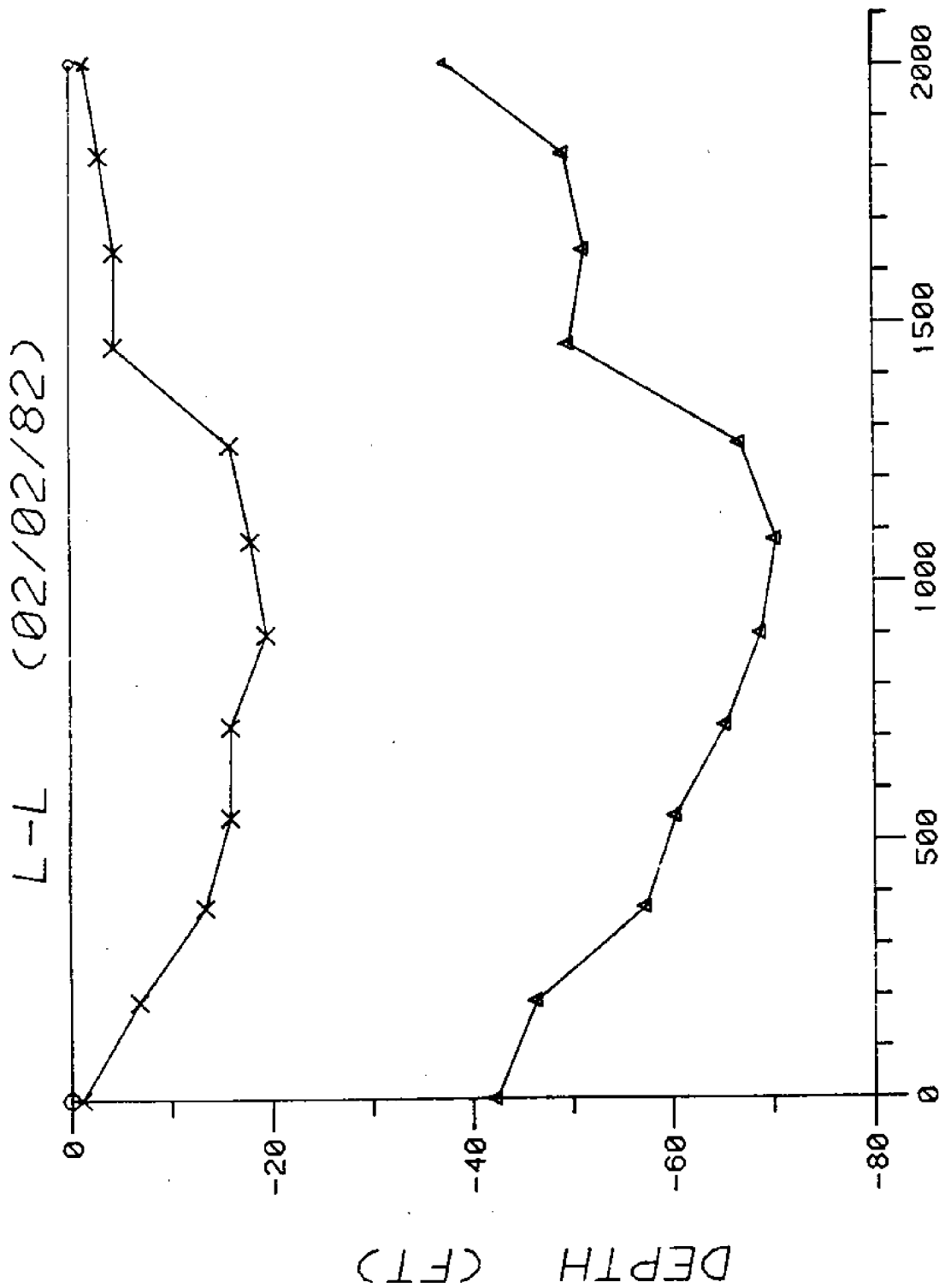


Figure A14. Velocity and Froude Number Distributions at Cross Section L-12; Feb. 11, 1982



DIST. FROM L-1 (FT)

Figure A15. Longitudinal Hanging Dam Profile Along Line L-L;
Feb. 2, 1982

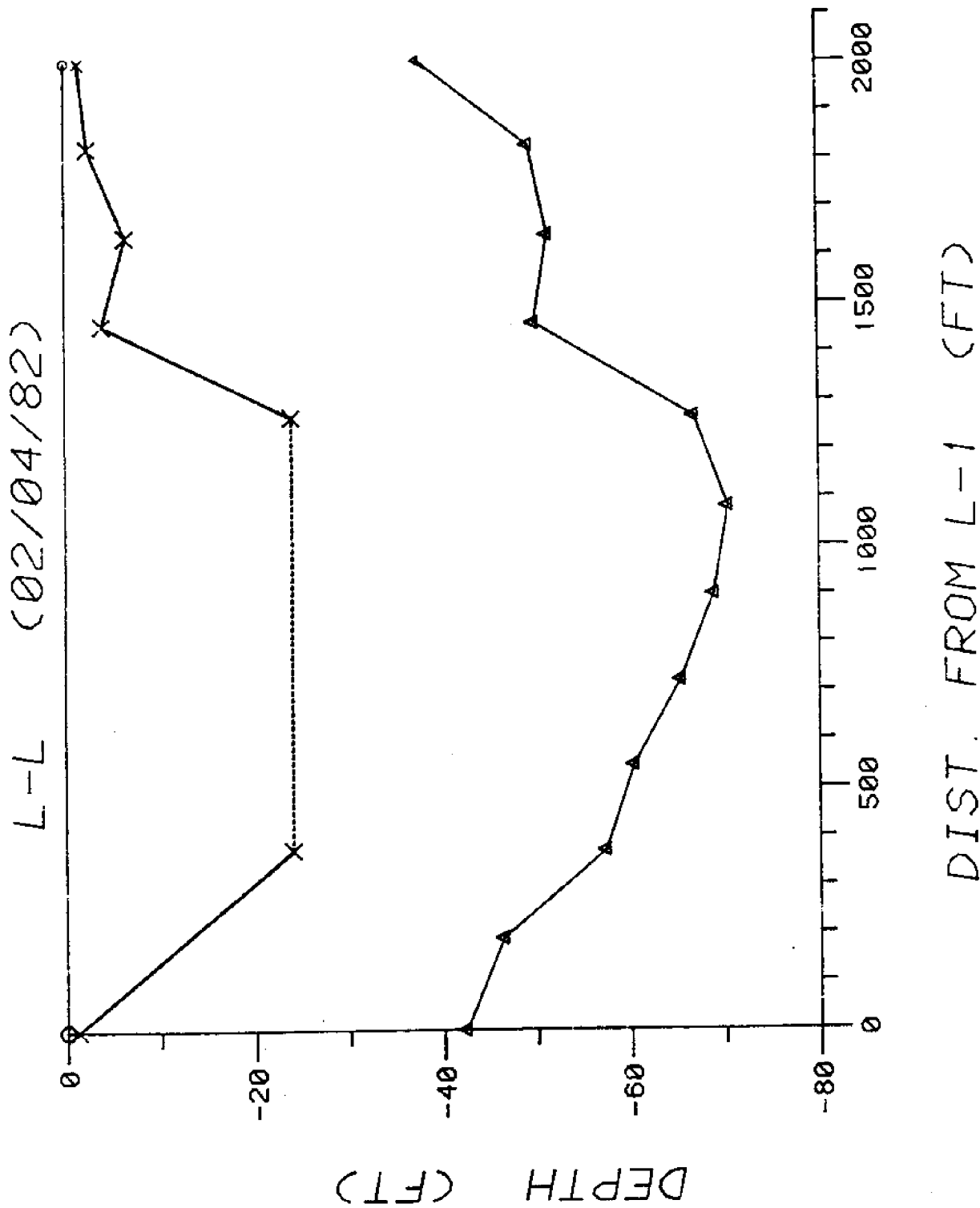
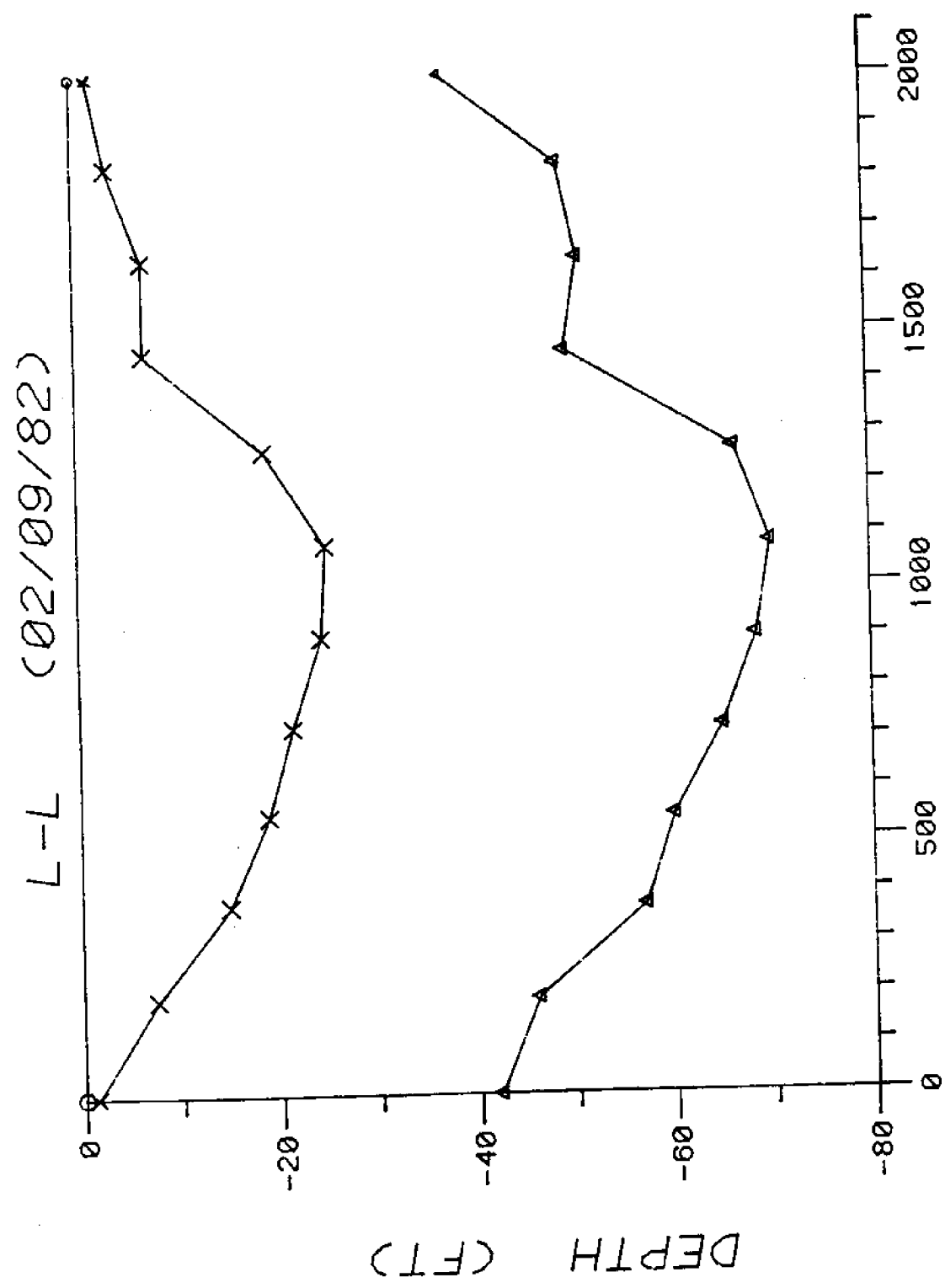
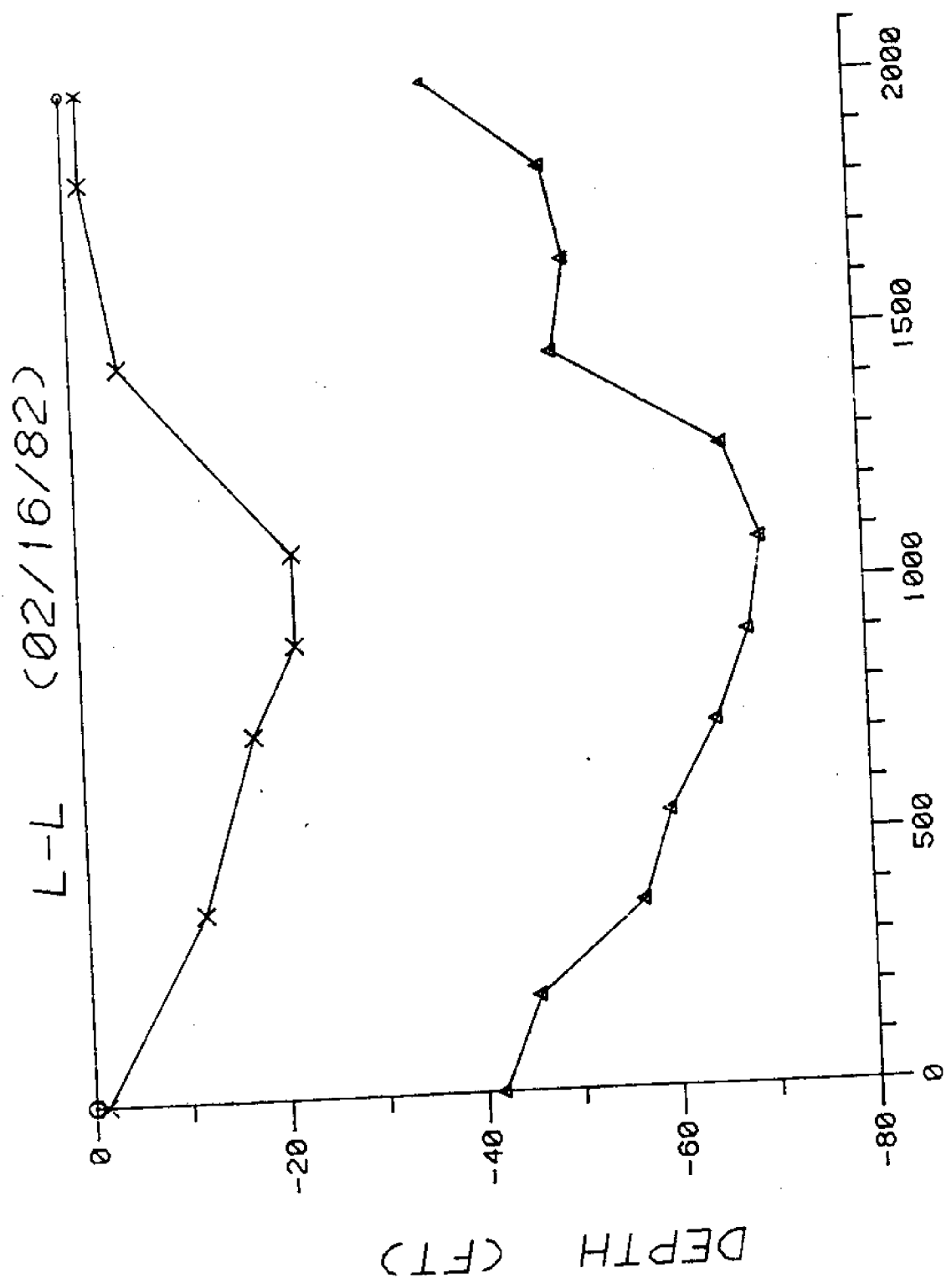


Figure A16. Longitudinal Hanging Dam Profile Along Line L-L;
Feb. 4, 1982



DIST. FROM L-1 (FT)

Figure A17. Longitudinal Hanging Dam Profile Along Line L-L; Feb. 9, 1982



DIST: FROM L-1 (FT)

Figure A18. Longitudinal Hanging Dam Profile Along Line L-L; Feb. 16, 1982

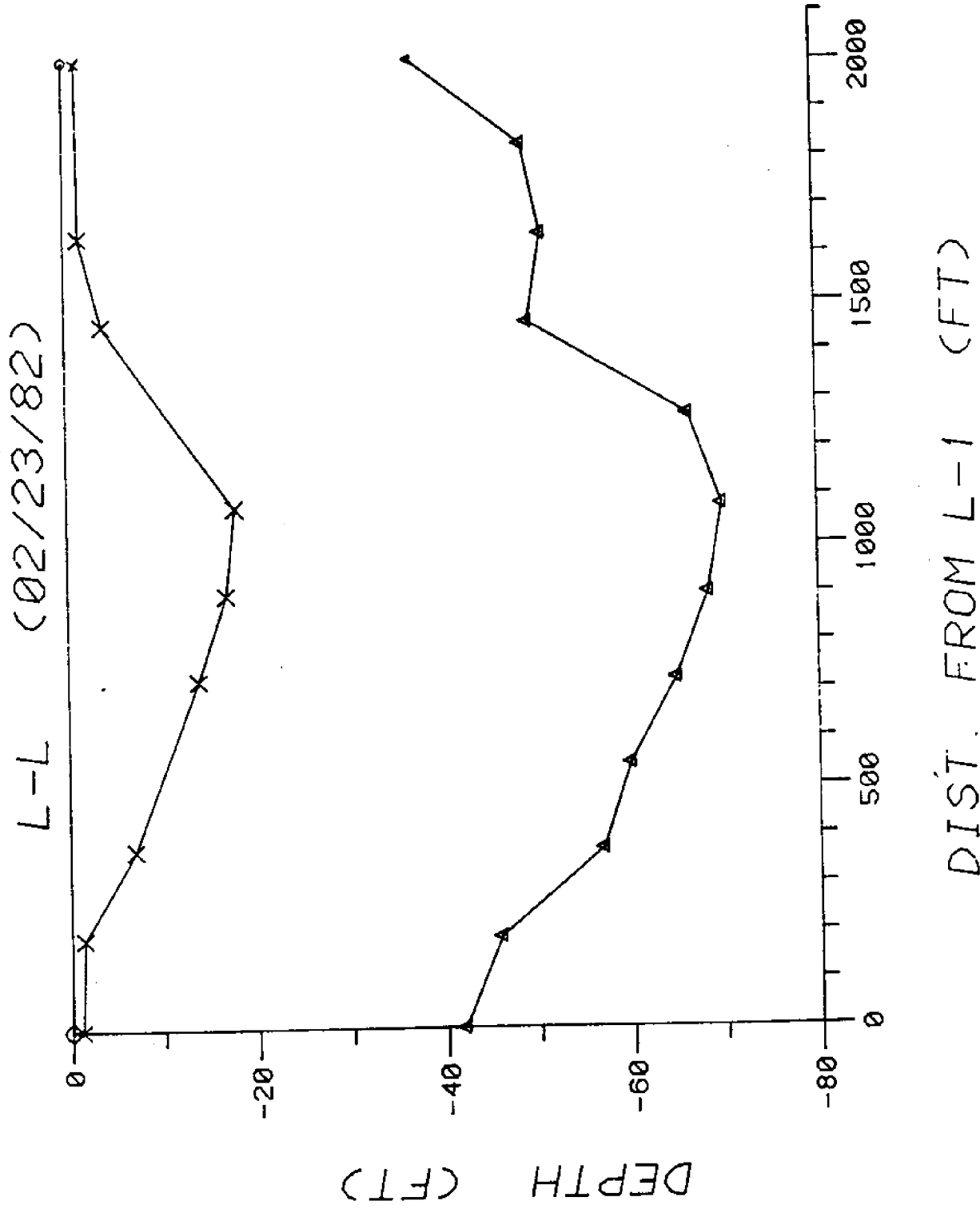


Figure A19. Longitudinal Hanging Dam Profile Along Line L-L; Feb. 23, 1982

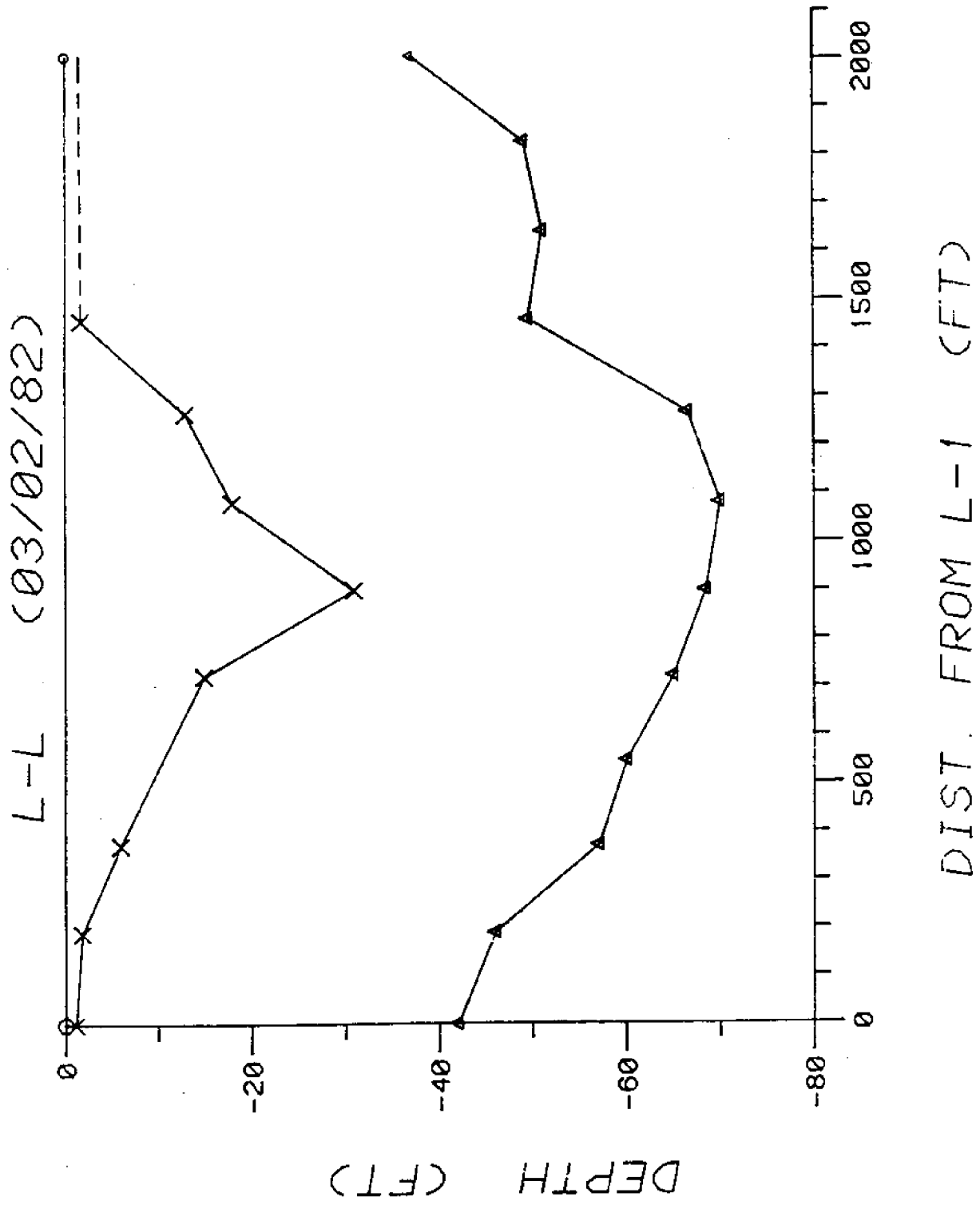


Figure A20. Longitudinal Hanging Dam Profile Along Line L-L; Mar. 2, 1982

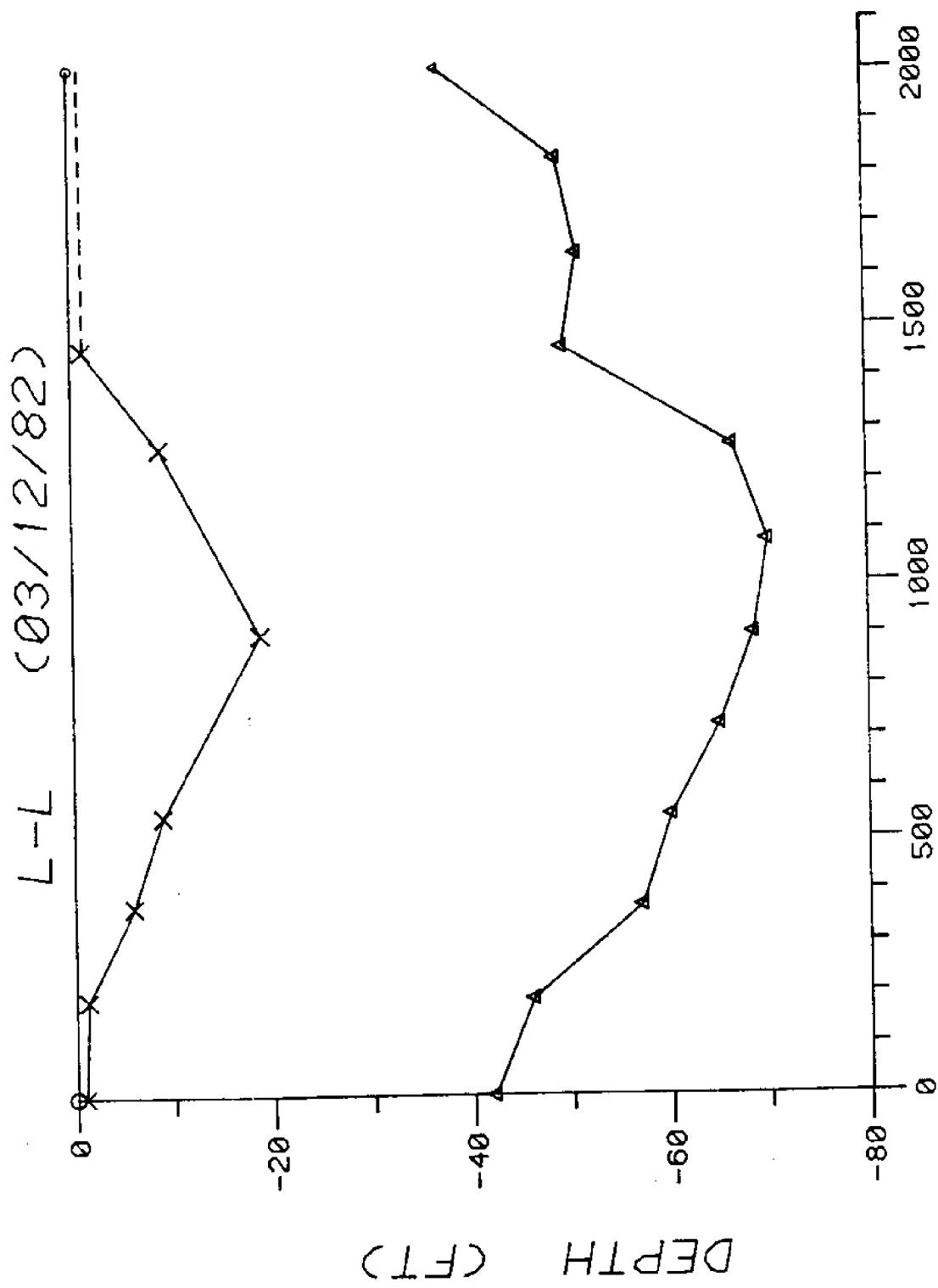


Figure A21. Longitudinal Hanging Dam Profile Along Line L-L; Mar. 12, 1982

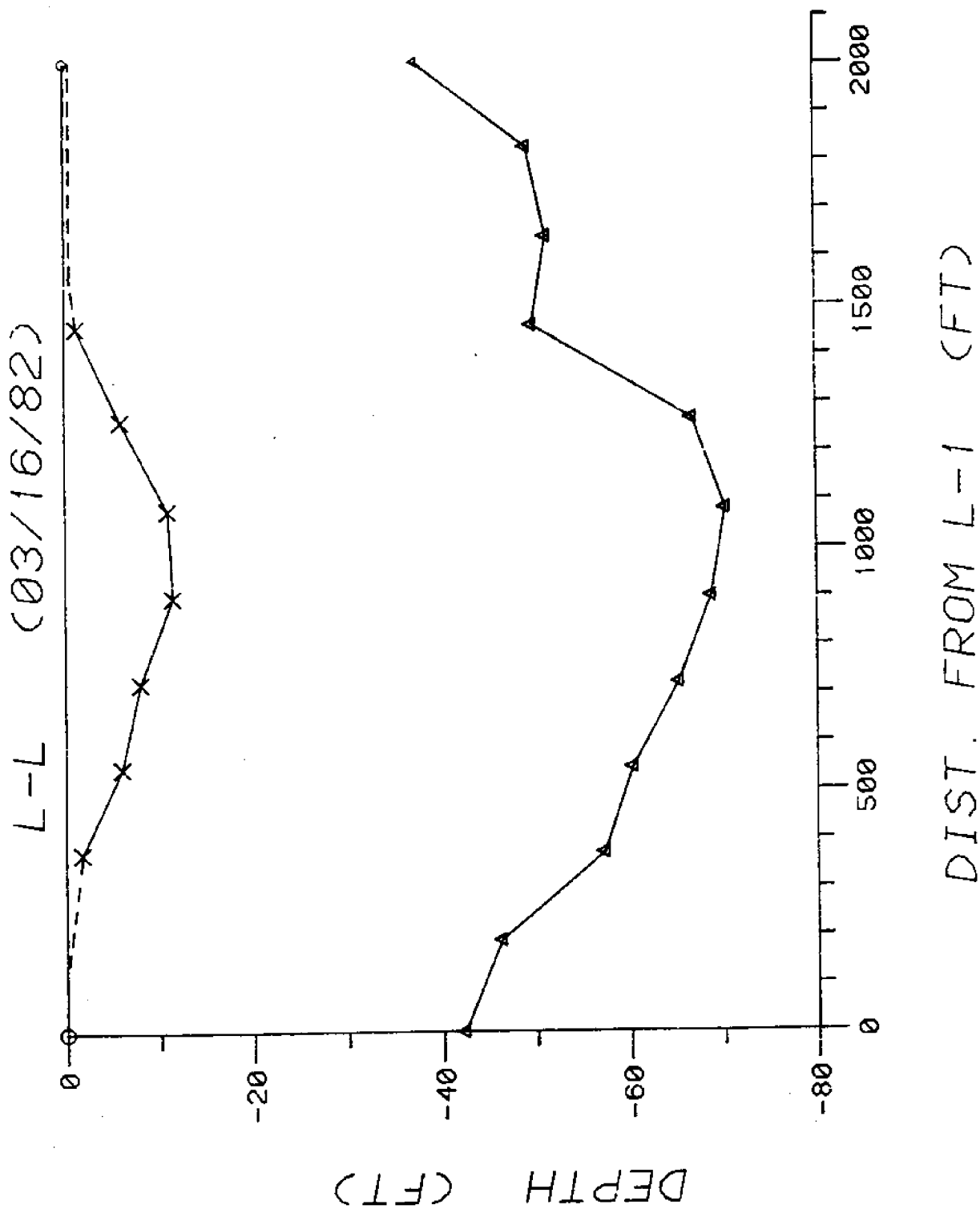


Figure A22. Longitudinal Hanging Dam Profile Along Line L-L; Mar. 16, 1982

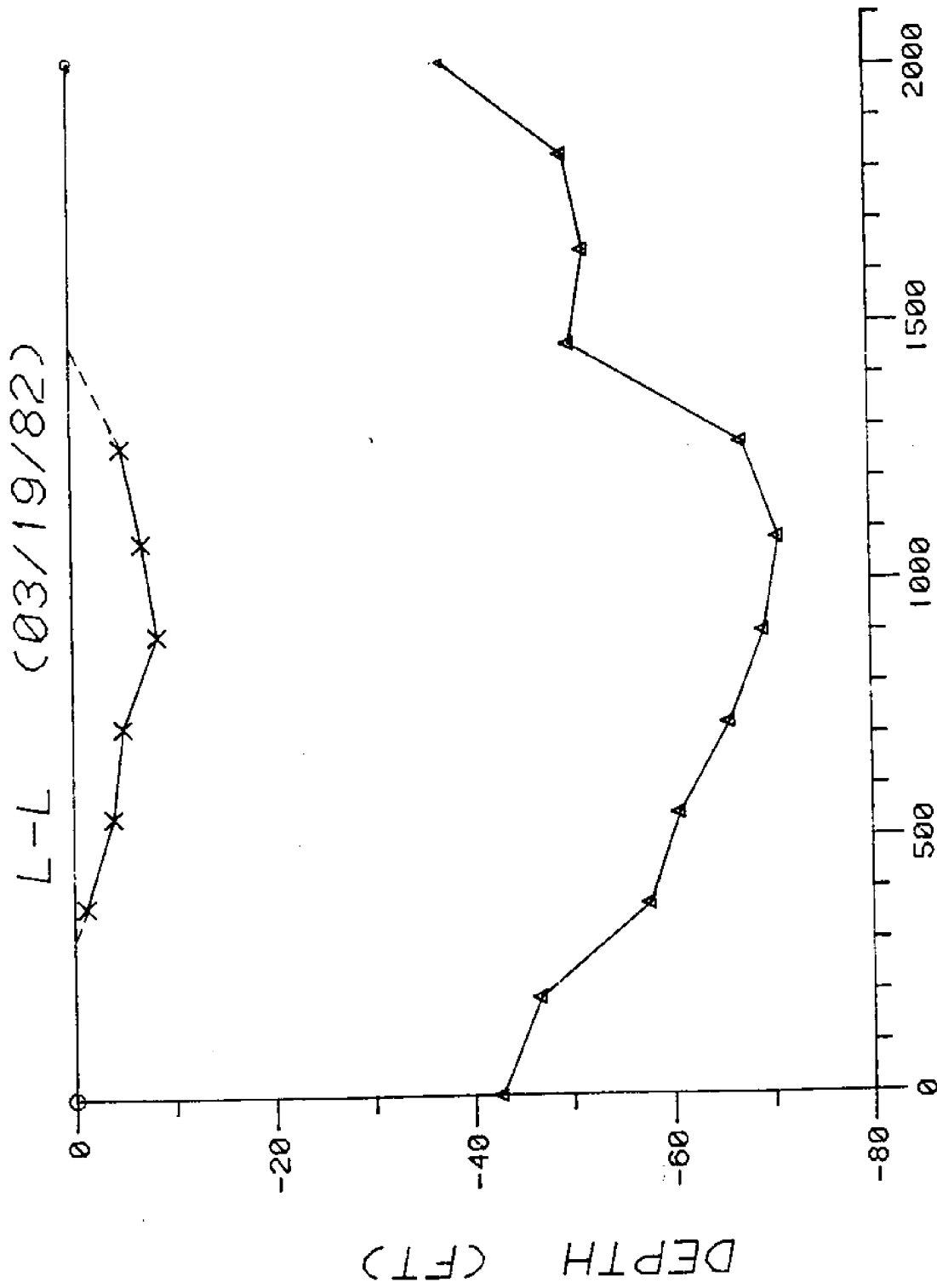


Figure A23. Longitudinal Hanging Dam Profile Along Line L-L; Mar. 19, 1982

APPENDIX B
Water Levels and Discharge

WATER LEVELS AND DISCHARGE - ST. LAWRENCE RIVER

DECEMBER 1981

DAY	KINGS	VINCE	DGDN	GALCP	CARDI	IRQHW	IRQTM	LEISH	WADIN	MORIS	SAUND	DISCHARGE
1	44.67	0.0	43.50	0.0	41.26	40.40	0.0	0.0	0.0	39.38	37.92	256937
2	44.73	0.0	43.72	0.0	41.41	40.59	0.0	0.0	0.0	39.46	38.08	297105
3	44.61	0.0	43.70	0.0	41.45	40.68	0.0	0.0	0.0	39.56	38.28	297298
4	44.60	0.0	43.69	0.0	41.34	40.56	0.0	0.0	0.0	39.42	38.17	296914
5	44.55	0.0	43.68	0.0	41.27	40.37	0.0	0.0	0.0	39.25	37.97	296314
6	44.51	0.0	43.68	0.0	41.07	40.23	0.0	0.0	0.0	39.16	37.87	255949
7	44.47	0.0	43.74	0.0	41.16	40.25	0.0	0.0	0.0	39.20	37.87	296263
8	44.47	0.0	43.68	0.0	40.93	40.09	0.0	0.0	0.0	39.00	37.60	295892
9	44.46	0.0	43.91	0.0	40.93	40.11	0.0	0.0	0.0	38.95	37.60	295882
10	44.44	0.0	0.0	0.0	40.93	40.14	0.0	0.0	0.0	38.96	37.66	296079
11	44.44	0.0	0.0	0.0	40.99	40.18	0.0	0.0	0.0	39.02	37.66	295829
12	44.43	0.0	0.0	0.0	40.91	40.06	0.0	0.0	0.0	38.94	37.53	294549
13	44.42	0.0	0.0	0.0	41.00	40.18	0.0	0.0	0.0	38.99	37.68	293999
14	44.42	0.0	43.33	0.0	41.02	40.20	0.0	0.0	0.0	39.04	37.71	293931
15	44.39	0.0	44.34	0.0	40.92	40.09	0.0	0.0	0.0	38.97	37.57	293834
16	44.40	0.0	43.42	0.0	40.91	40.06	0.0	0.0	0.0	38.94	37.59	293795
17	44.27	0.0	43.25	0.0	40.90	40.10	0.0	0.0	0.0	38.99	37.71	294153
18	44.30	0.0	43.15	0.0	40.69	39.86	0.0	0.0	0.0	38.77	37.31	293990
19	44.29	0.0	43.20	0.0	40.83	39.84	0.0	0.0	0.0	38.74	37.31	293845
20	44.28	0.0	43.30	0.0	40.89	40.00	0.0	0.0	0.0	38.84	37.49	294039
21	44.43	0.0	43.42	0.0	40.87	40.03	0.0	0.0	0.0	38.84	37.38	304836
22	44.35	0.0	43.33	0.0	40.87	40.03	0.0	0.0	0.0	38.81	37.39	305009
23	44.28	0.0	43.05	0.0	40.44	39.55	0.0	0.0	0.0	38.23	36.66	305100
24	44.28	0.0	43.53	0.0	40.84	39.93	0.0	0.0	0.0	38.54	37.14	305018
25	44.28	0.0	43.37	0.0	40.93	40.12	0.0	0.0	0.0	38.86	37.50	305216
26	44.13	0.0	43.02	0.0	40.50	39.62	0.0	0.0	0.0	38.35	36.81	310247
27	44.17	0.0	42.66	0.0	39.91	38.92	0.0	0.0	0.0	37.45	35.57	310122
28	44.21	0.0	43.07	0.0	40.22	39.18	0.0	0.0	0.0	37.61	35.94	310459
29	44.19	0.0	42.97	0.0	40.14	39.15	0.0	0.0	0.0	37.66	36.05	309513
30	44.16	0.0	43.01	0.0	40.18	39.23	0.0	0.0	0.0	37.72	36.10	309930
31	44.16	0.0	42.88	0.0	40.09	39.16	0.0	0.0	0.0	37.64	35.94	309889

WATER LEVELS AND DISCHARGE - ST. LAWRENCE RIVER

JANUARY 1982												
DAY	KINGS	VINCE	OGDEN	GALOP	CARDI	IRQHW	IRQTW	LEISH	WADIN	MORIS	SAUND	DISCHARGE
1	44.37	0.0	43.27	0.0	40.40	39.44	0.0	0.0	0.0	37.84	36.27	309969
2	44.02	0.0	42.86	0.0	40.23	39.32	0.0	0.0	0.0	37.96	36.44	310047
3	44.09	0.0	42.67	0.0	39.82	38.74	0.0	0.0	0.0	37.28	35.45	310482
4	44.22	0.0	42.55	0.0	39.81	38.70	0.0	0.0	0.0	37.14	35.30	309630
5	44.29	0.0	43.03	0.0	40.99	40.19	0.0	0.0	0.0	38.65	37.40	302842
6	44.21	0.0	43.19	0.0	41.24	40.38	0.0	0.0	0.0	39.41	38.15	252528
7	44.16	0.0	43.49	0.0	41.92	41.37	0.0	0.0	0.0	40.81	40.01	229645
8	44.19	0.0	43.45	0.0	42.13	41.65	0.0	0.0	0.0	41.19	40.41	230181
9	44.22	0.0	43.59	0.0	42.20	41.76	0.0	0.0	0.0	41.27	40.44	230052
10	44.47	0.0	43.82	0.0	42.31	41.85	0.0	0.0	0.0	41.34	40.42	229934
11	44.56	0.0	44.33	0.0	42.95	42.62	0.0	0.0	0.0	41.99	41.06	225105
12	44.20	0.0	43.57	0.0	42.11	41.76	0.0	0.0	0.0	40.61	39.51	210033
13	44.15	0.0	43.44	0.0	41.80	41.42	0.0	0.0	0.0	39.65	38.43	210042
14	44.18	0.0	43.47	0.0	41.78	41.00	0.0	0.0	0.0	38.91	37.65	209997
15	44.27	0.0	43.63	0.0	41.94	41.01	0.0	0.0	0.0	38.76	37.50	210083
16	44.51	0.0	43.83	0.0	42.15	41.16	0.0	0.0	0.0	38.98	37.75	210024
17	44.38	0.0	43.75	0.0	42.22	41.13	0.0	0.0	0.0	39.28	38.06	210109
18	44.36	0.0	43.71	0.0	42.18	41.03	0.0	0.0	0.0	39.06	37.87	215037
19	44.30	0.0	43.47	0.0	41.94	40.70	0.0	0.0	0.0	38.60	37.32	223333
20	44.10	0.0	43.19	0.0	41.76	40.48	0.0	0.0	0.0	38.19	36.79	229938
21	44.09	0.0	43.47	0.0	41.41	40.16	0.0	0.0	0.0	37.94	36.49	229941
22	44.42	0.0	43.32	0.0	41.37	40.18	0.0	0.0	0.0	37.82	36.38	230120
23	44.51	0.0	43.81	0.0	41.41	40.17	0.0	0.0	0.0	37.69	36.24	230178
24	44.29	0.0	43.50	0.0	41.89	40.64	0.0	0.0	0.0	38.22	36.83	229901
25	44.30	0.0	43.47	0.0	41.68	40.40	0.0	0.0	0.0	38.17	36.91	229990
26	44.22	0.0	43.35	0.0	41.65	40.12	0.0	0.0	0.0	38.11	36.85	230333
27	44.35	0.0	43.47	0.0	41.49	40.12	0.0	0.0	0.0	37.99	36.78	232162
28	44.31	0.0	43.60	0.0	41.43	39.93	0.0	0.0	0.0	37.63	36.26	240208
29	44.28	0.0	43.38	0.0	41.49	40.00	0.0	0.0	0.0	37.80	36.48	240148
30	44.04	0.0	43.38	0.0	41.24	39.78	0.0	0.0	0.0	37.70	36.22	240076
31	44.04	0.0	0.0	0.0	41.03	39.56	0.0	0.0	0.0	37.87	36.11	239979

WATER LEVELS AND DISCHARGE - ST. LAWRENCE RIVER

FEBRUARY 1982

DAY	KINGS	VINCE	DGDN	GALOP	CARDI	IROHW	IROTW	LEISH	WADIN	MORIS	SAUND	DISCHARGE
1	44.45	0.0	43.30	0.0	41.16	39.21	0.0	0.0	0.0	37.25	35.52	240064
2	44.28	0.0	43.12	0.0	40.97	39.03	0.0	0.0	0.0	36.87	35.30	240151
3	44.31	0.0	43.17	0.0	40.90	39.02	0.0	0.0	0.0	36.90	35.21	239864
4	44.37	0.0	43.24	0.0	40.99	39.19	0.0	0.0	0.0	37.11	35.48	240386
5	44.25	0.0	43.16	0.0	40.93	39.15	0.0	0.0	0.0	37.13	35.49	244987
6	44.46	0.0	43.35	0.0	41.10	39.31	0.0	0.0	0.0	37.28	35.58	244994
7	44.56	0.0	43.51	0.0	41.21	39.36	0.0	0.0	0.0	37.35	35.61	246968
8	44.40	0.0	43.38	0.0	41.04	39.16	0.0	0.0	0.0	37.15	35.43	250209
9	44.33	0.0	43.14	0.0	40.70	38.69	0.0	0.0	0.0	36.47	34.67	250638
10	44.42	0.0	43.25	0.0	40.77	38.75	0.0	0.0	0.0	36.42	34.61	250638
11	44.39	0.0	43.21	0.0	40.73	38.73	0.0	0.0	0.0	36.44	34.66	250054
12	44.25	0.0	43.13	0.0	40.69	38.68	0.0	0.0	0.0	36.43	34.64	250018
13	44.26	0.0	43.08	0.0	40.60	38.50	0.0	0.0	0.0	36.20	34.29	254892
14	44.23	0.0	43.03	0.0	40.56	38.47	0.0	0.0	0.0	36.14	34.19	255192
15	44.25	0.0	43.05	0.0	40.54	38.43	0.0	0.0	0.0	36.07	34.11	255120
16	44.20	0.0	42.98	0.0	40.44	38.47	0.0	0.0	0.0	36.17	34.29	255056
17	44.04	0.0	42.76	0.0	40.17	38.27	0.0	0.0	0.0	36.09	34.13	254974
18	44.17	0.0	42.76	0.0	40.13	38.16	0.0	0.0	0.0	36.07	33.97	255171
19	44.25	0.0	42.94	0.0	40.31	38.37	0.0	0.0	0.0	36.16	34.16	255041
20	44.15	0.0	42.96	0.0	40.37	38.53	0.0	0.0	0.0	36.42	34.48	255064
21	44.15	0.0	42.85	0.0	40.23	38.48	0.0	0.0	0.0	36.46	34.46	254955
22	44.21	0.0	42.94	0.0	40.29	38.57	0.0	0.0	0.0	36.55	34.76	254978
23	44.20	0.0	42.95	0.0	40.38	38.72	0.0	0.0	0.0	36.60	34.79	255143
24	43.95	0.0	42.78	0.0	40.21	38.63	0.0	0.0	0.0	36.71	34.88	254728
25	44.16	0.0	42.91	0.0	40.37	38.78	0.0	0.0	0.0	36.96	35.15	255488
26	44.15	0.0	42.93	0.0	40.50	38.98	0.0	0.0	0.0	37.15	35.35	255098
27	44.13	0.0	42.98	0.0	40.56	39.08	0.0	0.0	0.0	37.15	35.35	255098
28	44.05	0.0	42.89	0.0	40.48	39.01	0.0	0.0	0.0	37.15	35.34	254879

WATER LEVELS AND DISCHARGE - ST. LAWRENCE RIVER

MARCH 1982

DAY	KINGS	VINCE	OGDEN	GALCP	CARDI	IRQHW	IRQTW	LEISH	WADIN	MORIS	SAUND	DISCHARGE
1	44.00	0.0	42.84	0.0	40.41	38.93	0.0	0.0	0.0	36.99	35.18	255012
2	44.13	0.0	42.99	0.0	40.57	39.14	0.0	0.0	0.0	37.20	35.46	255103
3	44.03	0.0	42.94	0.0	40.45	39.06	0.0	0.0	0.0	37.22	35.40	255116
4	43.95	0.0	42.73	0.0	40.30	38.94	0.0	0.0	0.0	37.11	35.31	0
5	44.22	0.0	42.97	0.0	40.53	39.14	0.0	0.0	0.0	37.24	35.47	0
6	44.03	0.0	42.84	0.0	40.47	39.08	0.0	0.0	0.0	37.22	35.59	0
7	44.12	0.0	42.87	0.0	40.50	39.12	0.0	0.0	0.0	37.28	35.56	0
8	44.10	0.0	42.95	0.0	40.59	39.24	0.0	0.0	0.0	37.42	35.73	0
9	44.04	0.0	42.79	0.0	40.36	39.04	0.0	0.0	0.0	37.23	35.52	0
10	44.03	0.0	42.80	0.0	40.40	39.08	0.0	0.0	0.0	37.29	35.56	0
11	44.07	0.0	42.81	0.0	40.45	39.08	0.0	0.0	0.0	37.23	35.57	251135
12	44.08	0.0	42.86	0.0	40.51	39.14	0.0	0.0	0.0	37.33	35.58	251065
13	44.17	0.0	42.88	0.0	40.58	39.19	0.0	0.0	0.0	37.28	35.51	251082
14	44.25	0.0	43.11	0.0	40.89	39.45	0.0	0.0	0.0	37.53	35.84	251072
15	44.14	0.0	42.99	0.0	40.79	39.45	0.0	0.0	0.0	37.58	35.90	251073
16	44.05	0.0	42.87	0.0	40.68	39.36	0.0	0.0	0.0	37.50	35.75	251313
17	44.20	0.0	42.92	0.0	40.74	39.26	0.0	0.0	0.0	37.28	35.43	251732
18	44.27	0.0	43.11	0.0	41.00	39.53	0.0	0.0	0.0	37.53	35.70	251048
19	44.33	0.0	43.21	0.0	41.17	39.90	0.0	0.0	0.0	37.88	36.14	251157
20	44.29	0.0	43.19	0.0	41.24	40.16	0.0	0.0	0.0	38.22	36.47	255952
21	44.42	0.0	43.25	0.0	41.34	40.87	0.0	0.0	0.0	38.46	36.69	255918
22	44.49	0.0	43.53	0.0	41.70	40.96	0.0	0.0	0.0	38.93	37.21	256177
23	44.47	0.0	43.49	0.0	41.66	40.96	0.0	0.0	0.0	39.28	37.62	256003
24	44.45	0.0	43.49	0.0	41.83	41.06	0.0	0.0	0.0	39.54	37.98	256013
25	44.52	0.0	43.50	0.0	41.83	41.28	0.0	0.0	0.0	40.03	38.57	256061
26	44.75	0.0	43.89	0.0	42.16	41.61	0.0	0.0	0.0	40.44	39.12	256379
27	44.74	0.0	43.94	0.0	42.27	41.77	0.0	0.0	0.0	40.71	39.43	261846
28	44.70	0.0	43.92	0.0	42.27	41.70	0.0	0.0	0.0	40.61	39.30	262057
29	44.68	0.0	43.92	0.0	42.26	41.73	0.0	0.0	0.0	40.64	39.34	261973
30	44.64	0.0	43.74	0.0	42.05	41.52	0.0	0.0	0.0	40.46	39.17	262039
31	44.81	0.0	43.90	0.0	42.24	41.72	0.0	0.0	0.0	40.78	39.55	262023

WATER LEVELS AND DISCHARGE - ST. LAWRENCE RIVER

DAY	APRIL 1982													DISCHARGE
	KINGS	VINCE	OGDEN	GALCP	CARDI	IRQHW	IROTW	LEISH	WADIN	MORIS	SAUND			
1	44.90	0.0	44.28	0.0	42.81	42.39	0.0	0.0	0.0	41.57	40.75	0.0	252238	
2	44.81	0.0	44.17	0.0	42.99	42.62	0.0	0.0	0.0	41.95	41.29	0.0	239724	
3	45.07	0.0	44.23	0.0	42.93	42.55	0.0	0.0	0.0	41.79	40.98	0.0	244543	
4	45.33	0.0	45.00	0.0	43.74	43.37	0.0	0.0	0.0	42.61	42.09	0.0	256196	
5	45.10	0.0	44.37	0.0	43.14	42.69	0.0	0.0	0.0	42.03	41.32	0.0	269477	
6	44.93	0.0	43.83	0.0	42.15	41.63	0.0	0.0	0.0	40.70	39.70	0.0	276874	
7	45.05	0.0	43.97	0.0	42.08	41.51	0.0	0.0	0.0	40.47	39.50	0.0	276804	
8	45.12	0.0	0.0	0.0	42.21	41.61	0.0	0.0	0.0	40.57	39.56	0.0	276646	
9	45.21	0.0	0.0	0.0	42.39	41.83	0.0	0.0	0.0	40.82	39.71	0.0	277278	
10	45.23	0.0	0.0	0.0	42.57	41.97	0.0	0.0	0.0	40.99	39.97	0.0	284259	
11	45.20	0.0	0.0	0.0	42.49	41.90	0.0	0.0	0.0	40.53	39.94	0.0	284373	
12	45.19	0.0	44.27	0.0	42.46	41.85	0.0	0.0	0.0	40.85	39.89	0.0	284004	
13	45.39	0.0	44.38	0.0	42.54	41.94	0.0	0.0	0.0	40.89	39.96	0.0	283936	
14	45.28	0.0	44.36	0.0	42.68	42.15	0.0	0.0	0.0	41.17	40.33	0.0	284334	
15	45.20	0.0	44.24	0.0	42.43	41.68	0.0	0.0	0.0	40.87	39.89	0.0	283908	
16	45.23	0.0	44.23	0.0	42.40	41.81	0.0	0.0	0.0	40.74	39.81	0.0	284235	
17	45.34	0.0	44.30	0.0	42.42	41.78	0.0	0.0	0.0	40.68	39.71	0.0	296373	
18	45.42	0.0	44.75	0.0	42.89	42.26	0.0	0.0	0.0	41.11	40.41	0.0	254617	
19	45.30	0.0	44.46	0.0	43.05	42.60	0.0	0.0	0.0	41.79	41.05	0.0	247333	
20	45.36	0.0	44.48	0.0	43.15	42.75	0.0	0.0	0.0	42.05	41.18	0.0	246780	
21	45.58	0.0	44.99	0.0	43.67	43.32	0.0	0.0	0.0	42.56	42.05	0.0	246955	
22	45.53	0.0	44.87	0.0	43.70	43.39	0.0	0.0	0.0	42.11	42.11	0.0	248100	
23	45.62	0.0	45.05	0.0	43.81	43.50	0.0	0.0	0.0	42.62	42.16	0.0	247527	
24	45.58	0.0	44.91	0.0	43.72	43.41	0.0	0.0	0.0	42.63	41.97	0.0	261535	
25	45.57	0.0	44.69	0.0	43.12	42.63	0.0	0.0	0.0	42.56	40.78	0.0	292486	
26	45.54	0.0	44.51	0.0	42.74	42.17	0.0	0.0	0.0	41.01	40.04	0.0	298560	
27	45.60	0.0	44.44	0.0	42.46	41.77	0.0	0.0	0.0	40.61	39.54	0.0	304601	
28	45.55	0.0	44.32	0.0	42.28	41.55	0.0	0.0	0.0	40.37	39.27	0.0	297736	
29	45.59	0.0	44.48	0.0	42.56	41.89	0.0	0.0	0.0	40.75	39.79	0.0	285337	
30	45.64	0.0	44.60	0.0	42.86	42.25	0.0	0.0	0.0	41.20	40.33	0.0	281331	

APPENDIX C

Ice Cover Thickness at
Selected Cross Sections*

*Data provided by Ontario Hydro. Cross
section locations are given in Ref. 23.

CROSS SECTION A(Power Dam), Feb. 22, 1982

<u>Location</u>	<u>Ice Thickness</u>	<u>and</u>	<u>Remarks</u>
0+00	Barnhart Island		
1+50	16" Solid Ice		
3+00	17" Solid Ice		
4+50	19" Solid Ice		
6+00	17" Solid Ice		
7+50	15" Solid Ice		
9+00	18" Solid Ice		
10+50	18½" Solid Ice		
12+00	25" Solid Ice		
13+50	21" Solid Ice		
15+00	21" Solid Ice		
16+50	18" Solid Ice		
18+00	21" Solid Ice		
19+50	16" Solid Ice		
21+00	21" Solid Ice		
22+50	26" Solid Ice		
24+00	20" Solid Ice		
26+50	18" Solid Ice		
28+00	21" Solid Ice		
29+50	Canadian Shore		

CROSS SECTION B1 (Waddington), Feb. 22, 1982

<u>Location</u>	<u>Ice Thickness</u>	<u>and</u>	<u>Remarks</u>
0+00	U.S. Mainland		
1+50	21" Consolidated Broken Pack	No Slush	
3+00	16" Consolidated Broken Pack	No Slush	
4+50	19" Consolidated Broken Pack	No Slush	
6+00	18" Consolidated Broken Pack	No Slush	
7+50	18" Consolidated Broken Pack	No Slush	
9+00	18" Consolidated Broken Pack	No Slush	
10+50	18" Consolidated Broken Pack	No Slush	
12+00	20" Consolidated Broken Pack	No Slush	
13+50	21" Consolidated Broken Pack	No Slush	
15+00	Ogden Island		

CROSS SECTION C (Pinetree Pt.), Feb. 23, 1982

<u>Location</u>	<u>Ice Thickness</u>	<u>and</u>	<u>Remarks</u>
1+50	23" Solid Ice	No Slush	
3+00	17" Solid Ice	No Slush	
4+50	20" Consolidated Broken Pack	No Slush	
6+00	18" Consolidated Broken Pack	Waferlike ice crystals evident in hole	
7+50	18" Consolidated Broken Pack	Waferlike ice crystals evident in hole	
9+00	22" Consolidated Broken Pack	No Slush	
10+50	17" Consolidated Broken Pack	No Slush	
12+00	22" Consolidated Broken Pack	No Slush	Underside of cover rough
13+50	30" Broken pack and slush	- silt evident	
15+00	19" Consolidated Broken Pack	No Slush	
16+50	18" Consolidated Broken Pack	No Slush	
18+00	17" Consolidated Broken Pack	No Slush	
19+50	26" Broken pack and slush	- silt evident	
21+00	21" Consolidated Broken Pack	Waferlike ice crystals evident in hole	
22+50	23" Solid Ice	No Slush	
23+25	United States Mainland		

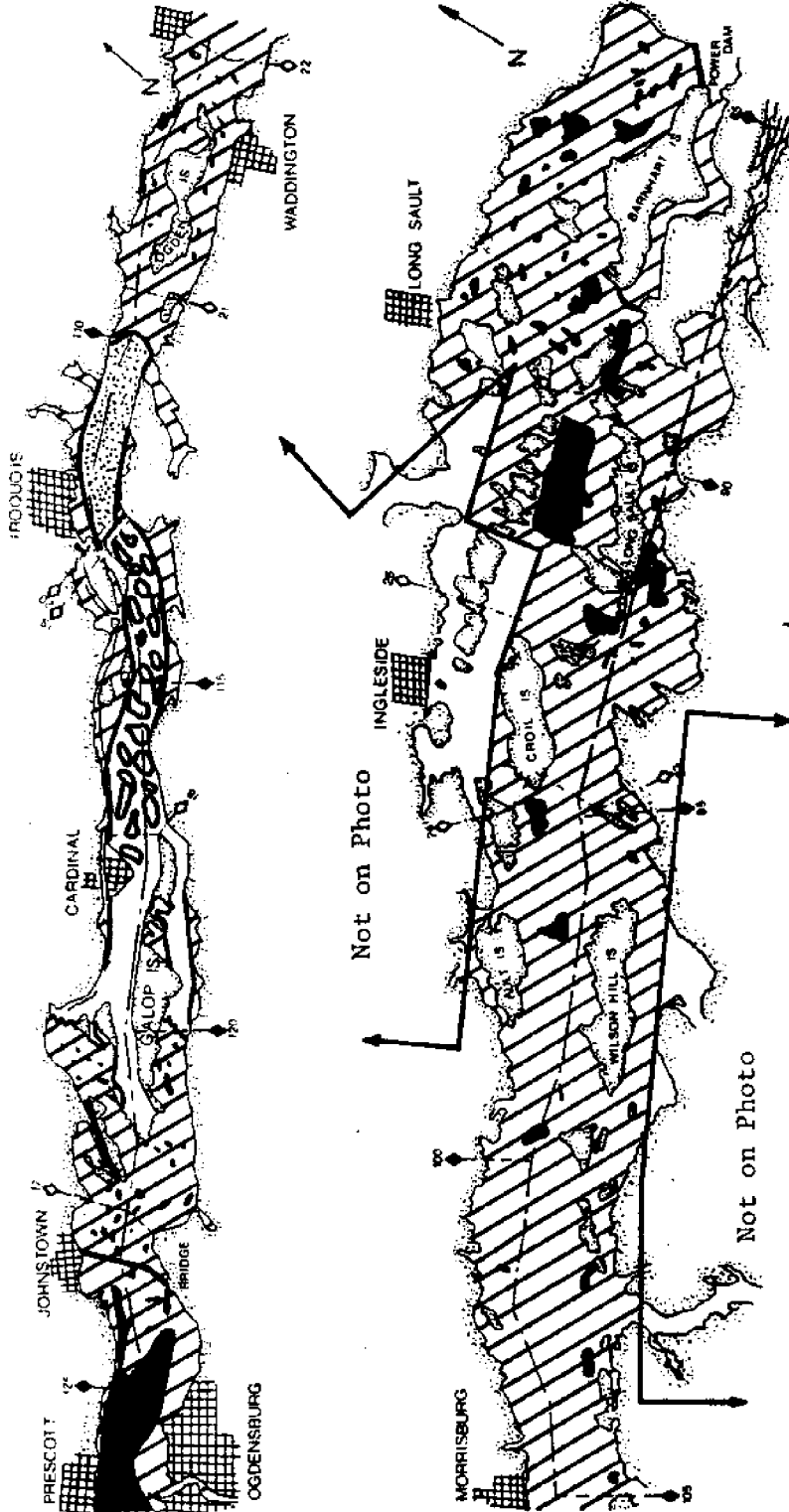
CROSS SECTION D(Cardinal), Feb. 24, 1982

<u>Location</u>	<u>Ice Thickness</u>	<u>and</u>	<u>Remarks</u>
1+50	17½" Solid Ice		No Slush
3+00	13" Consolidated Broken Pack		No Slush
4+50	15" Consolidated Broken Pack		No Slush
6+00	16" Consolidated Broken Pack		No Slush
7+50	17" Consolidated Broken Pack		No Slush
9+00	20" Consolidated Broken Pack		No Slush
10+50	20½" Consolidated Broken Pack		No Slush
12+00	10½" Consolidated Broken Pack		21' Heavy Slush
13+50	19½" Consolidated Broken Pack		22'4" Heavy Slush
15+00	20" Consolidated Broken Pack		18'4" Heavy Slush
16+50	21" Consolidated Broken Pack		11'3" Heavy Slush
18+00	21" Consolidated Broken Pack		6'4" Medium Slush
19+50	5'8" Broken Pack		Light Slush
21+00	5'1" Broken Pack		Light Slush
22+50	18" Solid Ice		18" Light Slush
24+00	15" Solid Ice		No Slush
25+50	16" Solid Ice		No Slush
27+00	20" Solid Ice		12" Light Dirty Slush
27+50	American Shore		

APPENDIX D

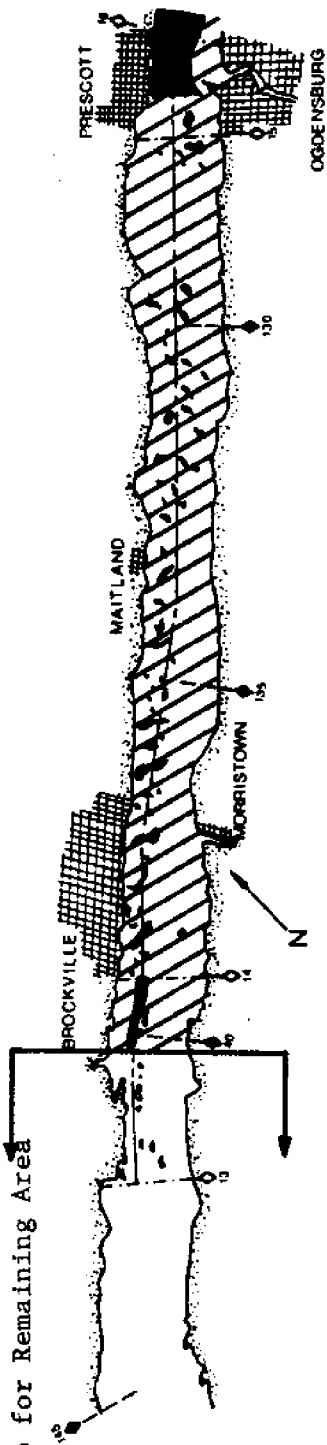
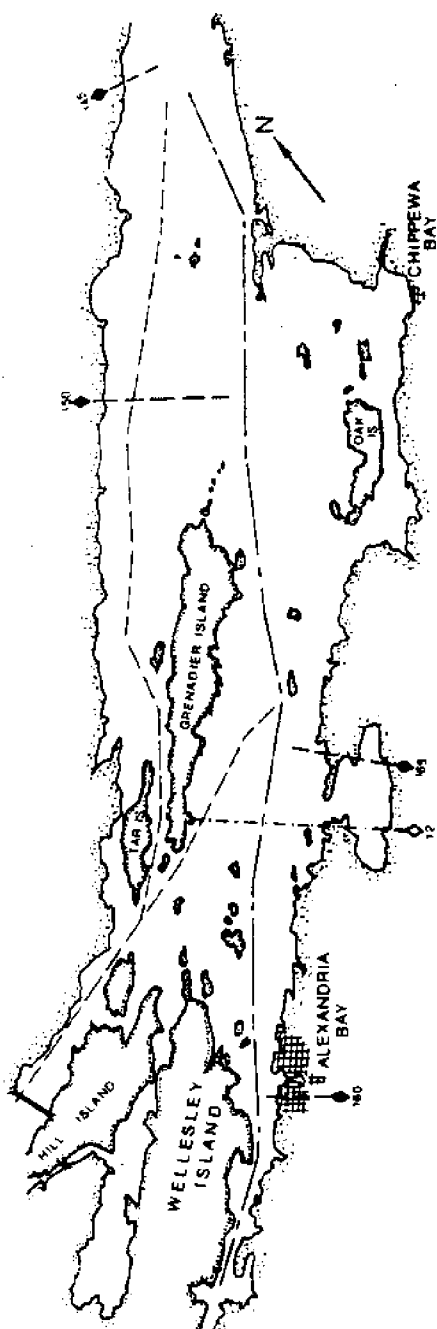
Ice Cover Condition Maps*

*Based on aerial photographs by the St.
Lawrence Seaway Development Corporation.

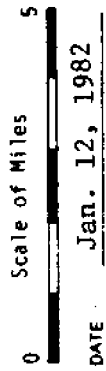


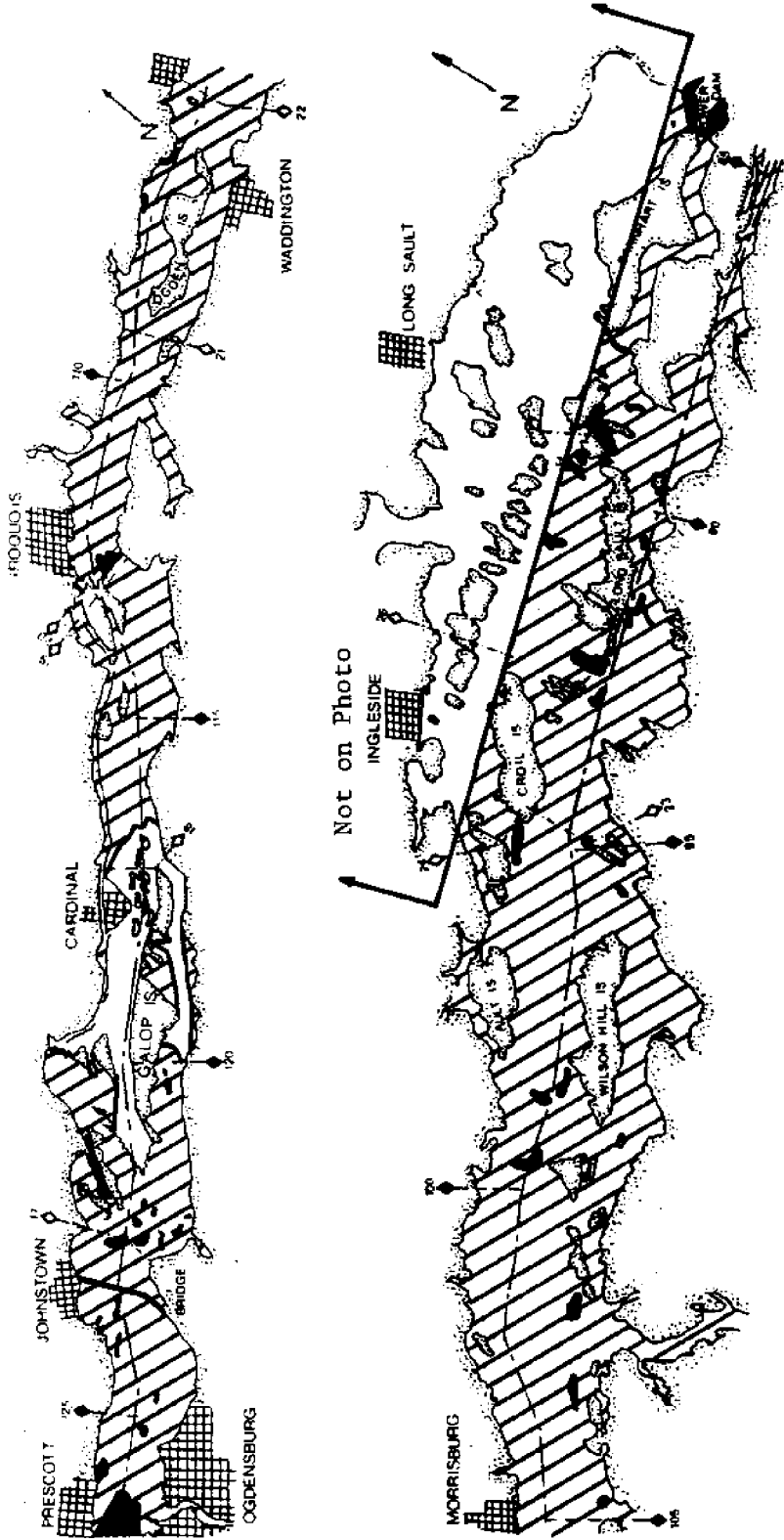
0 Scale of Miles 5

DATE Jan. 12, 1982

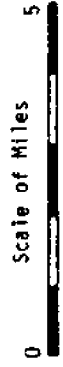


No Photo for Remaining Area

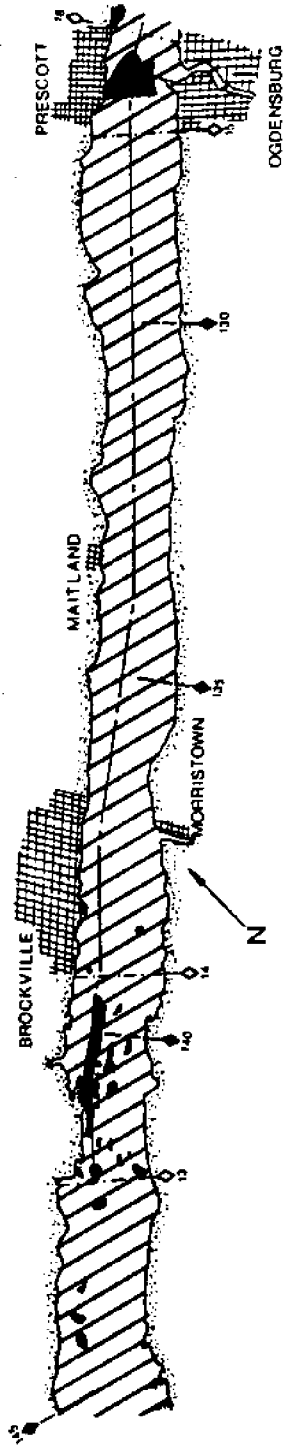
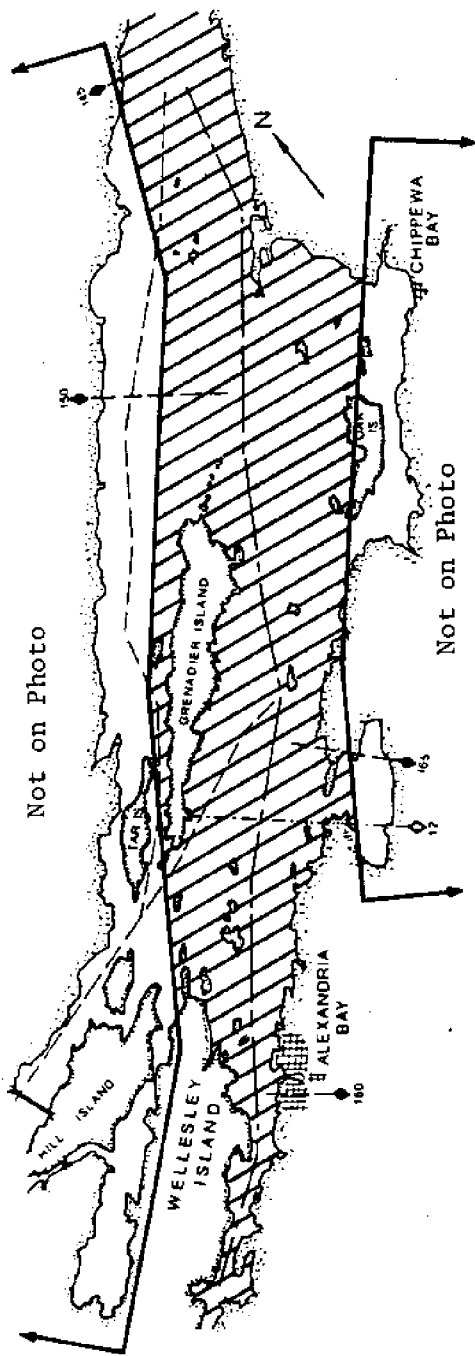




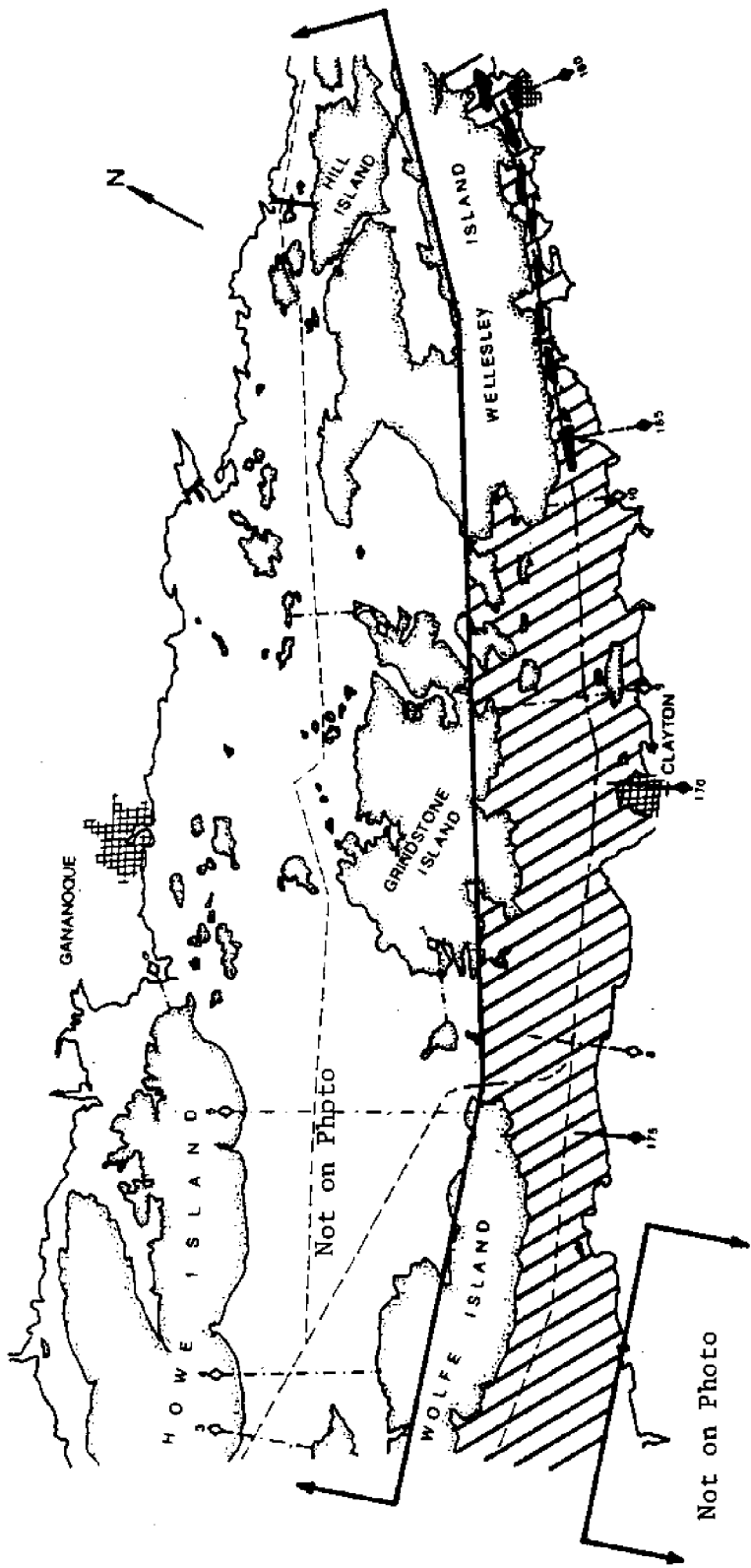
Not on Photo



DATE Jan. 19, 1982

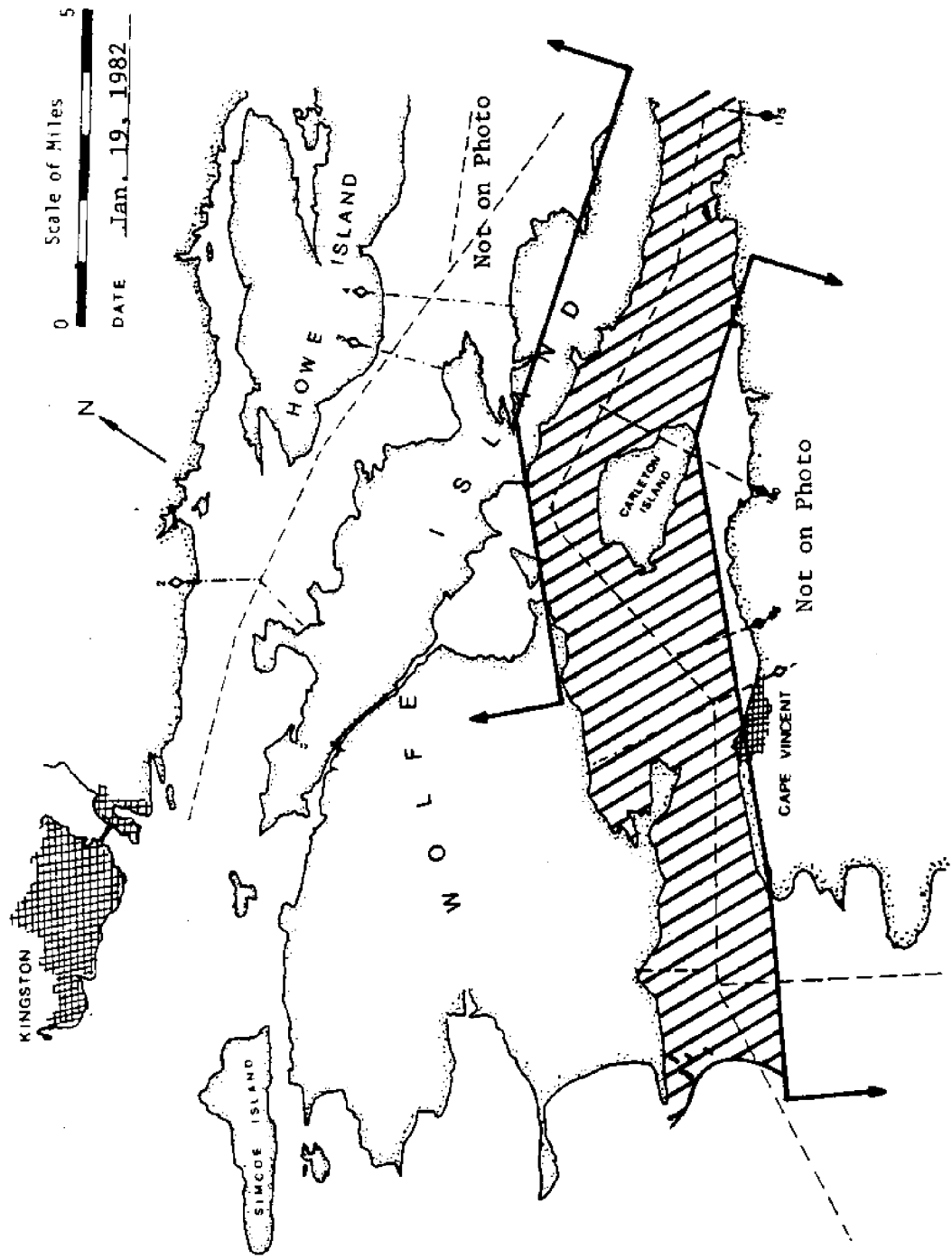


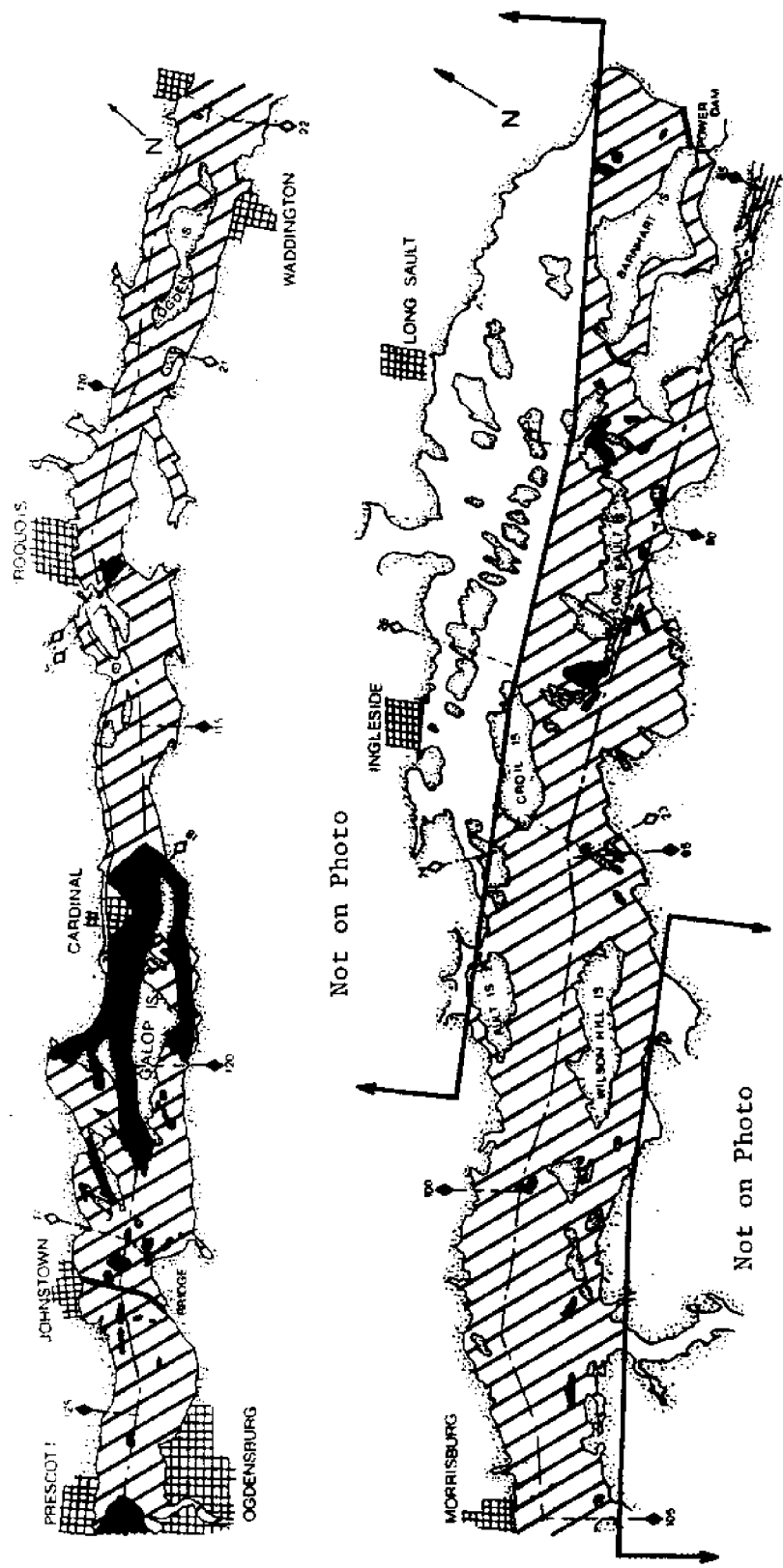
0 Scale of Miles 5
 DATE Jan. 19, 1982

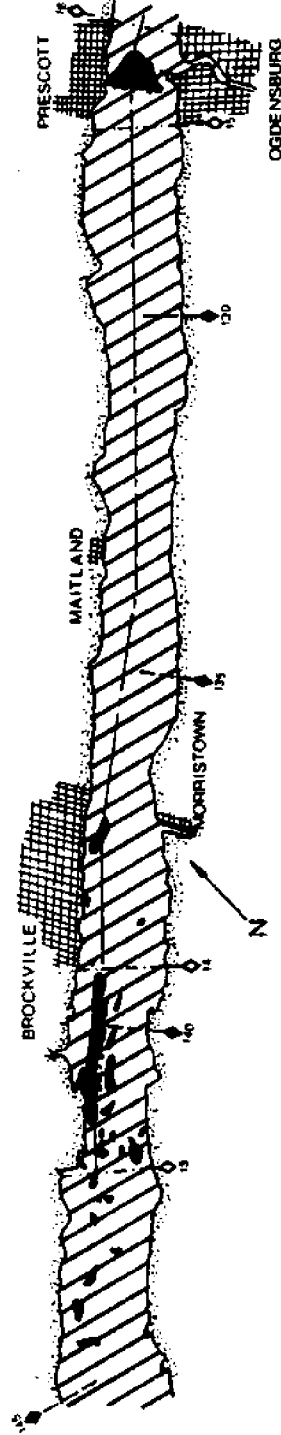
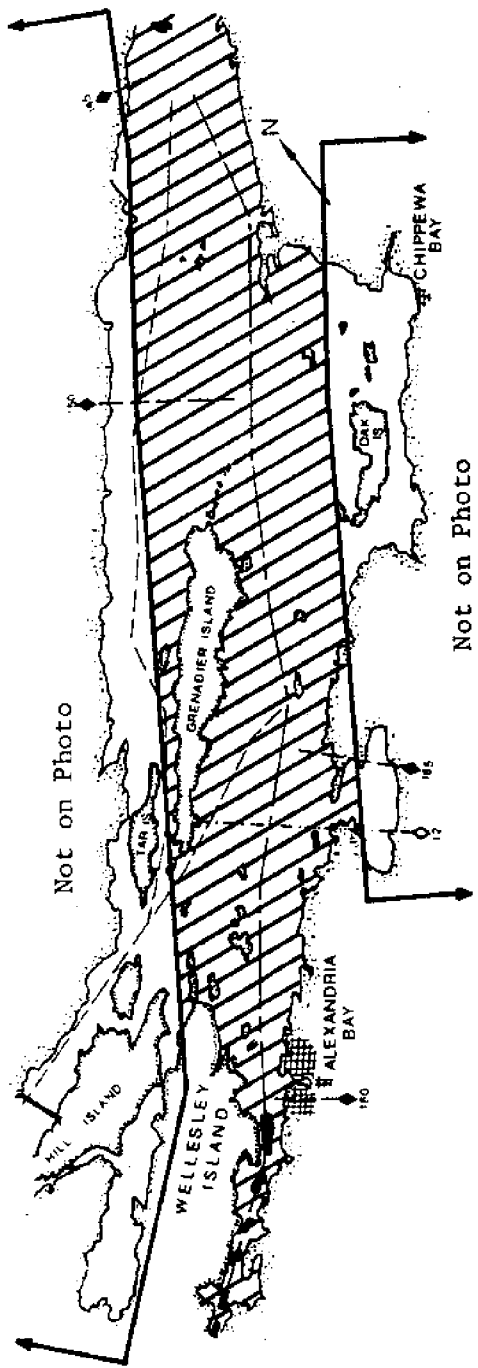


0 Scale of Miles 5

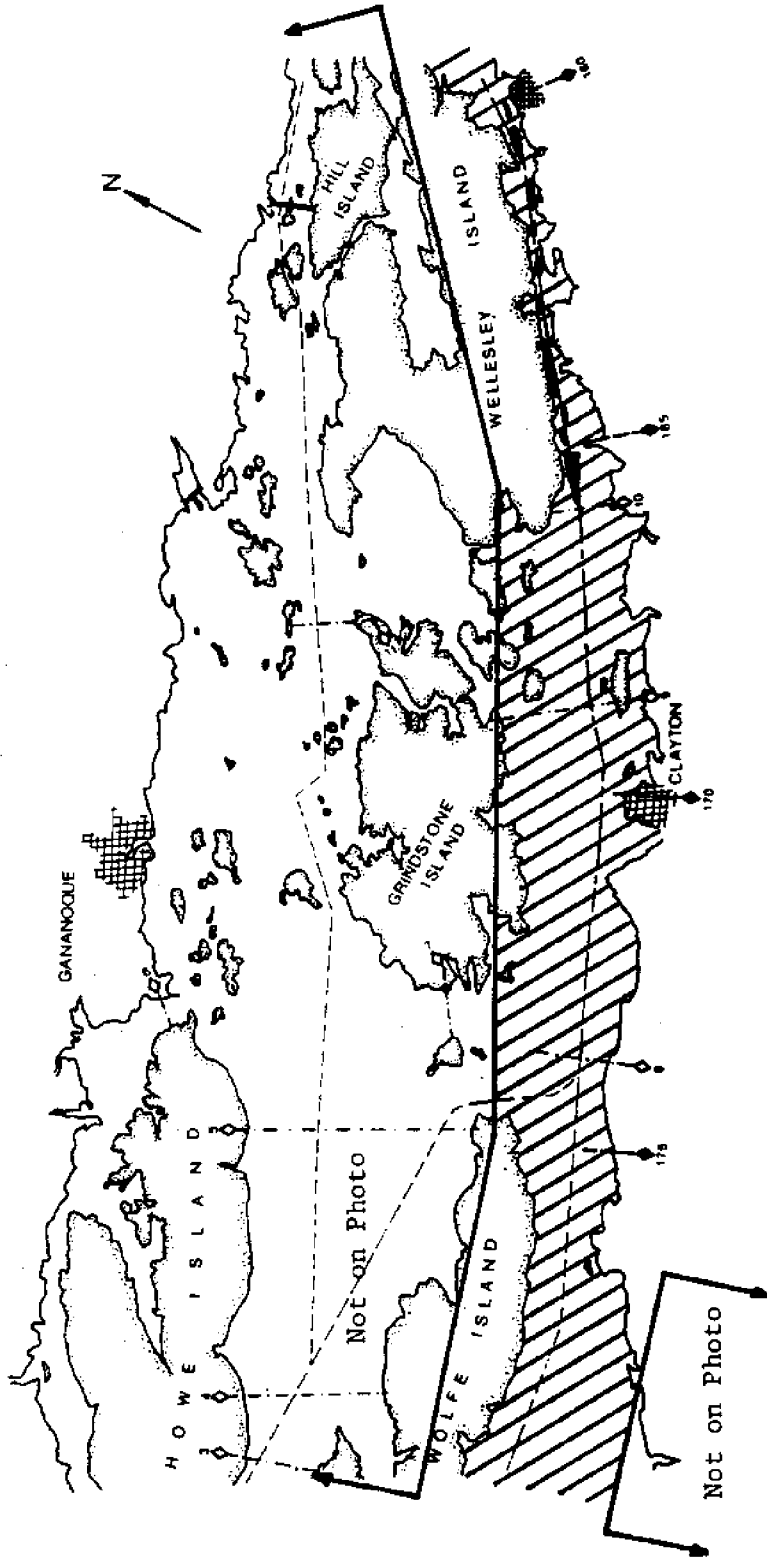
DATE: Jan. 19, 1982





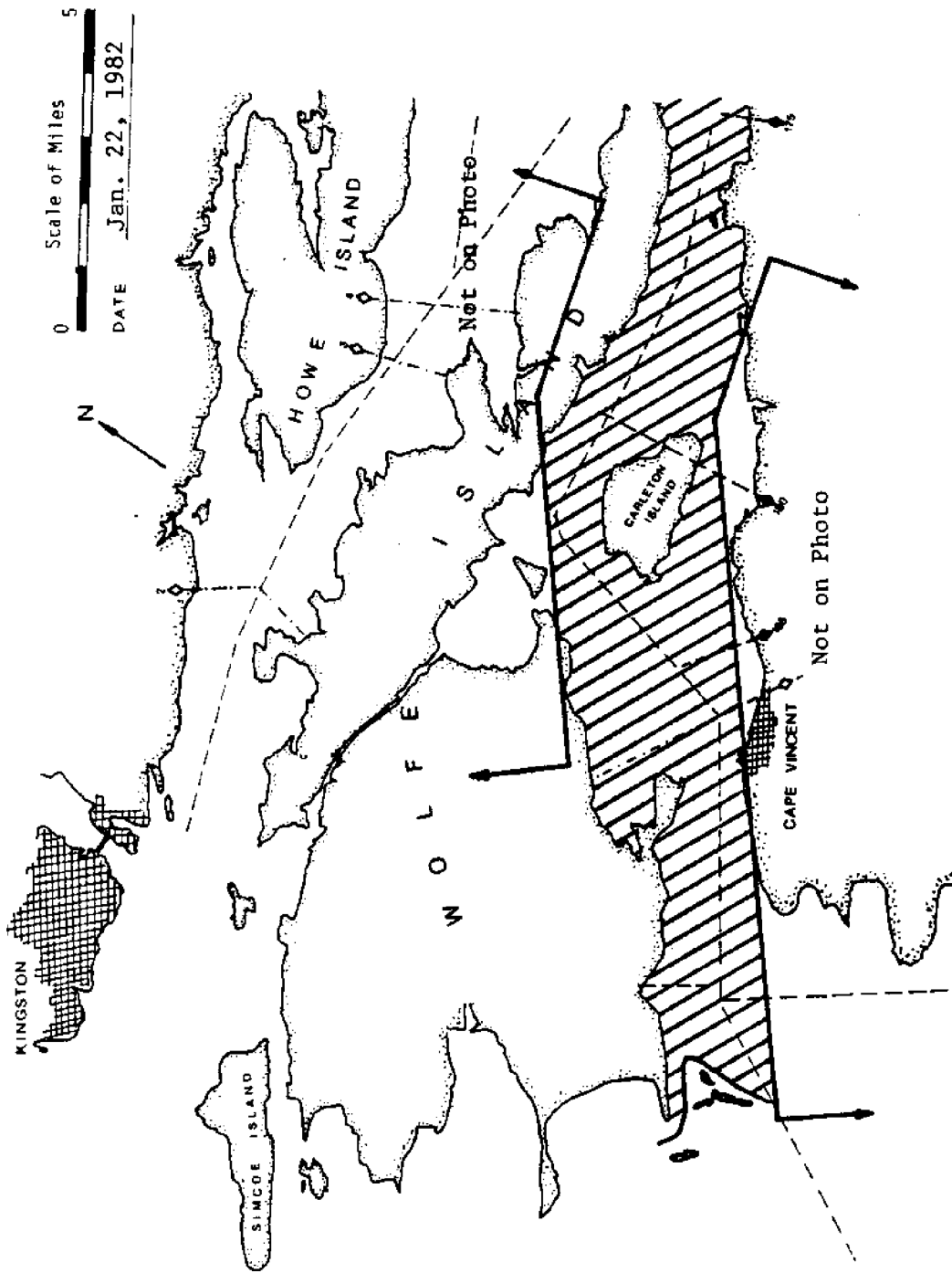


0 Scale of Miles 5
 DATE Jan. 22, 1982



0 Scale of Miles 5

DATE Jan. 22, 1982



Scale of Miles 0 5
DATE Jan. 22, 1982

KINGSTON

SIMCOE ISLAND

HOWE ISLAND

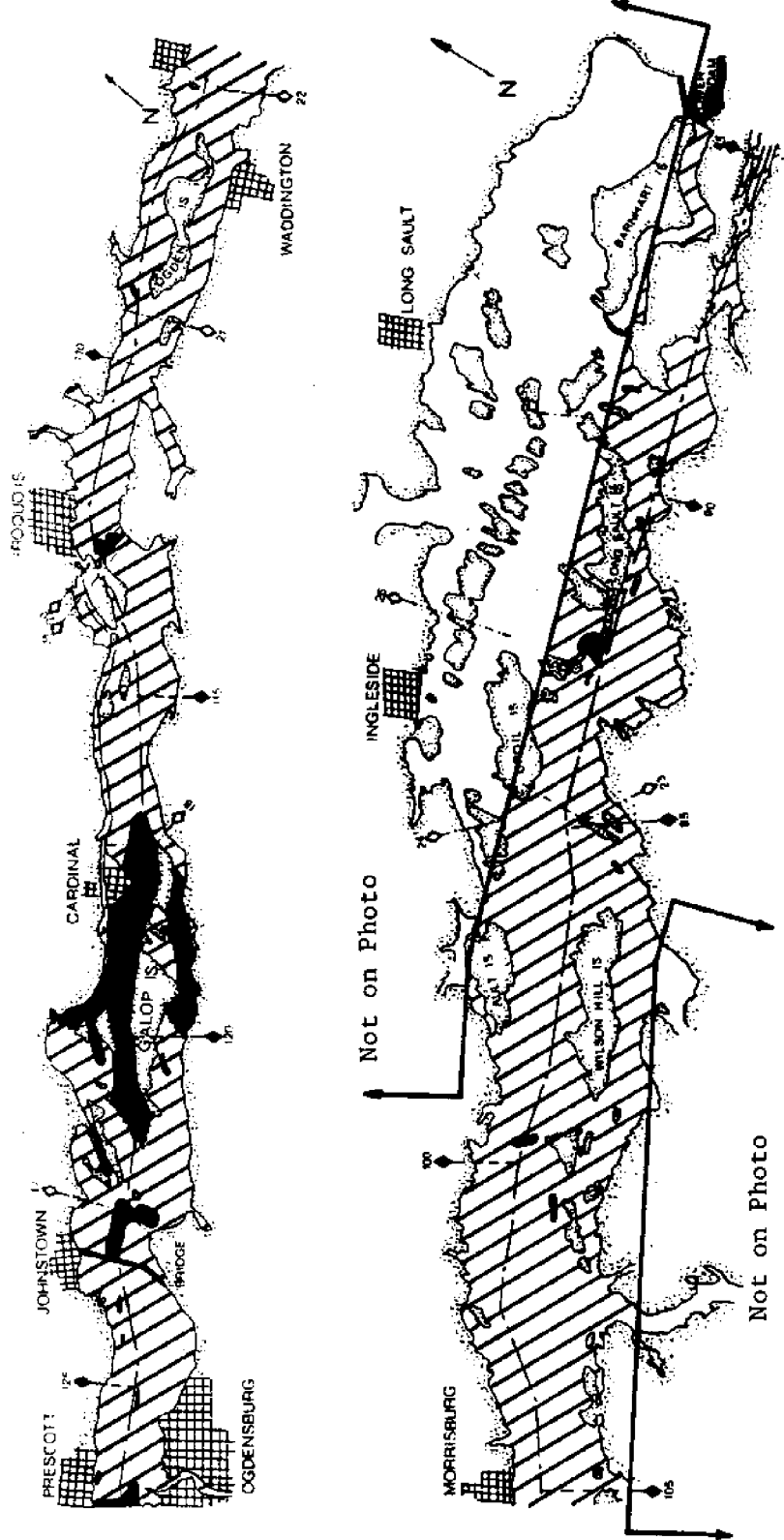
CARLETON ISLAND

CAPE VINCENT

WOLF ISLANDS

Not on Photo

Not on Photo

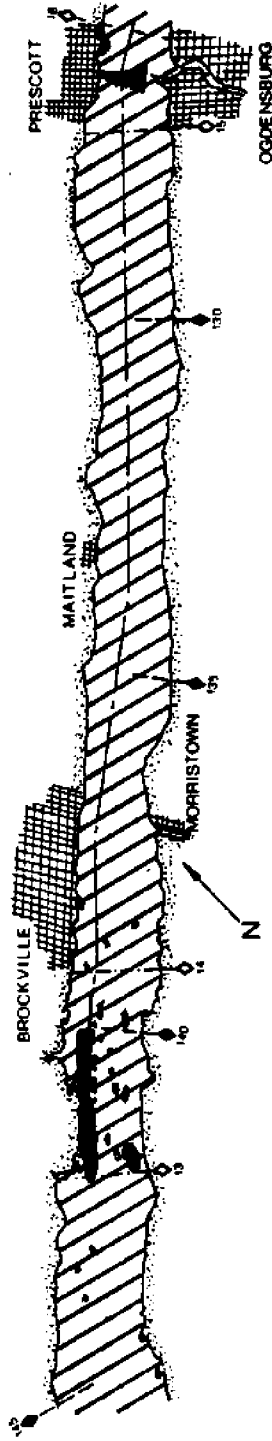
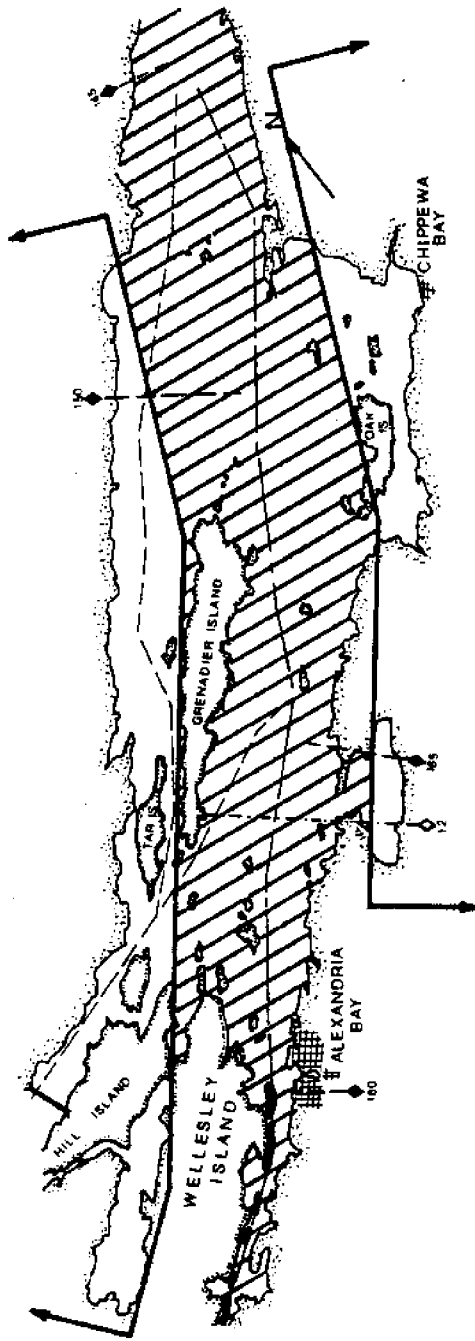


0 Scale of Miles 5

DATE Feb. 17, 1982

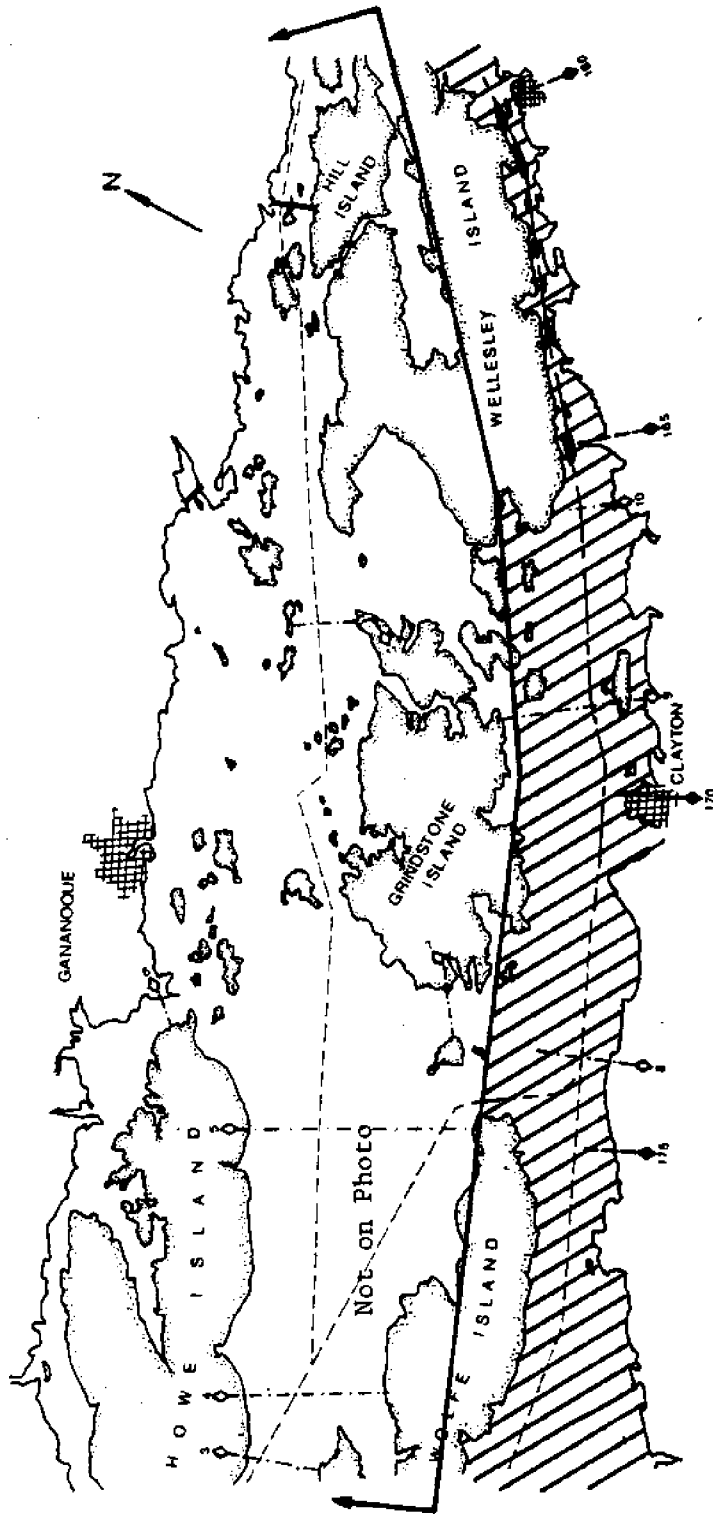
Not on Photo

Not on Photo



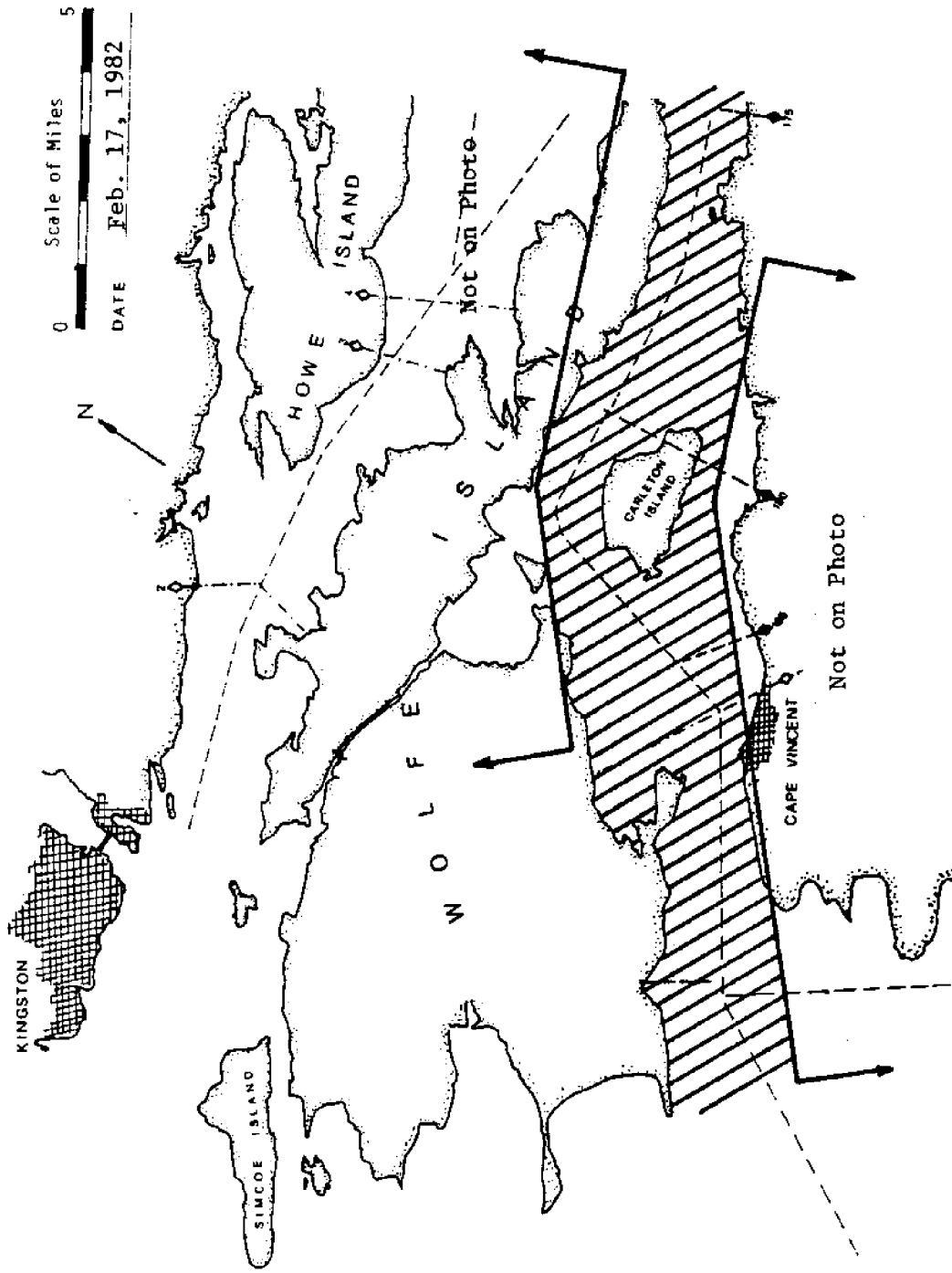
0 Scale of Miles 5

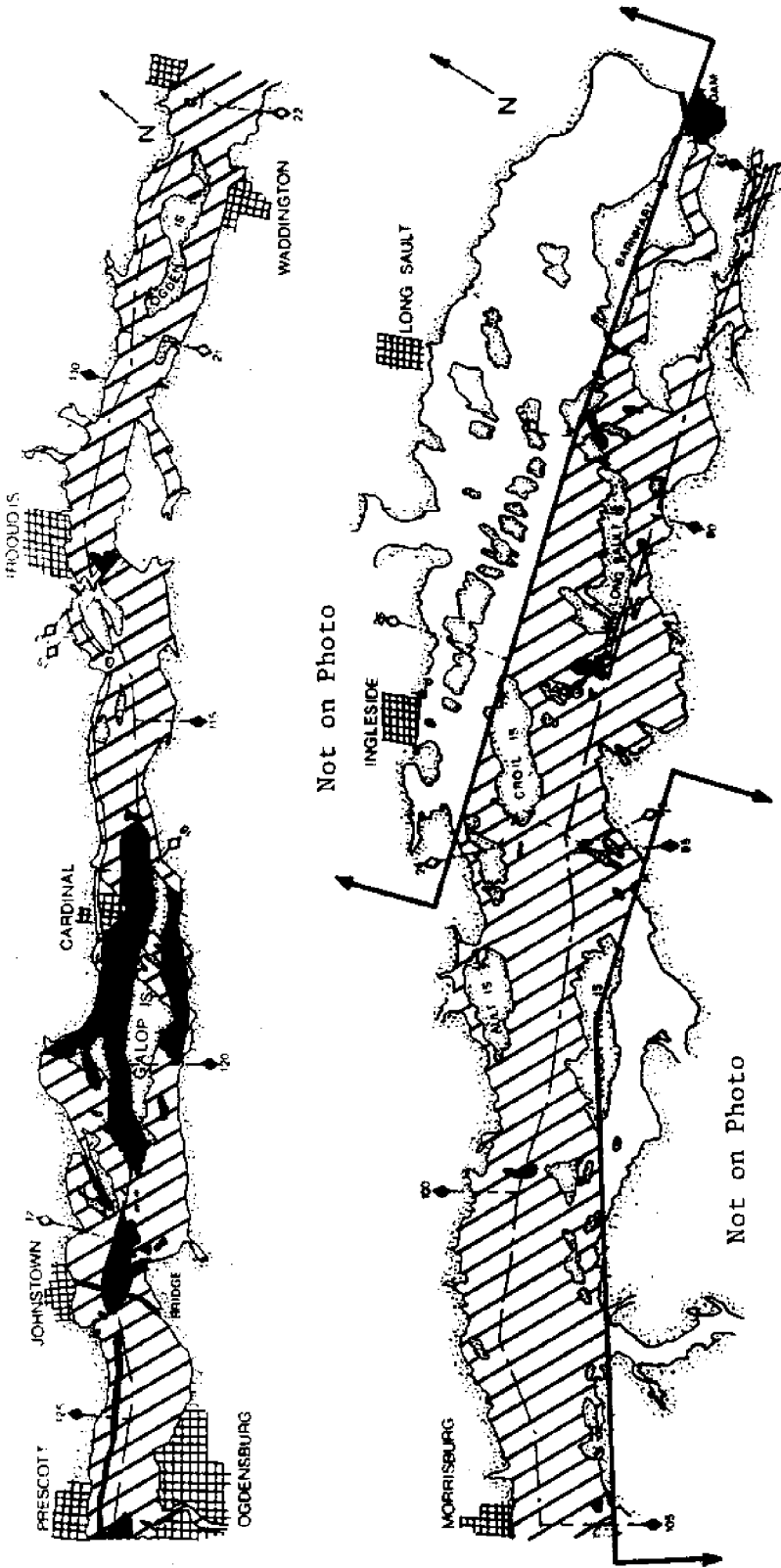
DATE Feb. 17, 1982



Scale of Miles
0 5

DATE Feb. 17, 1982



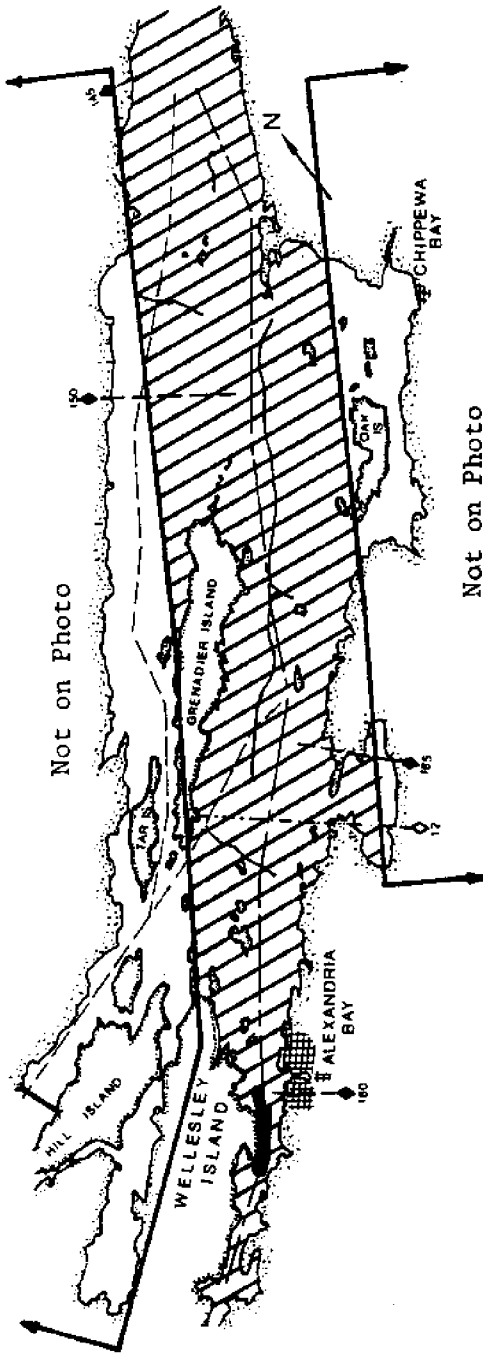


Not on Photo

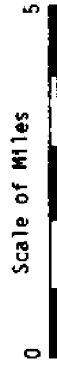
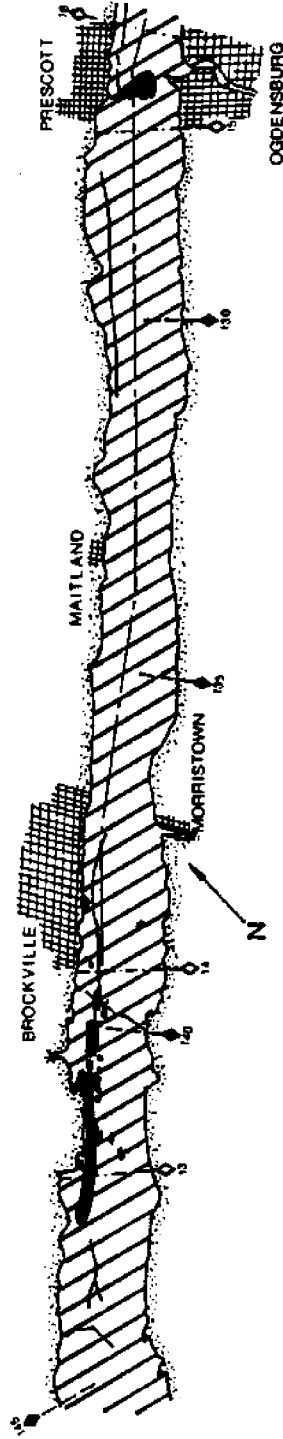
Not on Photo

0 Scale of Miles 5

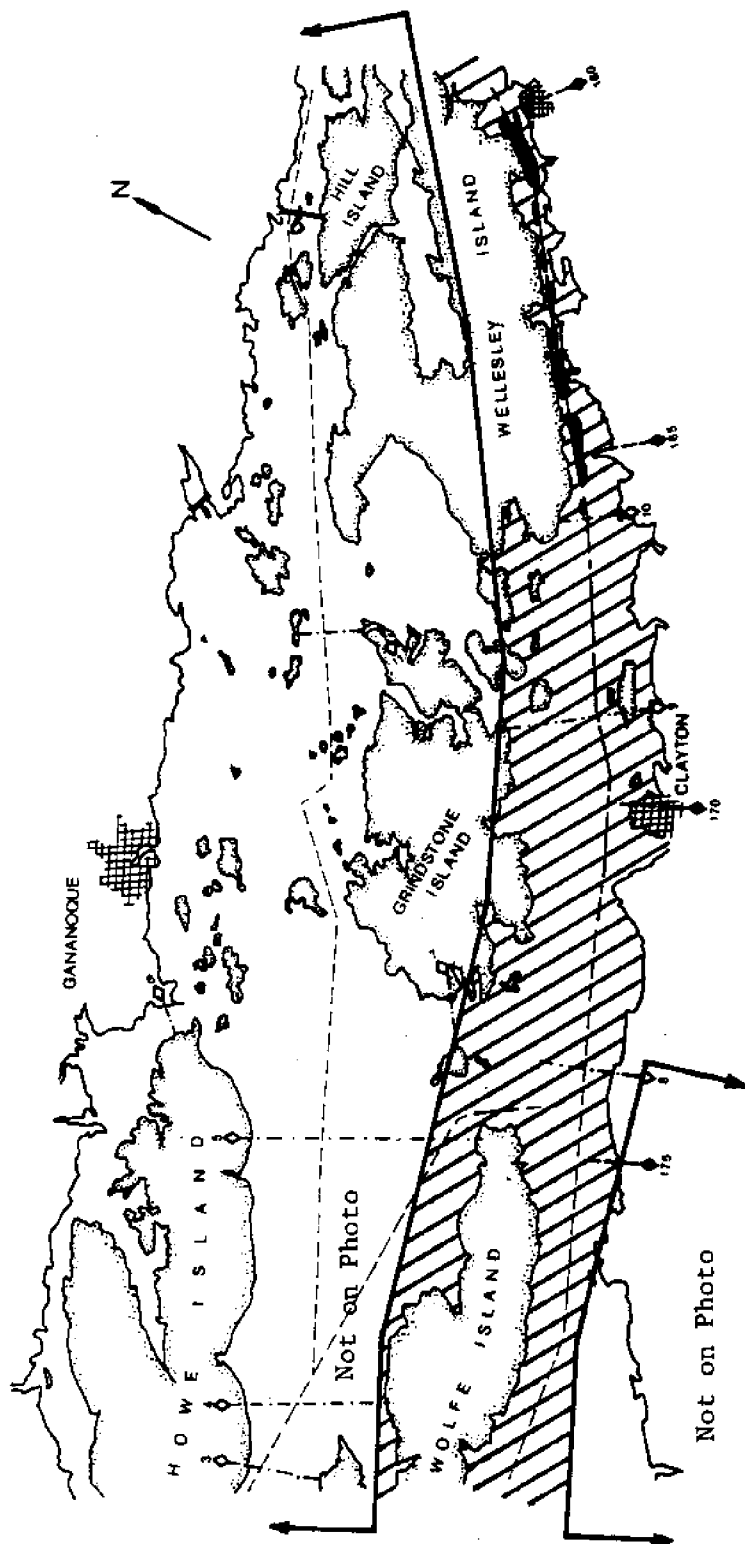
DATE March 6, 1982



Not on Photo



DATE: March 6, 1982

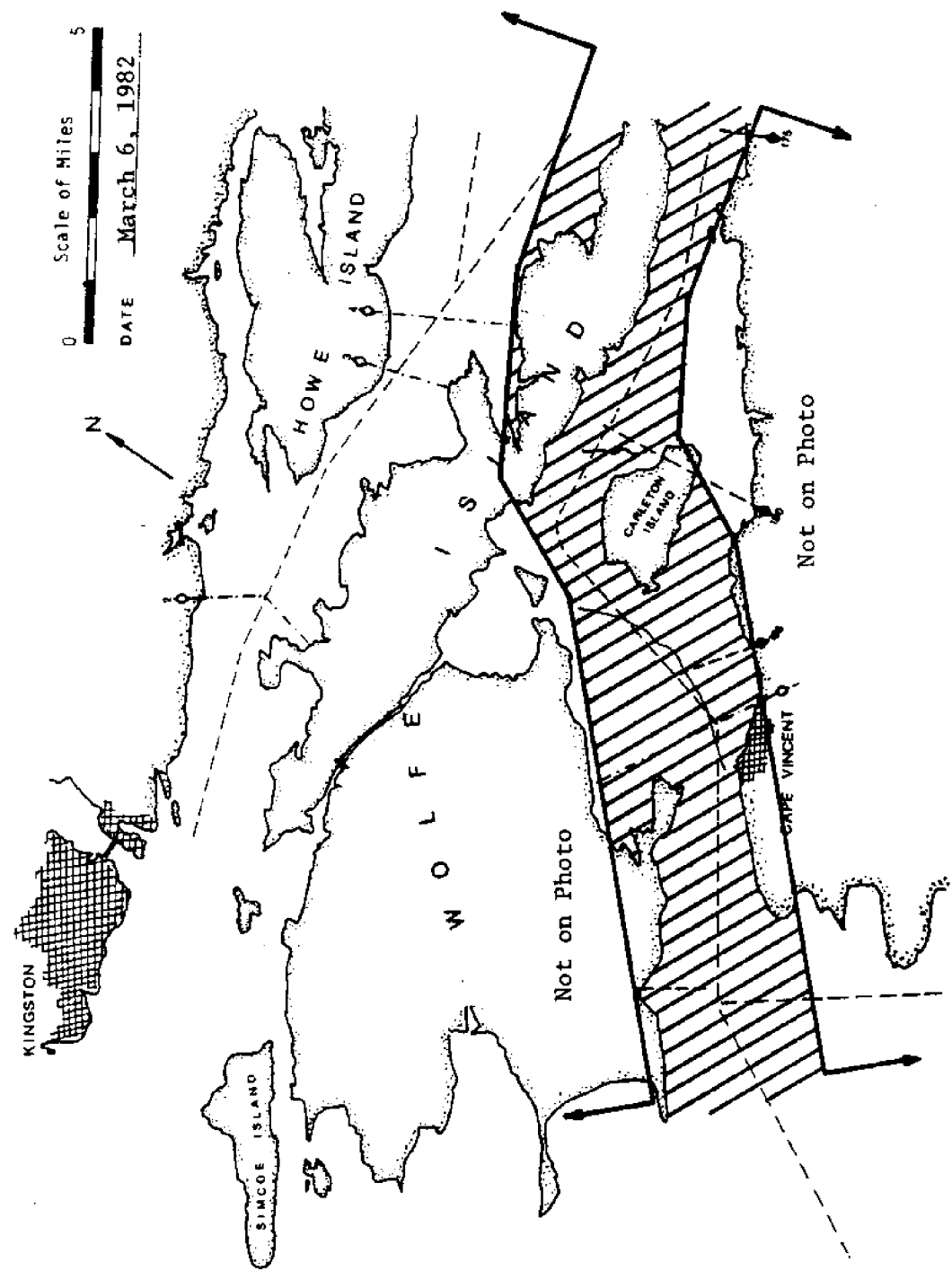


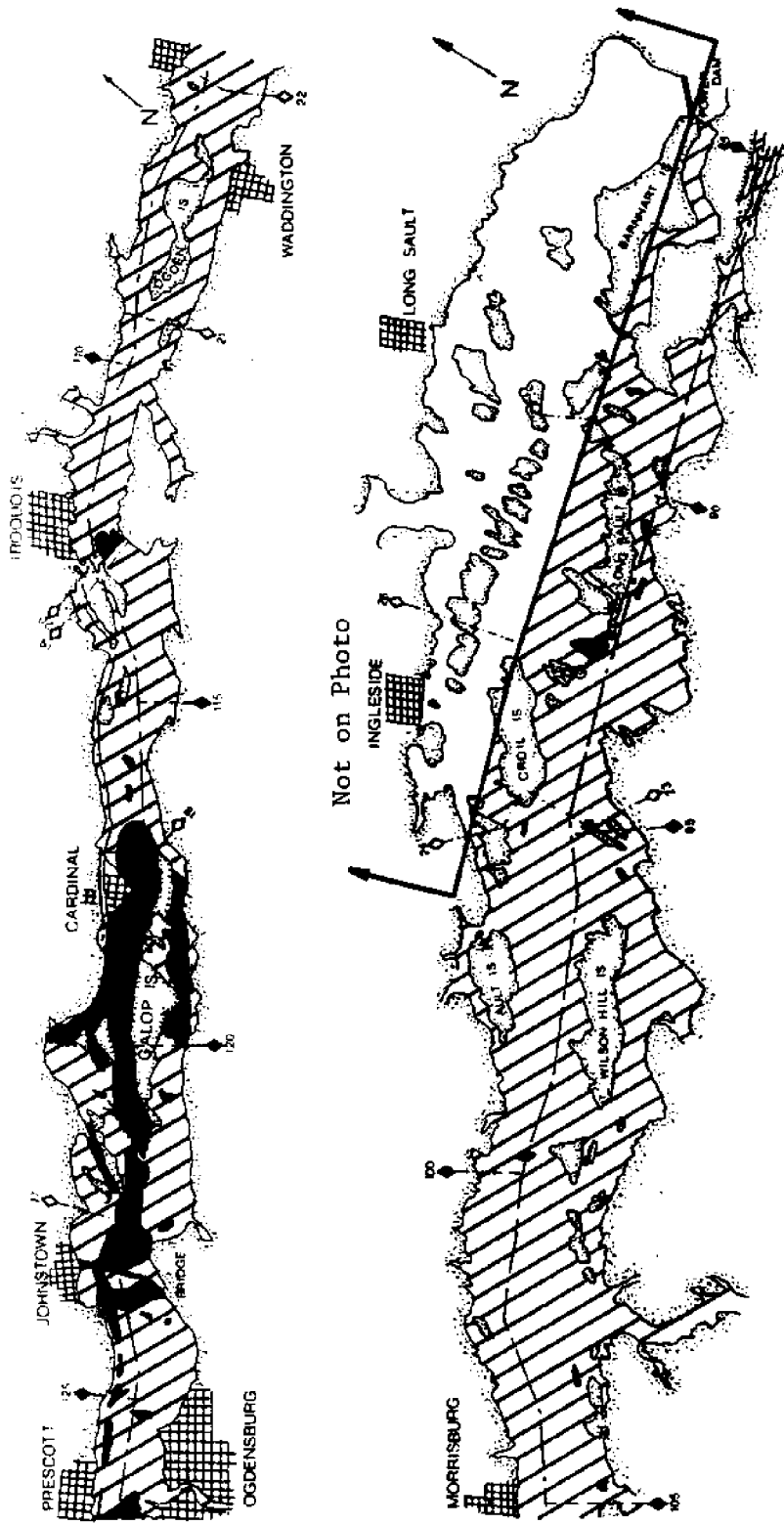
0 Scale of Miles 5

DATE March 6, 1982

Not on Photo

Not on Photo

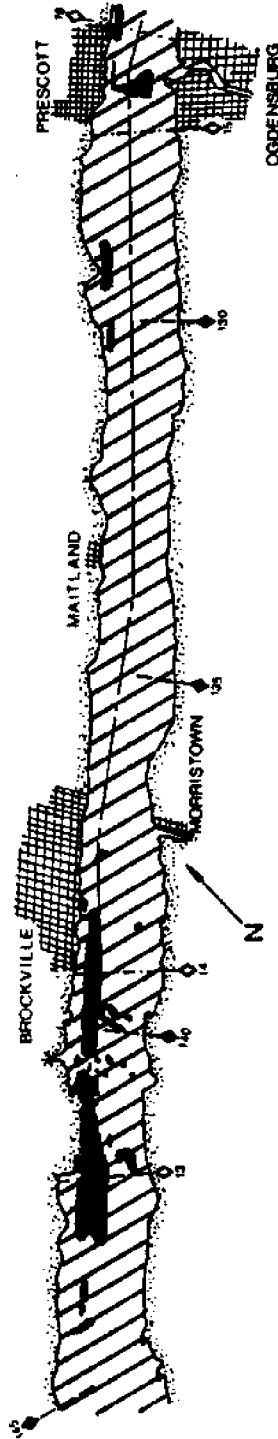
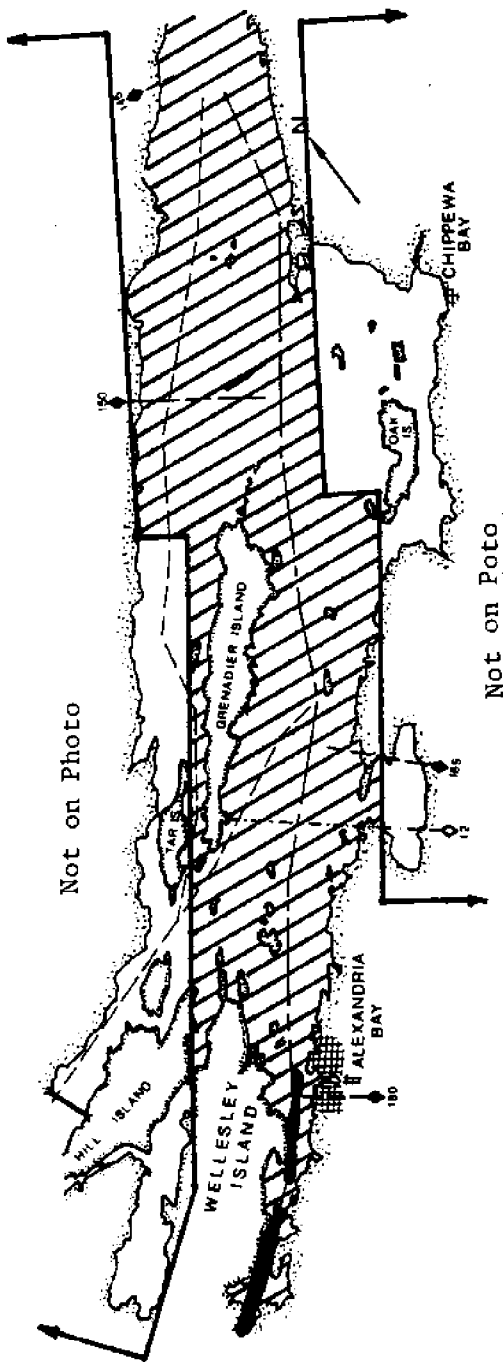




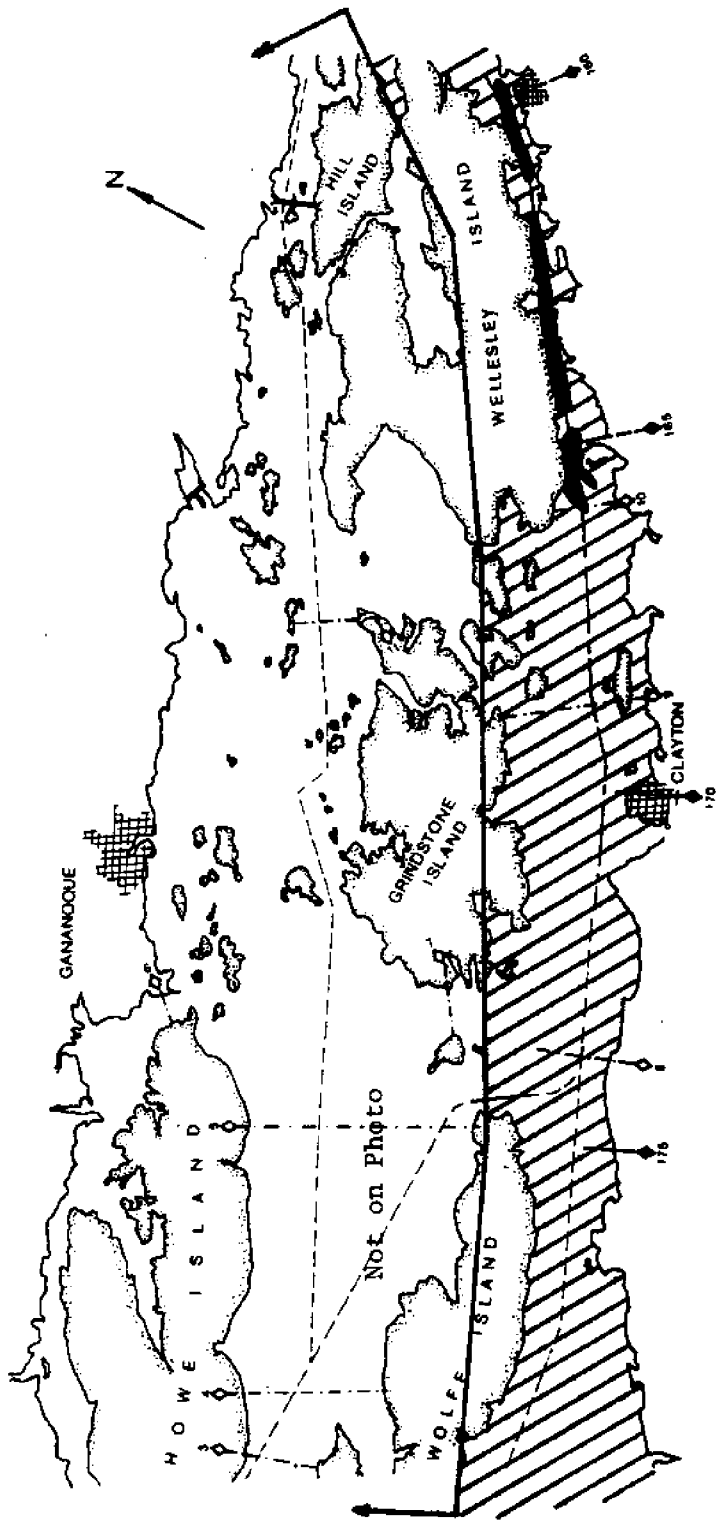
Not on Photo

0 Scale of Miles 5

DATE March 15, 1982

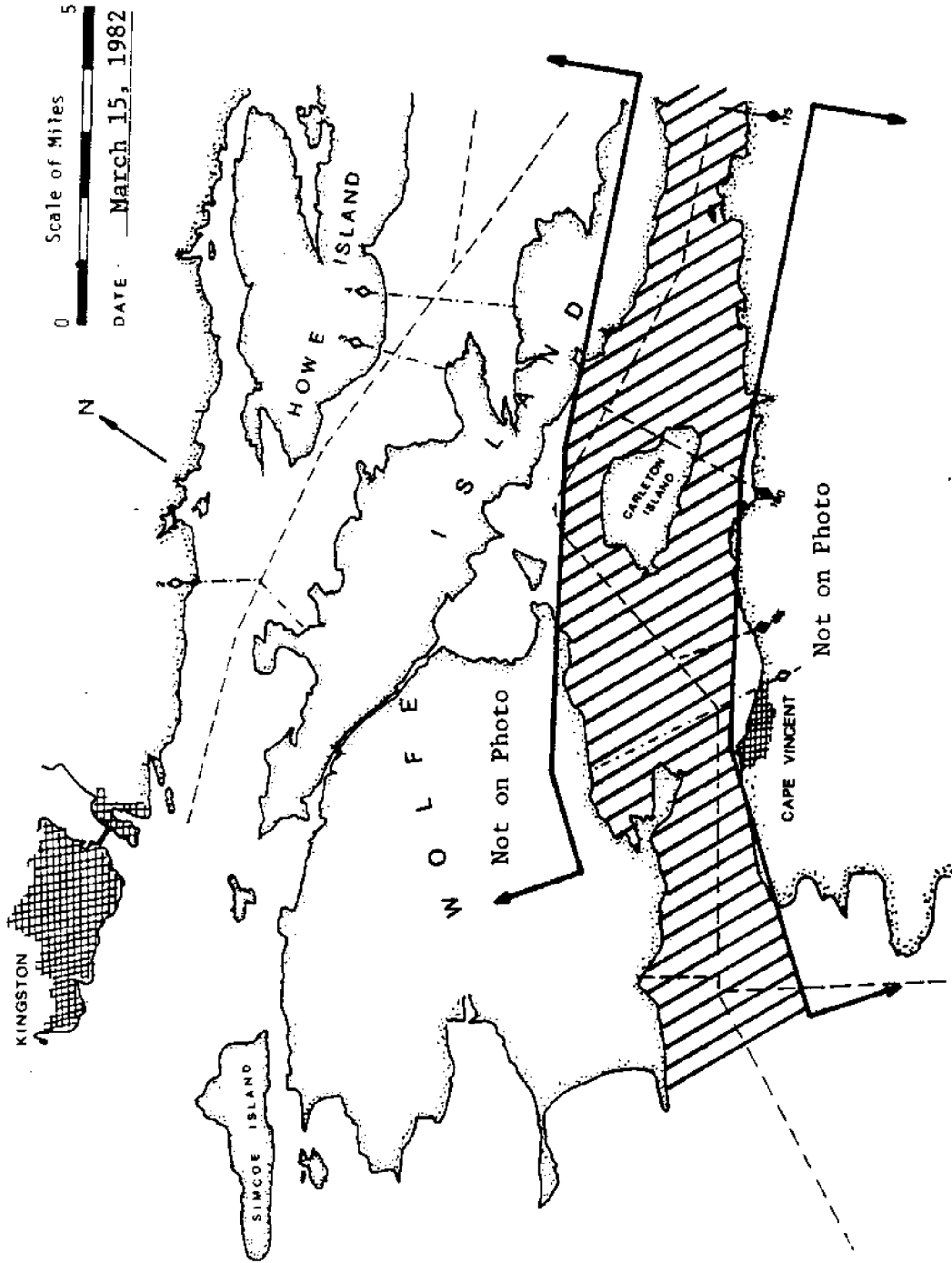


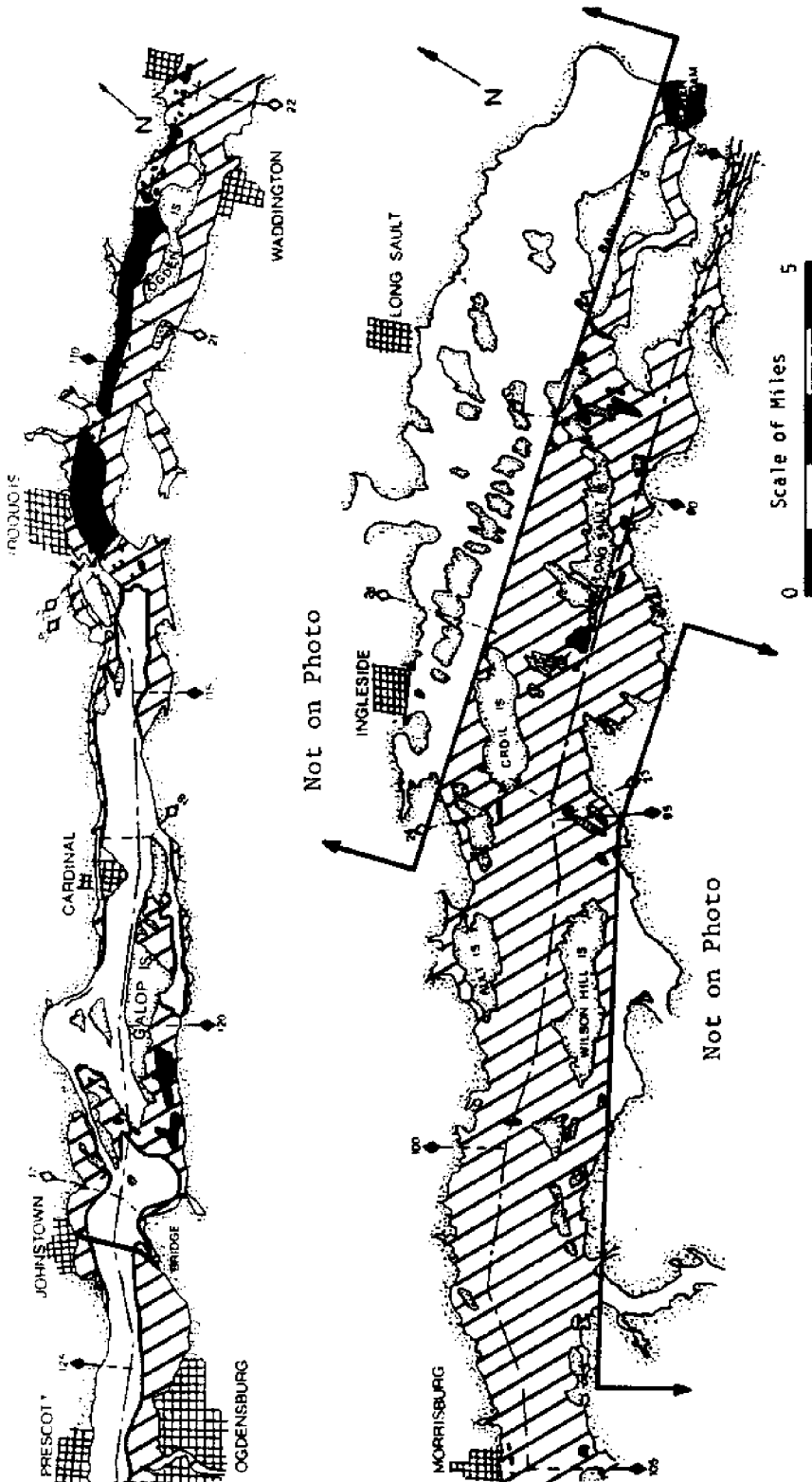
DATE: March 15, 1982

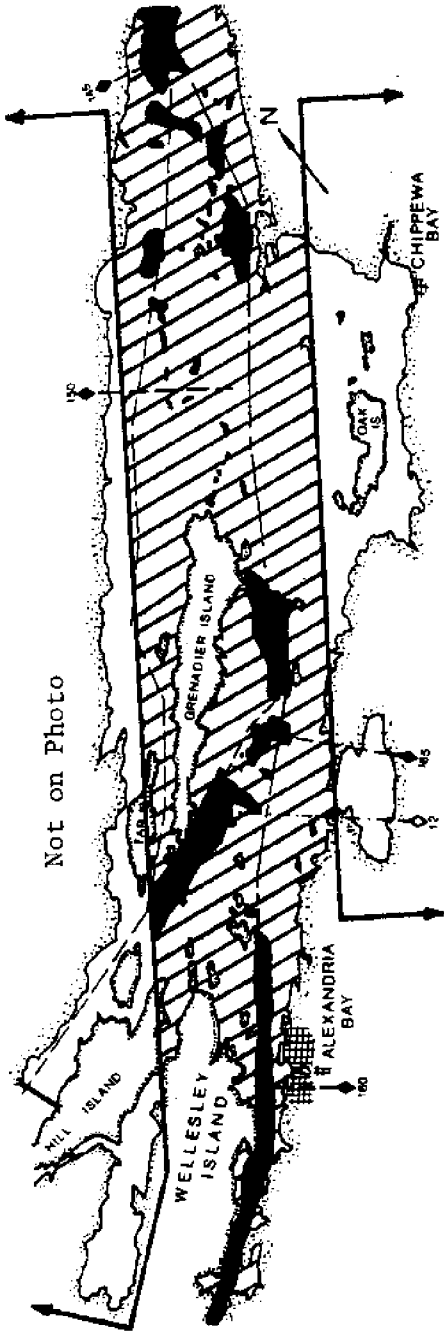


0 Scale of Miles 5

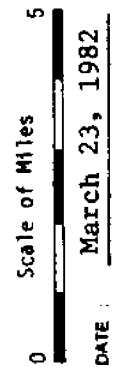
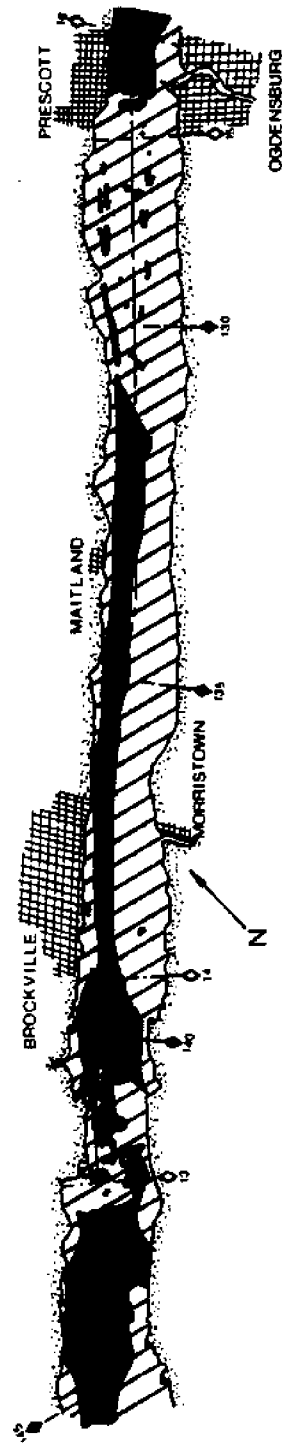
DATE: March 15, 1982

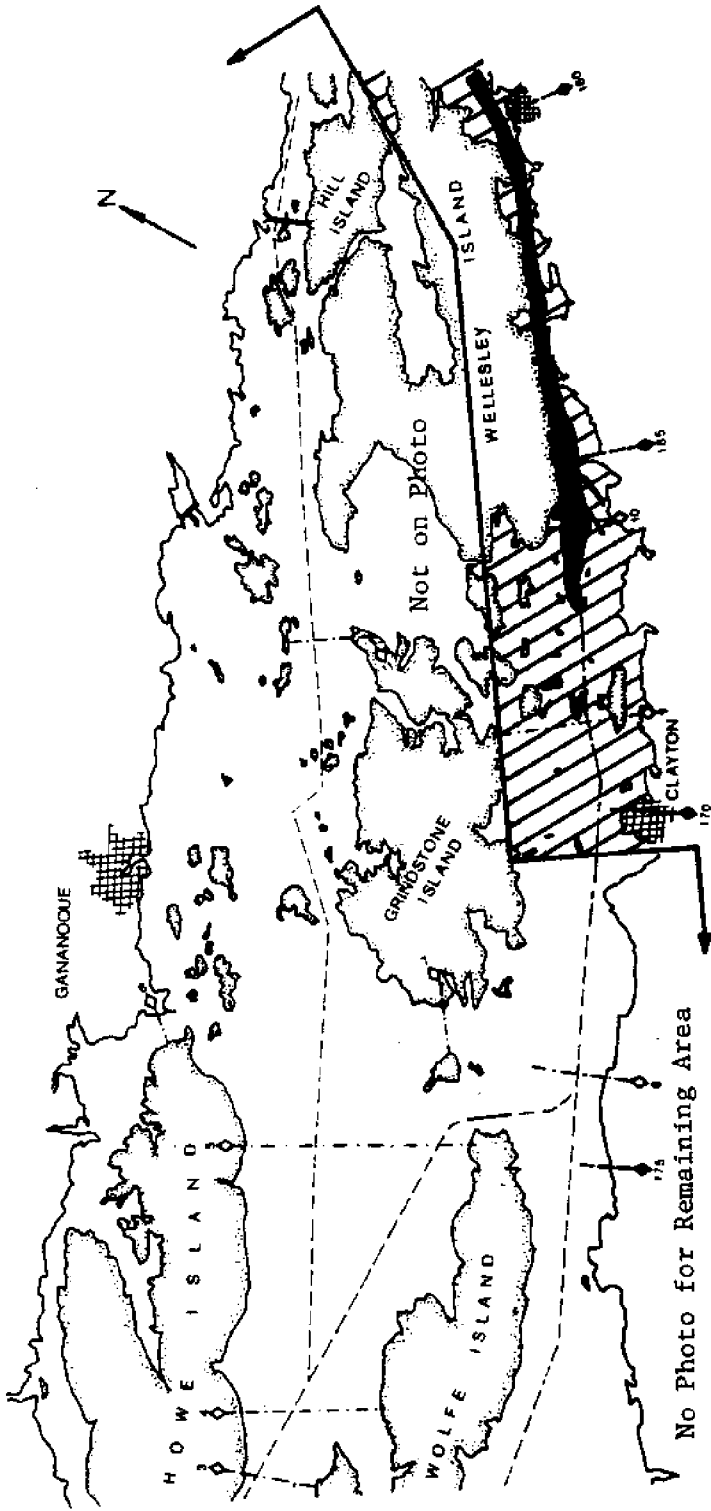






Not on Photo

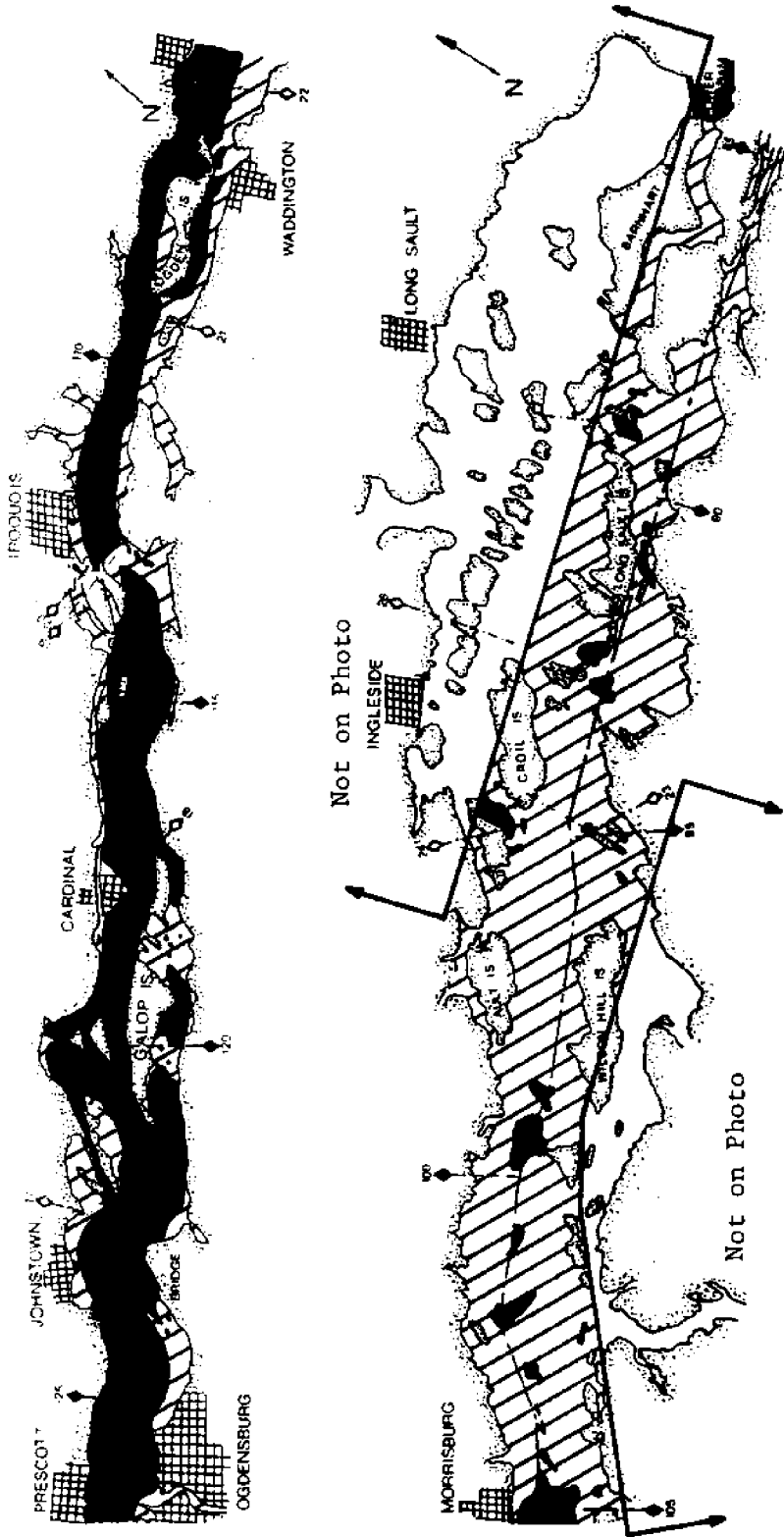


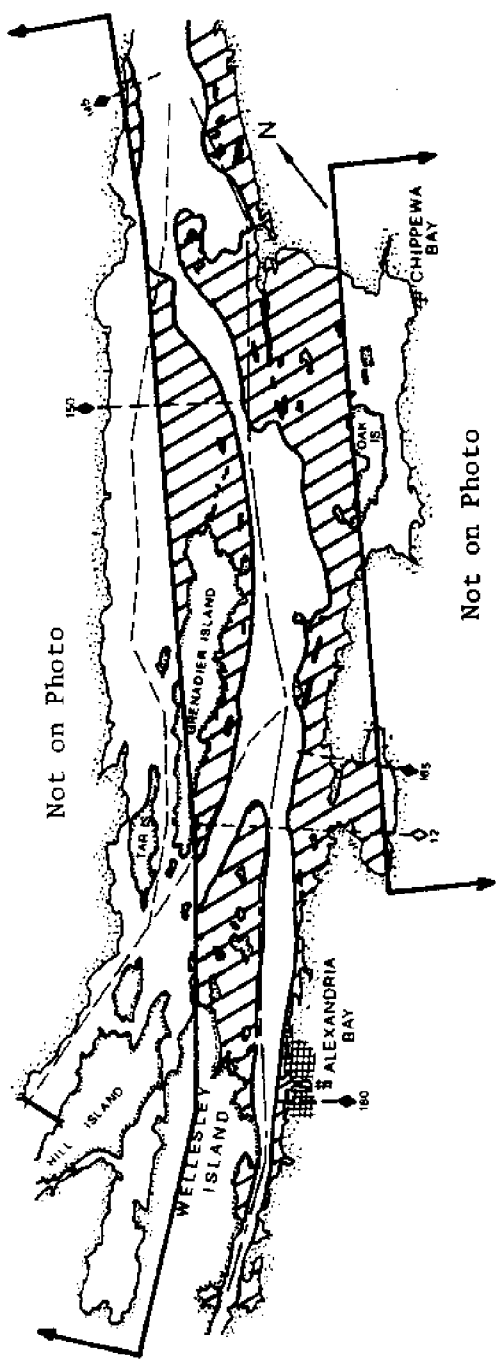


0 Scale of Miles 5

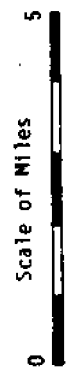
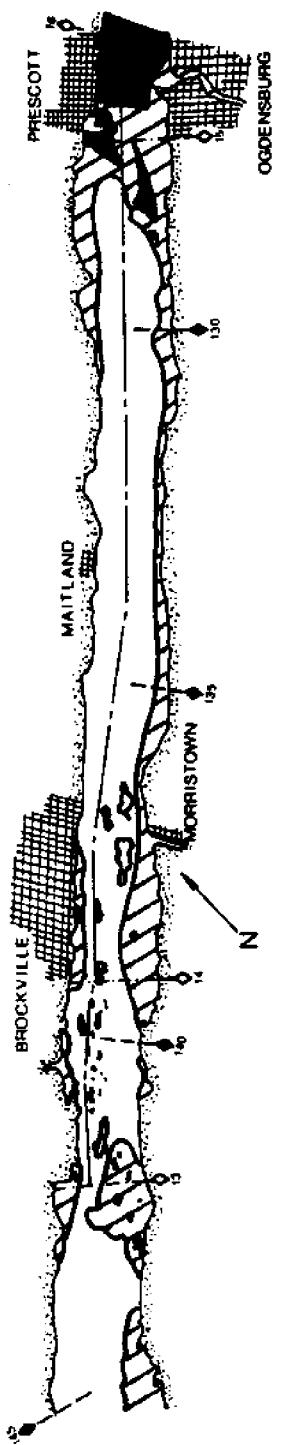
DATE: March 23, 1982

No Photo for Remaining Area

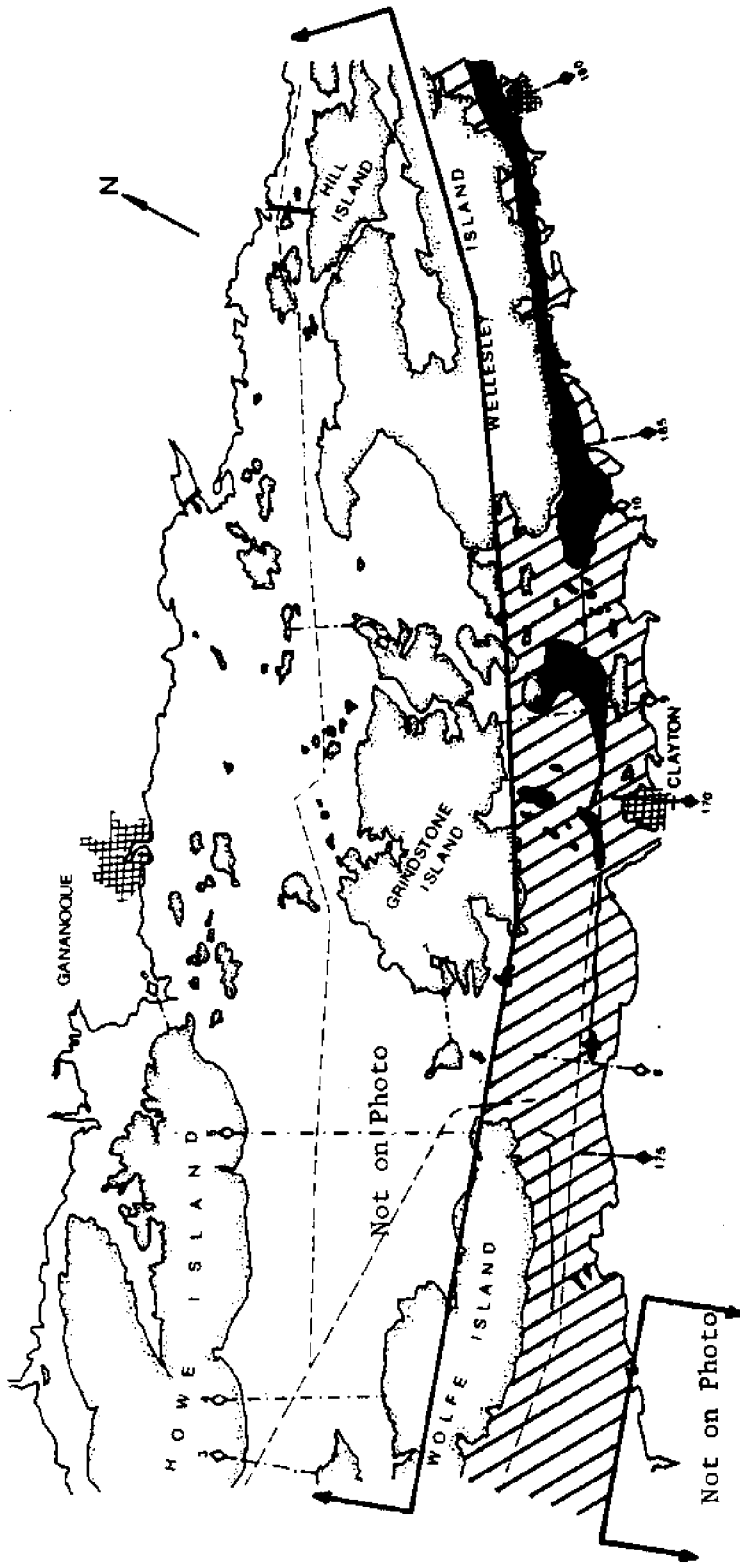




Not on Photo

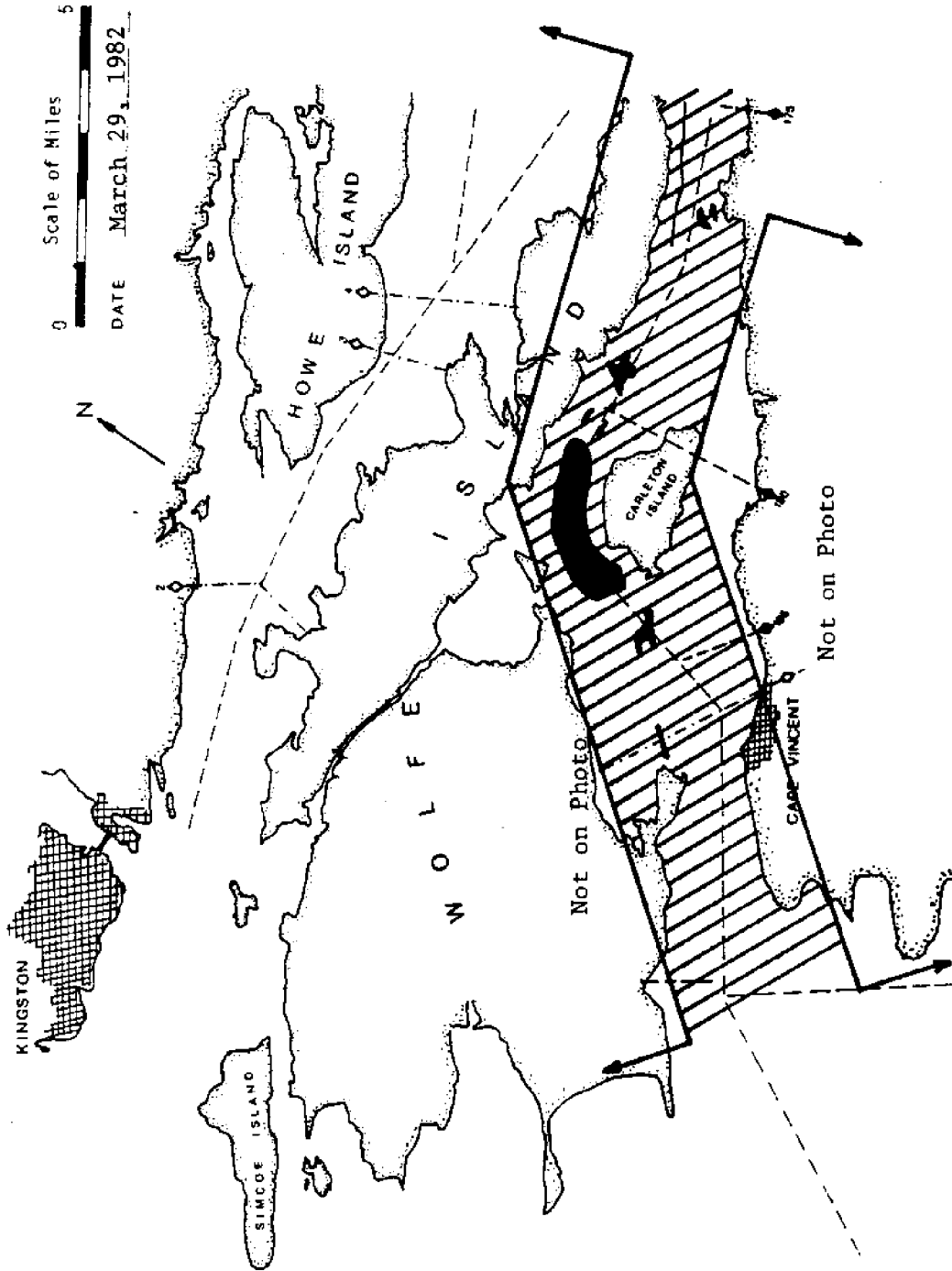


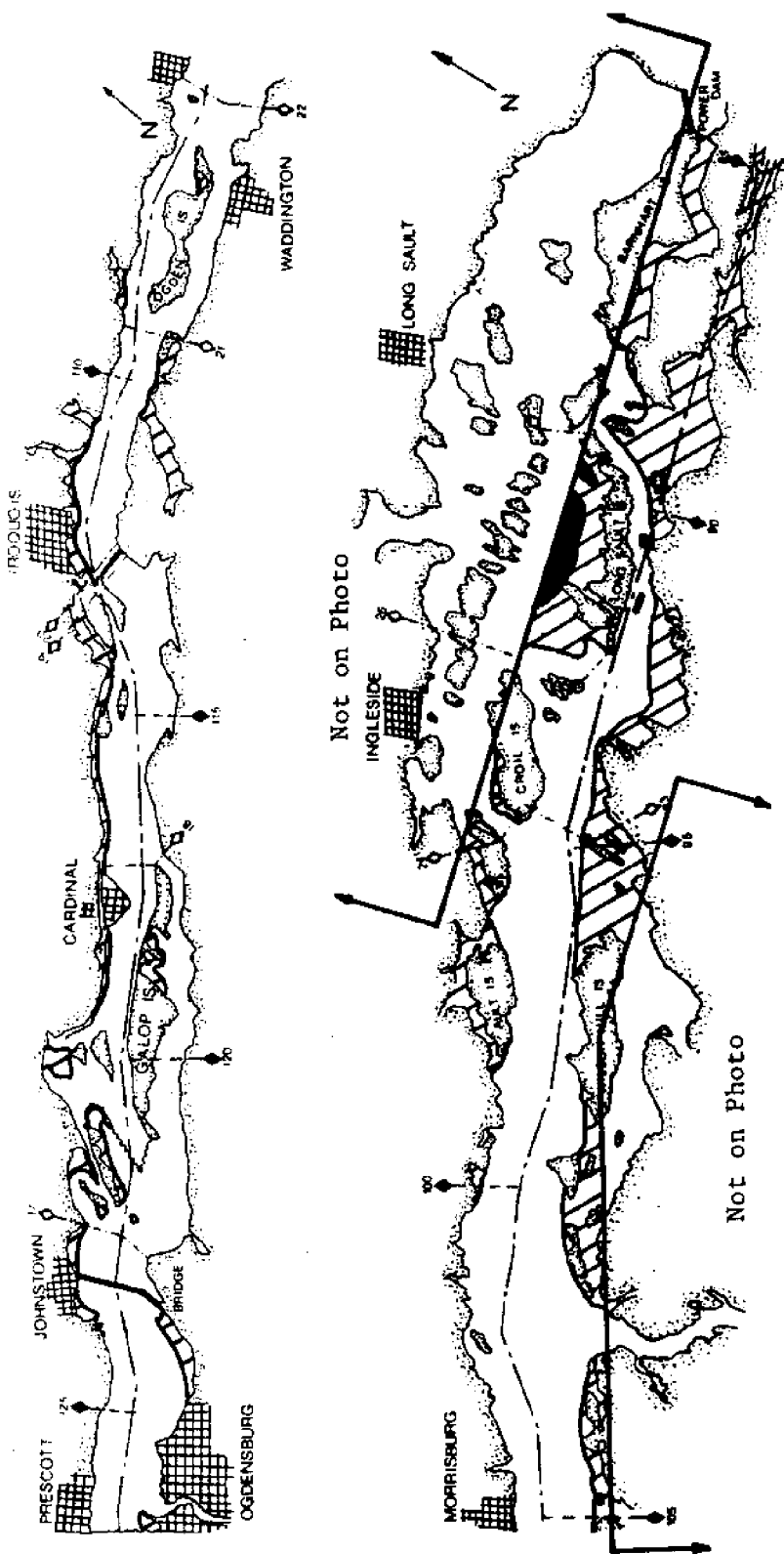
DATE March 29, 1982

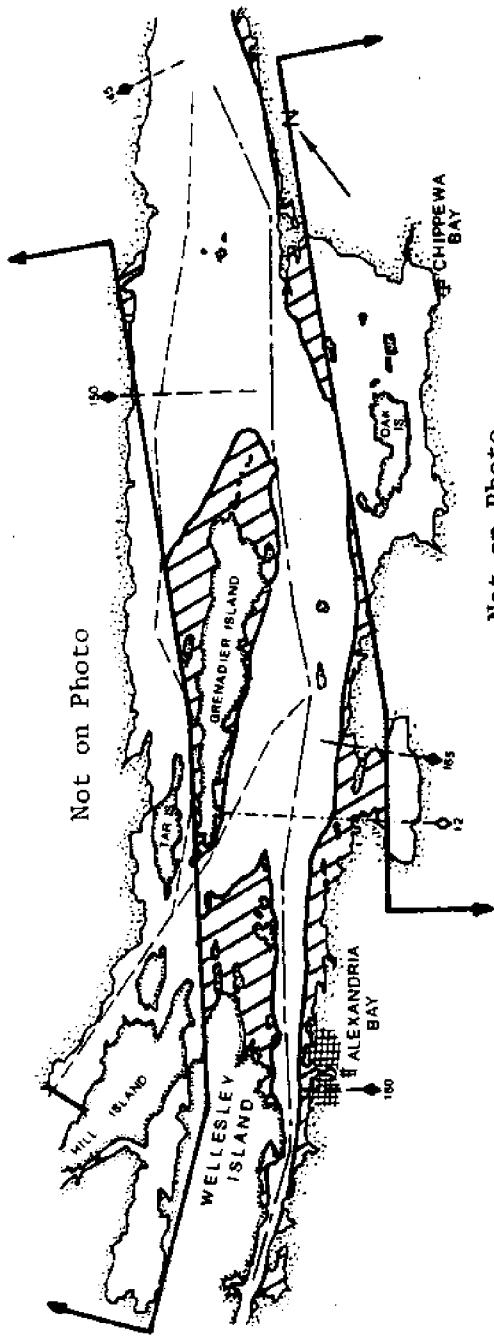


0 Scale of Miles 5

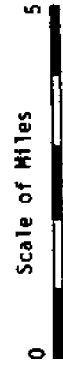
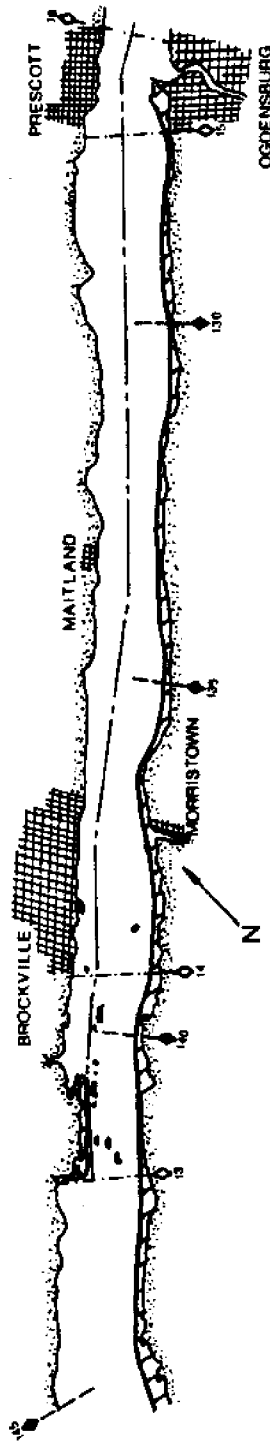
DATE March 29, 1982



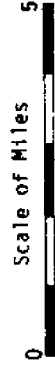
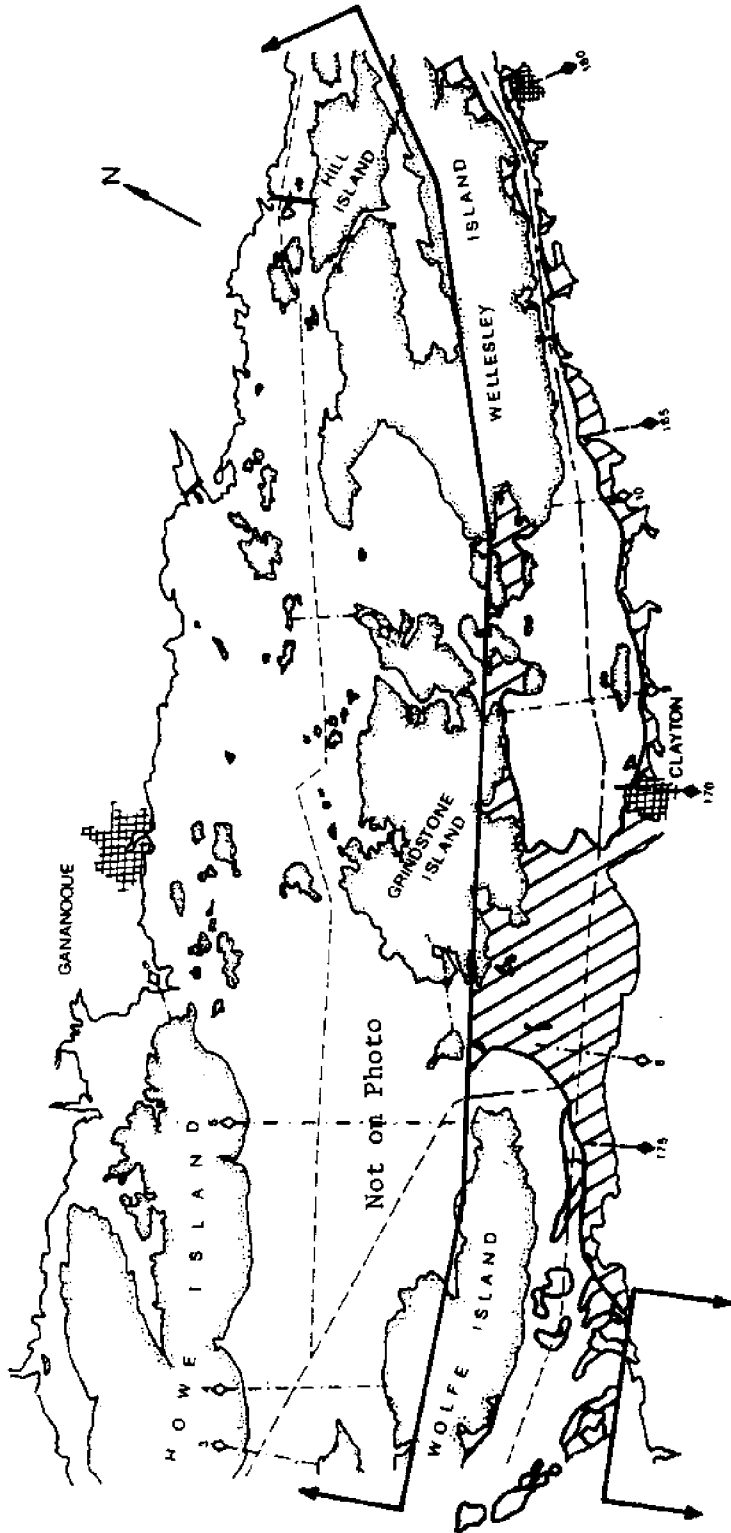




Not on Photo



DATE: April 5, 1982



DATE April 5, 1982

